EPA-650/2-75-062
August 1975

Environmental Protection Technology Series

REMOTE MEASUREMENT OF POWER PLANT SMOKE STACK EFFLUENT VELOCITY

U.S. Environmental Protection Agency
Office of Research and Development
Washington, D. C. 20460

EPA-650/2-75-062

REMOTE MEASUREMENT OF POWER PLANT SMOKE STACK EFFLUENT VELOCITY

by

C. R. Miller and C. M. Sonnenschein

Raytheon Company
528 Boston Post Road
Sudbury, Massachusetts 01776

Contract No. 68-02-1752
ROAP No. 26AAP-85
Program Element No. 1AA010

EPA Project Officer: William F. Herget

Chemistry and Physics Laboraotory
National Environmental Research Center
Research Triangle Park, North Carolina 27711

Prepared for

U. S. ENVIRONMENTAL PROTECTION AGENCY
OFFICE OF RESEARCH AND DEVELOPMENT
WASHINGTON, D. C. 20460

August 1975

EPA REVIEW NOTICE

This report has been reviewed by the National Environmental Research Center - Research Triangle Park, Office of Research and Development, EPA, and approved for publication. Approval does not signify that the contents necessarily reflect the views and policies of the Environmental Protection Agency, nor does mention of trade names or commercial products constitute endorsement or recommendation for use.

RESEARCH REPORTING SERIES

Research reports of the Office of Research and Development, U.S. Environmental Protection Agency, have been grouped into series. These broad categories were established to facilitate further development and application of environmental technology. Elimination of traditional grouping was consciously planned to foster technology transfer and maximum interface in related fields. These series are:

1. ENVIRONMENTAL HEALTH EFFECTS RESEARCH
2. ENVIRONMENTAL PROTECTION TECHNOLOGY
3. ECOLOGICAL RESEARCH
4. ENVIRONMENTAL MONITORING
5. SOCIOECONOMIC ENVIRONMENTAL STUDIES
6. SCIENTIFIC AND TECHNICAL ASSESSMENT REPORTS
9. MISCELLANEOUS

This report has been assigned to the ENVIRONMENTAL PROTECTION TECHNOLOGY series. This series describes research performed to develop and demonstrate instrumentation, equipment and methodology to repair or prevent environmental degradation from point and non-point sources of pollution. This work provides the new or improved technology required for the control and treatment of pollution sources to meet environmental quality standards.

This document is available to the public for sale through the National Technical Information Service, Springfield, Virginia 22161.

Publication No. EPA-650/2-75-062

ABSTRACT

This report describes the successful demonstration of the ability a CO_2 Laser Doppler Velocimeter to measure remotely the velocity of the effluent from a power plant smoke stack. The basis of the technique is that laser radiation backscattered from particulates in the effluent is Doppler shifted in frequency in proportion to the velocity of the effluent.

Measurements were made against a coal burning power plant equipped with electrostatic precipitators to remove particulates from the boiler flue gases. The measurement site was approximately 400 m slant range from the stack. Backscattered signals from the stack effluents were detected, processed and recorded on magnetic tape. The taped data was analyzed to determine: (1) agreement between LDV and in-stack velocity measurements, (2) correlation of backscatter signal strength and the cross-stack optical transmission, (3) estimates of the effluent backscatter coefficient at 10.6-μm, (4) profiles of the stack exit velocity distribution at various heights above the stack lip, and (5) the effect of turbulence on the backscattered Doppler spectra.

As a result of exit velocity measurements in the 25 to 45 m/sec range, it was concluded that an LDV can remotely measure stack exit velocities to an accuracy of at least 1.5 m/sec. The potential for making particulate concentration measurements with the same instrument was also demonstrated by establishing a relationship between the intensity of the scattered radiation and the optical opacity of the exit gases.

Based on the results of the measurements a study on the design of an LDV optimized for the measurement of power plant effluent velocities was performed.

This report was submitted in fulfillment of EPA contract number 68-02-1752 by Raytheon Company, Equipment Division, Electro-Optics Department carried out under the joint sponsorship of the Environmental Protection Agency, and the National Aeronautics and Space Administration. Work was completed as of June 1975.

TABLE OF CONTENTS

CONTENTS (Continued)

ILLUSTRATIONS

ILLUSTRATIONS (Continued)

ILLUSTRATIONS (Continued)

ILLUSTRATIONS (Continued)

LIST OF TABLES

ACKNOWLEDGEMENTS

The work effort in this project has involved a number of companies and governmental agencies. The authors would like to acknowledge the extensive technical assistance of R. E. Schaaf and the managerial direction of A. V. Jelalian of the Electro-Optics Department of Raytheon Company's Equipment Division, Sudbury Engineering Facility. The analysis of turbulence effects was performed under sub-contract by J. A. L. Thomson of Physical Dynamics, Inc. The cooperation of the personnel of Duke Power's River Bend Steam Station in support and performance of the experimental measurements is gratefully acknowledged. The authors would like to thank W. F. Herget and R. Rollins of the EPA's NERC, for their technical assistance. Acknowledgement is made to Environmental Science and Engineering, Inc., for the in-stack measurements. The contribution of R. M. Huffaker of NASA, MSFC, as a technical advisor to the program is greatly appreciated.

SECTION 1

INTRODUCTION AND SUMMARY

Most conventional methods for monitoring particulate flow rates from stationary sources such as power plants are expensive and quite time-consuming. These methods require the use of highly specialized teams to install monitoring equipment on a stack, make the required measurements, and analyze the data. New methods for stationary source monitoring are now being developed which are based on remote measurement of the electromagnetic properties of the polluting species in the stack effluent. Since the new instrumentation can be operated without even requiring access to the power plant property, a complete test can be done with a minimum of preparation and time.

Two types of measurements are needed to calculate a mass flow rate by remote techniques: species concentration and velocity. The U. S. Environmental Protection Agency's Chemistry and Physics Laboratory and Stationary Source Enforcement Division are currently evaluating various remote measurement techniques. Research over the past ten years by NASA and other government agencies has shown that remote measurement of wind velocities at ranges of a kilometer are possible using a Laser Doppler Velocimeter (LDV). The basis of the technique is that laser radiation scattered from particulates in the air is Doppler shifted in frequency, and measurement of this Doppler frequency shift yields the velocity of the particulates and hence of the wind. The method has excellent potential for use in the determination of smoke stack gas exit velocities and particle concentrations. The instrumentation for the remote wind velocity measurement is in existence. Particulate concentration measurements can be made with the same instrument by relating the intensity of the scattered radiation to the emission concentration.

The objective of this program was to prove the feasibility of remote measurement of smoke stack velocity using an LDV. To accomplish this a CO_2 Laser Doppler Radar system was assembled into

a mobile van, and measurements were made on an EPA instrumented smoke stack at the River Bend Steam Station of the Duke Power Company in Mt. Holly, North Carolina. This facility is a coal burning power plant with four boilers. Each boiler drives a turbine generator capable of producing an output up to 150 MW. Each boiler unit is equipped with electrostatic precipitators which remove over 99% of the particulate matter from the smoke. The measurement site was approximately 400 meters slant range from the stack exit. The elevation angle to the stack lip was about 8°. In-stack measurements of the flue gas velocities and the cross-stack optical transmission were supplied by the EPA for comparison to the remote data.

After alignment and calibration of the LDV system at the Duke Power site, backscatter signals, representing the particulate characteristics of the effluents from a smoke stack, were detected, processed, and recorded on magnetic tape for further analysis. Approximately 5,500 meters of taped data were recorded during the first field test period of 24 to 31 August 1974. Another 11,000 meters of taped data were recorded in the second field test period of 12 to 19 January 1975. The data were analyzed to determine (1) profiles of the stack exit velocity at various heights above the stack lip, (2) stack exit velocities as a function of the in-stack velocities, (3) effluent backscatter coefficients at 10.6 μm, (4) correlation of backscatter signal strength and cross-stack optical transmission, and (5) the effect of turbulence on the backscattered Doppler spectra.

The results of the measurements definitely prove the feasibility of using a LDV to remotely measure smoke stack effluent velocities. The velocity data from the LDV, taken at the top of the stack, and the in-stack velocity data, taken from pitot tube traverses at the base of the stack, agreed to within 14%. It is thought that the majority of this error is due to miscalibration (e.g. in the pitot-tube velocity measurements or in the measurement of the LDV elevation angles.) and that the actual LDV measurement accuracy is about 1.5 m/sec for stack exit velocities in the 25 to 40 m/sec range. Estimates

for the backscatter coefficient at 10.6-μm vary from 10^{-7} to 10^{-3} m^{-1} depending on the number of precipitators in use. Definite correlations exist between the 10.6-μm backscatter signal strength and the attenuation coefficient measured in the visible. Since a correlation can be made between the attenuation coefficient and mass concentration, the LDV can be used to measure the mass concentration exhausting from a given smoke stack. Turbulence effects were shown to flatten the exit velocity distribution across the top of the stack. This flattening relaxes the spatial alignment requirements necessary for an accurate velocity measurement. The turbulent velocities in the stack broaden the backscattered Doppler spectra. The broadening is relatively independent of elevation angle, and it was found that suitable effluent velocity measurements can be made with elevation angles between 8° and 45°.

The LDV system used in the first field tests is described in detail in Section 2. Section 3 presents the results of the first experimental phase, while Section 4 describes various system changes and gives the results of the second set of field tests. The design studies for an optimized LDV for smoke stack emission measurements are presented in Section 5. Conclusions and recommendations for additional work are proposed in Section 6.

SECTION 2

SYSTEM DESCRIPTION

2.0 INTRODUCTION

A block diagram of the LDV system used to make effluent velocity measurements is shown in Figure 2-1. The optical portion of the system consists of a 20 watt CO_2 laser, a Mach-Zehnder interferometer, a 30 cm diameter, f/8 telescope and a copper-doped germanium detector, all of Raytheon manufacture. This equipment is shown schematically in Figure 2-2 and pictorially in Figure 2-3. These equipments are mounted on an aluminum base which is in turn shock mounted on a support table to protect against vibration. The transmitted beam is directed by a Raytheon scanner utilizing an elliptical flat with a 46 cm major axis. The signals are viewed on a Hewlett Packard 8552B/8553B Spectrum Analyzer for visual monitoring and processed by a Raytheon Frequency Tracker. Data from the spectrum analyzer and frequency tracker as well as a voice channel was recorded on a Precision Instruments Magnetic Tape Recorder. These various components, as well as the Raytheon laser test van, are described in the following sections.

2.1 CO_2 LASER

The Raytheon Model LS10A CO_2 laser shown in Figure 2-4 was a water cooled semi-sealed unit having a nominal output of 20 watts. Sealing of the system was through a vacuum valve which permitted refilling of the laser in the field if necessary. Refilling was accomplished using the gas bottle and pumping station located in the power unit which also contained the laser power supply, the closed cycle laser cooling system and a high voltage supply for tuning the laser by PZT control of the cavity length.

The laser head contained a split discharge tube closed off with non-hygroscopic zinc selenide windows mounted at Brewster's angle. The orientation of the windows determined the polarization of the

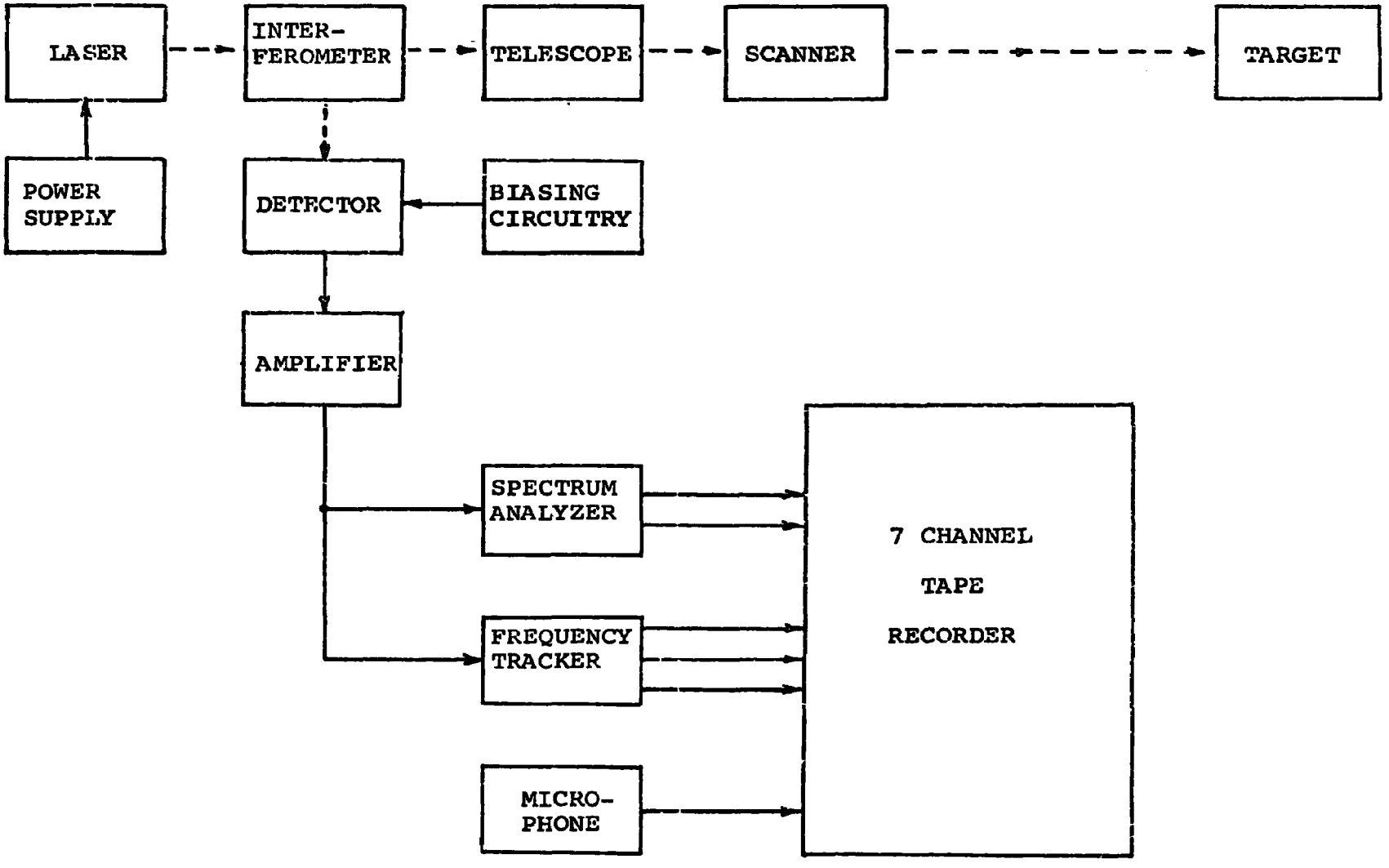

Figure 2-1. Block Diagram of the EPA Effluent Detection System

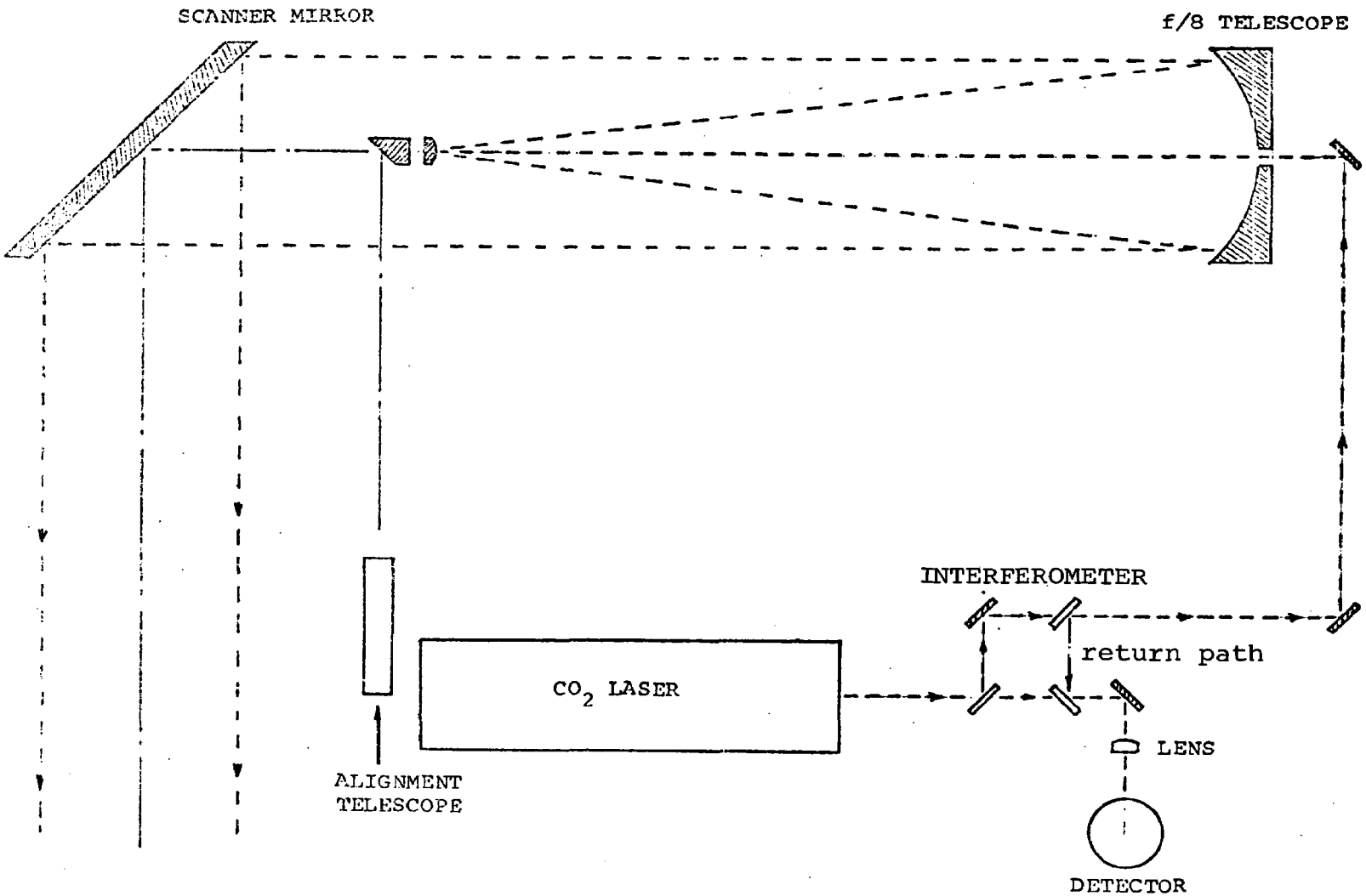

Figure 2-2. Optical Layout of the EPA Effluent Detection System

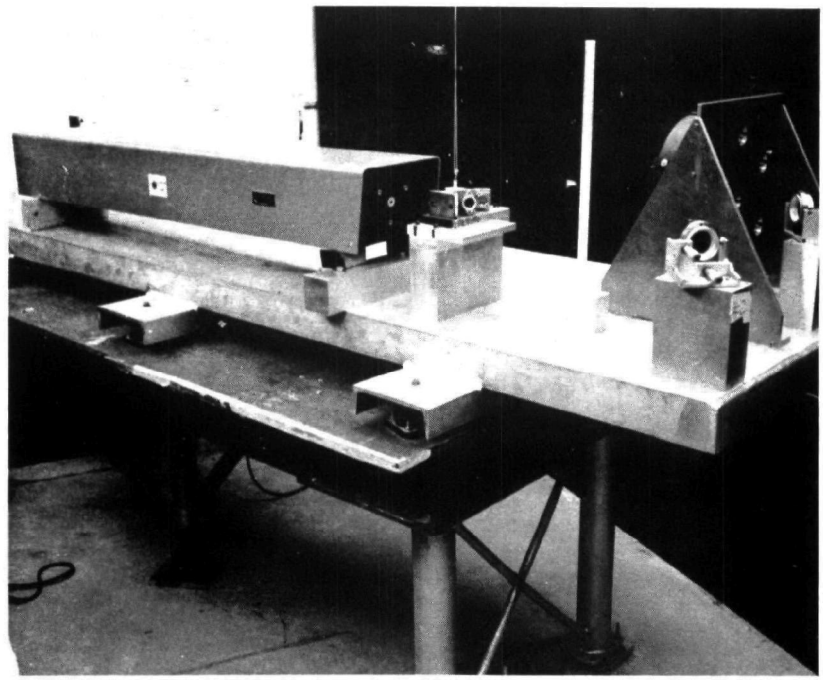

Figure 2-3. Photograph of Laser Doppler Velocimeter.

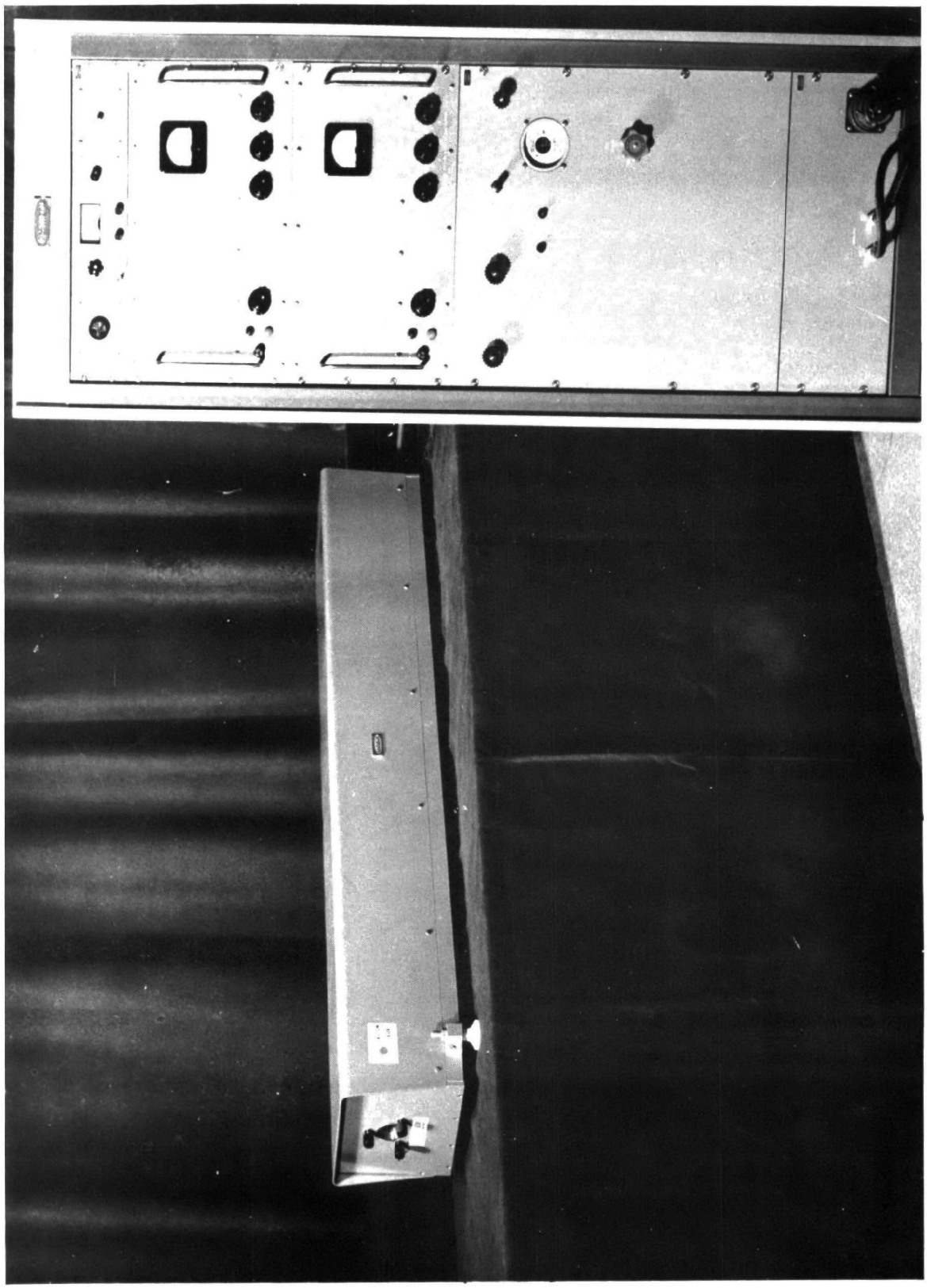

Figure 2-4. Raytheon Model LS10A CO_2 Laser

output beam. The discharge tube was mounted between a plane output mirror and a four meter radius of curvature rear reflector. The mirrors and discharge tube were mounted on a frame utilizing four Invar bars for thermal stability. The cavity configuration and mechanical structure assured a stable TEM_{oo} output beam.

2.2 THE INTERFEROMETER

A Mach Zehnder interferometer was used in the LDV system. The configuration is shown in Figure 2-5.

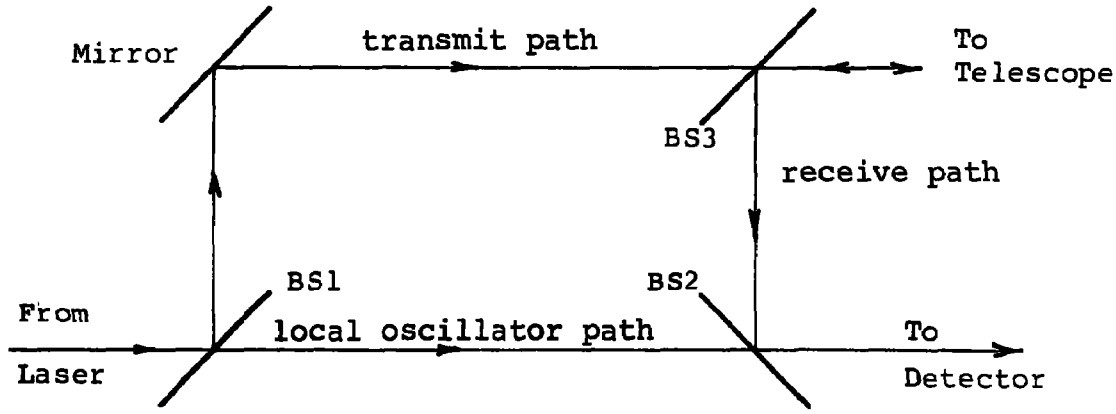

Figure 2-5. Mach Zehnder Interferometer Configuration

The laser beam enters from the left, is reflected by the beamsplitter (BS1) and mirror and goes through the beamsplitter BS3 to the telescope. The signal beam, which consists of that portion of the scattered light which has retained the polarization of the output beam, comes from the telescope, is reflected by BS3 and BS2 to the detector where it is mixed with the local oscillator beam which has come from the laser through BS1 and BS2. The beamsplitters

BS1 and BS2 are chosen so that the product of their transmission yields the correct local oscillator level for the detector being used.

In order to eliminate the need for independently maintaining alignment of the various mirrors and beamsplitters, Raytheon constructed interferometers from precision machined blocks of solid Invar. This resulted in an interferometer which is mechanically rigid and thermally stable and which is aligned by a simple tilt, rotation or translation of the interferometer as a unit rather than of each of the components.

2.3 TELESCOPE

The telescope was a reflecting telescope of the Cassegrain type. It is partially visible in Figure 2-3 and shown schematically in Figure 2-2. The primary is a 30 cm diameter, f/8 spherical mirror and is fed by a 2.54 cm diameter spherical secondary. Focussing of the telescope is achieved by a calibrated translation of the secondary on a micrometer driven stage. Both components of the telescope are mounted on the aluminum shock mounted optical table.

The use of reflecting elements in the telescope allowed it to be aligned in the visible as well as aimed visually, since reflecting elements aligned in the visible are also aligned at the laser wavelength in the infrared. The use of reflecting elements also permitted aiming of the system without transmitting a laser beam, thereby avoiding a possible safety hazard.

2.4 DETECTOR AND RECEIVER ELECTRONICS

A copper-doped germanium detector with a quantum efficiency of 10% was used in the LDV system. The liquid helium cooled Ge:Cu detector requires more than 20 milliwatts to become shot noise limited and can be operated with 50-100 milliwatts if desired. At these higher powers, the power reflected by the secondary of the Cassegrainian telescope is negligible and no saturation effects occur. In addition, the Ge:Cu detector is nearly impossible to damage if excessive optical power is applied.

The detector was properly matched to the bias circuit and the preamplifier in order to obtain the frequency response desired and to assure that the shot noise will exceed the thermal noise of the preamplifier and load resistor which are the major noise sources. The Ge:Cu detector used in the measurements is shown in Figure 2-6.

2.5 OPTICAL SCANNER

An optical scanner was necessary to direct the 30 cm diameter laser beam toward a target of interest, which, in this case, was the effluent of a smoke stack. The scanner provided sufficient deflection in both elevation and azimuth to accommodate various target sighting geometries and to correct for the rough positioning of the van.

The elliptical scan mirror was of sufficient aperture so that the entire laser beam was intercepted at all scan angles. The mirror surface was flat to $\lambda/10$ at 10.6-μm under ambient temperature changes and various mirror positions. The scanner mechanism provided a precise, smooth adjustment in both elevation and azimuth so that target positioning could be easily accomplished. In addition, once the target had been aligned, the scanner was able to be locked in position so that the laser beam remained on the target.

A scanner was built and tested which met the general requirements and had the following specifications:

Mirror size:	48 cm x 33 cm x 5 cm
Mirror Flatness:	$\lambda/10$ @ 10.6 μ
Mirror coating:	Aluminum with SiO overcoating
Azimuth scan angle:	$\pm 8^{\circ}$
Elevation scan angle:	0° to 20°

The scanner had micrometer drives on both the azimuth and elevation scan controls. It was possible for the scanner to easily maintain alignment accuracies of $\pm$100 μradians. A photograph of the scanner is shown in Figure 2-7.

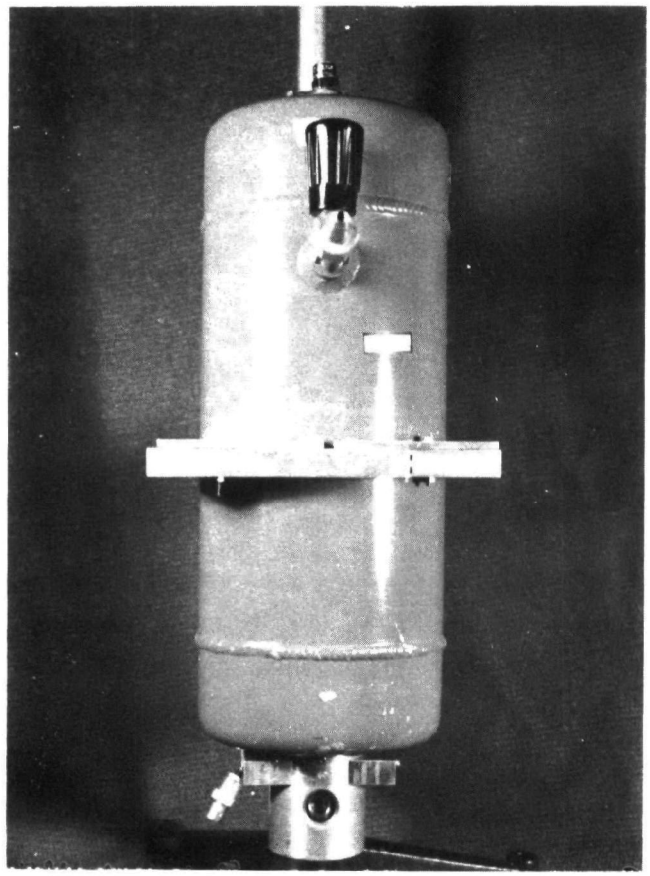

Figure 2-6. A Liquid Helium Cooled Copper Doped Germanium Detector.

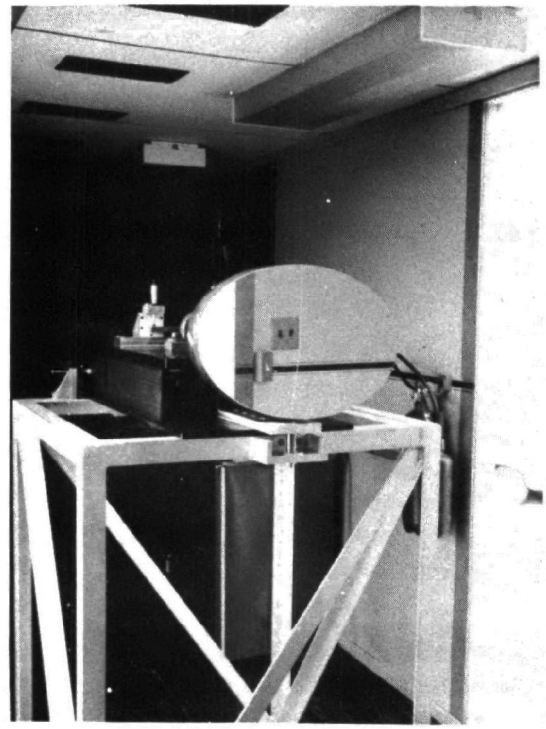

Figure 2-7. Scanning Mirror.

2.6 SIGNAL PROCESSING

The return signal from the smoke stack effluent was processed in two manners. The spectral density of the returned signal was determined by passing the signal through an HP 8552B/8553B spectrum analyzer. The velocity of the smoke stack effluents could be determined from the doppler shift of returned signals.

A frequency tracker was also used to process return signals. The frequency tracker was basically an FM demodulator with negative feedback. It, therefore, became a tracking filter with a variable center frequency. It produced a DC voltage proportional to the mean spectral frequency as well as signals indicating signal dropout and signal fluctuations.

The outputs of both the frequency tracker and the spectrum analyzer were recorded on magnetic tape for further data processing.

2.7 THE LASER TEST VAN

The LDV system was incorporated into Raytheon's laser test van. This van is a specially modified 12 meter trailer from the Fruehauf Corporation. Some of its features are listed below.

a. An air conditioning system capable of handling all electrical power dissipation with three men in the van, for outside air temperatures as high as 52°C.

b. A heating system capable of maintaining a 20°C internal van temperature at an outside air temperature as low as -18°C.

c. Full thermal wall and floor insulation.

d. Full fluorescent lighting fixtures.

e. Ample 60 and 400 Hz power outlets in van walls.

f. Three large 0.9 m square windows (one in rear, one each side) for transmitting the laser beam.

g. Four heavy truck jacks (with sand shoes) were provided for maximum stabilization of the van when on site.

h. A 1300 kg capacity hydraulic lift platform was installed at one of the side doors for heavy equipment loading.

A 25 kW, 60 cycle generator was used to power the van. The generator was gasoline powered. Two views of the van are shown in Figure 2-8 and 2-9.

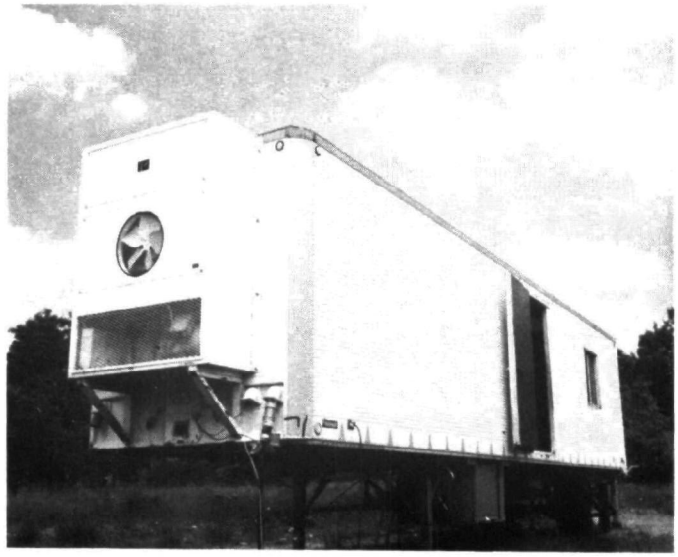

Figure 2-8. Raytheon Trailer.

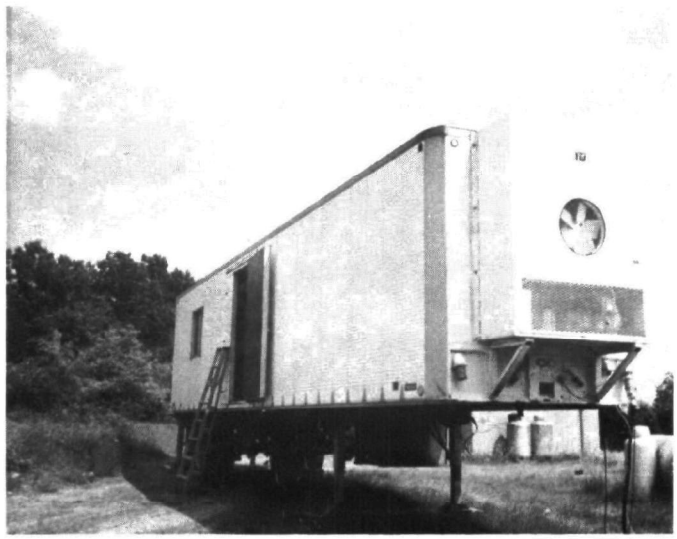

Figure 2-9. Raytheon Trailer.

SECTION 3

RESULTS OF THE FIRST FIELD TESTS

3.0 INTRODUCTION

The first phase of field testing a LDV system for the remote detection of effluents from smoke stacks was completed during the week of 23 - 31 August 1974. A CO_2 Laser Doppler Velocimeter was assembled in a 12 meter semi-trailer and taken to the River Bend Steam Station of Duke Power Company in Mount Holly, North Carolina. A photograph of the test site is shown in Figure 3-1.

After assembly and calibration of the LDV system at the Duke Power Test Site, backscatter signals representing the velocity distribution of the effluents from the smoke stacks were detected and recorded. All data was taken at a slant range of 400 m as measured by a laser range finder. The elevation angle to the stack lip was measured with a transit and found to be 8^{o} from the horizontal. Under these conditions, the effluent exit velocity is related to the doppler IF frequency by the equation:

$$v(m/sec) = 3.81 \times 10^{-3} \quad \Delta\nu_D(Hz) \qquad (3\text{-}1)$$

Measurements of effluent exit velocities were made under a variety of operating conditions including: (1) various power plant load conditions from 80 MW to 140 MW to vary the output velocity and (2) various precipitator operating conditions to vary the effluent opacity. Velocity profiles across the stack lip and at various heights above the stack were made. In all approximately 5,500 meters of taped data were obtained for later processing.

The primary direction of the program during the first field tests was to show the feasibility for remote effluent velocity measurements. Hence, the reduction of the data was directed primarily toward the determination of the mean effluent velocity from the power plant smoke stacks. Most of the data were collected from the EPA instrumented smoke stack, which is the third stack from the

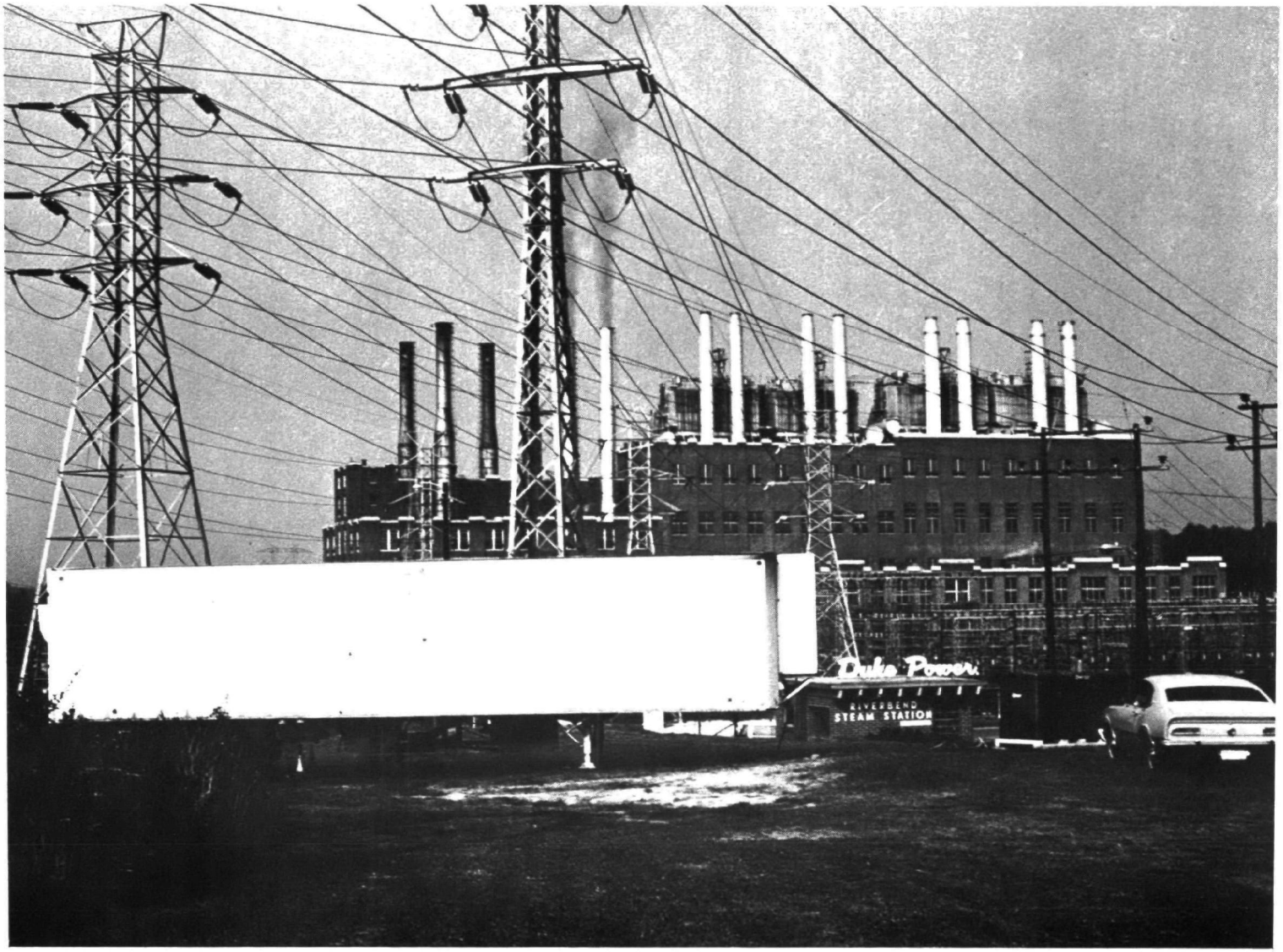

Figure 3-1. The Raytheon Data Van at the Duke Power River Bend Steam Station.

right as seen in Figure 3-1. At Duke Power, this stack is commonly referred to as the number six smoke stack. The EPA contracted with Environmental Science and Engineering, Inc. to perform in-stack pitot-tube velocity measurements at the same time as the remote LDV velocity measurements were being made. The in-stack monitoring was done through sampling ports located about 1.6m above the base of the smoke stack as shown in Figure 3-2. The in-stack monitoring also included the measurement of particle size distributions and mass emission rates.

The constriction of the smoke stack at the top from 2.94 m to 1.96 m caused an increase in velocity. The gas velocity measured at the base had to be multiplied by a factor of 2.32 in order to obtain an estimate of the exit velocity. The use of such a factor assumed that there is no significant cooling or compression of the exhaust gases between the sampling ports and the stack exit.

3.1 PROCESSING METHODS

The recorded data was reduced in basically two different manners. In one procedure the recorded spectrum analyzer traces were played back into a 564 Tektronix storage oscilloscope. Thirty-eight sequential traces were photographed in one composite photograph (a 2 second exposure). Typically, three or four composite photographs were taken at each stack profile position. During CW runs between 9 and 16 composite pictures were used to determine the average effluent velocities. A typical composite photograph is shown in Figure 3-3a.

In order to justify the above procedure as an accurate processing method, a one minute interval of data was evaluated. Thirty 2 second composite photographs were taken at 2 second intervals. These photographs were used to determine the mean velocity and the velocity distribution width of the smoke stack effluents. A data interval from Tape #6 on 29 August 1974 was used in these measurements. The thirty, 2 second composite photographs indicated a mean effluent velocity of 50.9 $\pm$ 3.0 m/sec, where the $\pm$ 3.0 m/sec factor represents the standard deviation in velocity from the thirty

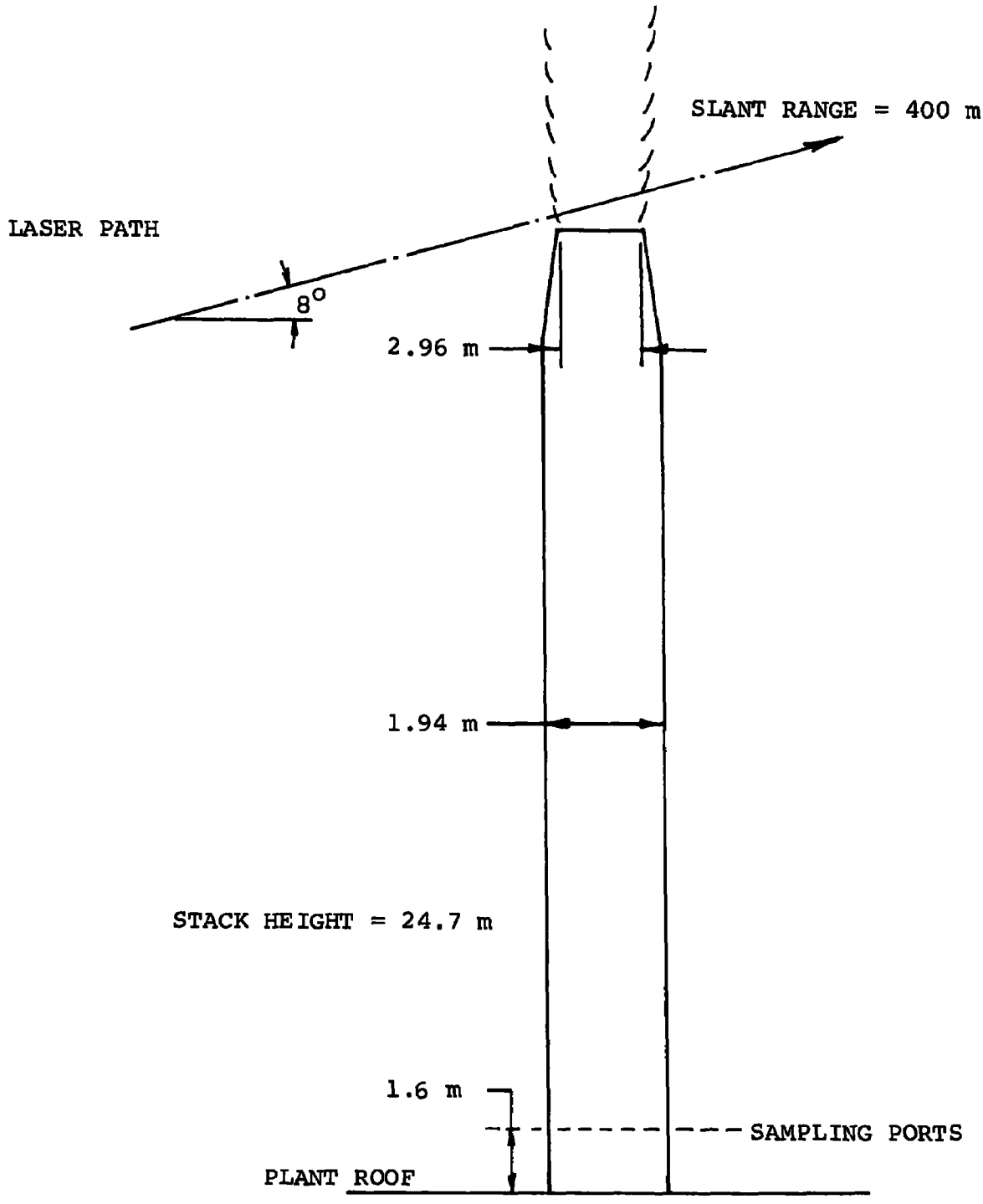

Figure 3-2. Smoke Stack Geometry for LDV Effluent Velocity Measurements.

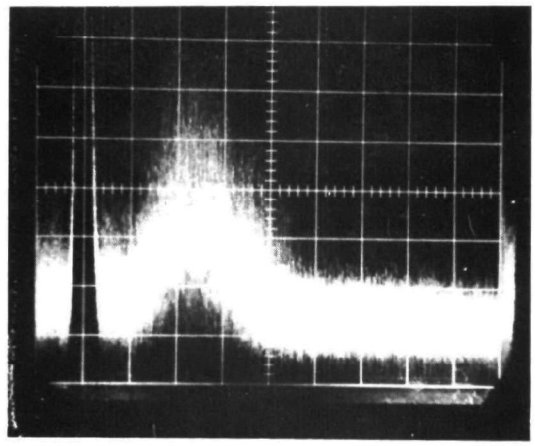

Figure 3-3a. Typical Composite Photograph of 2 Second Average Spectrum Analyzer Signals.

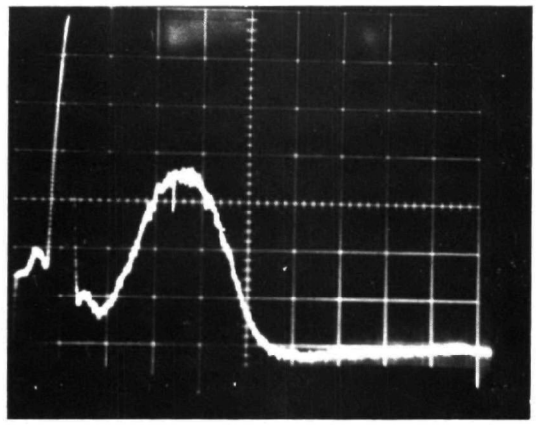

Figure 3-3b. Typical Photograph of 7 Second Average Spectrum Analyzer Signals.

photographs. Similarly, the average -3 dB velocity width of the effluents was 53.0 $\pm$ 5.8 m/sec. Since the standard deviations are less than 11% of the average values of both the velocity and velocity width, the process of using randomly spaced 2 second composite photographs to estimate effluent velocity parameters appears justified.

Another procedure utilized a signal averager. The recorded vertical output of the spectrum analyzer was played back into the signal averager. During CW runs 512 sweeps were averaged over a 28 second period and were photographed at 30 second intervals. A typical photograph of the averaged signal is shown in Figure 3-3b. These photographs were then analyzed to determine the mean effluent velocity as a function of time. To determine the velocity profile across the top of the smoke stack, 128 sweeps were averaged over a 7 second period and photographed at approximately 10 second intervals. Typically, five or six photographs were obtained at each profile position. The results from these photographs were averaged to determine a mean effluent velocity for each profile position.

Efforts were also made to utilize the frequency tracker as a data processor. Strip charts of effluent velocity as a function of time were made for most of the CW data runs. However, the tracker was meant to be used against signals which were considerably narrower than those generated by the smoke stack effluents. As a consequence, the tracker performance was questionable, particularly in the presense of widely varying signal amplitudes. Hence the frequency tracker data are suspect and are not presented in this report.

Frequency calibrations were made by introducing a 3.0 MHz frequency standard into the spectrum analyzer at the beginning of each data run.

3.2 EXPERIMENTAL RESULTS

Seven tapes of data were recorded on 28 and 29 August 1974. Six of these tapes contained reducible data and are discussed in detail below. A summary of the taped data is given in Table 1.

Table 3-1

Summary of Data Tapes

TAPE	RUN	TIME	DATE	SUBJECT	PROCESSING
1	1	10:00	08/28/74	CW Run - 2nd stack from right	None - tape not reduced - calibration questionable
2	1	14:30	08/28/74	CW Run - 0.3 m above #6 stack *	2 second composite photographs 28 sec, 512 sweep average
2	2	16:10	08/28/74	Velocity profile - 0.3 m above #6 stack	2 second composite photographs 7 sec, 128 sweep average
3	1	22:00	08/28/74	Power reduction directly above #6 stack - 140 MW-100MW power level	2 second composite photographs 7 sec, 128 sweep average
4	1&2	12:17	08/29/74	CW Run - directly above #6 stack	2 second composite photographs 28 sec, 512 sweep average
5	1	14:05	08/29/74	CW Run - directly above #6 stack	2 second composite photographs 28 sec, 512 sweep average
6	1	14:50	08/29/74	CW Run - directly above #6 stack	2 second composite photographs 28 sec, 512 sweep average
6	2	15:05	08/29/74	Velocity profile directly above #6 stack	2 second composite photographs 7 sec, 128 sweep average
7	1	15:59	08/29/74	Velocity profile - 1.8 m above #6 stack	2 second composite photographs 7 sec, 128 sweep average
7	2	16:43	08/29/74	Velocity profile directly above #6 stack	2 second composite photographs 7 sec, 128 sweep average

* Stacks on the main building are numbered from 1 to 8 from left to right as seen in Figure 3-1.

3.2.1 TAPE #1, RUN #1

Tape #1, Run #1 was recorded between 10:00 and 10:30 on 28 August 1974. The laser beam was positioned just above the center of the second stack from the right. Efforts were made to record backscatter signals during the period when the precipitators were being turned off. Due to coordination difficulties the time when the precipitators were off was not recorded. Nor was a good calibration obtained. The data on this tape was therefore suspect and was not reduced.

3.2.2 TAPE #2, RUN #1

Tape #2, Run #1 was recorded between 14:30 and 14:45 on 28 August 1974. The laser beam was positioned approximately 0.3 m above the center of the number six smoke stack. The laser beam was not moved during the run. The power load during this run was constant at 140 MW.

The data from this run were reduced by means of 2 second duration composite photographs. The mean effluent velocity measured by averaging 11 composite photographs was 50.0 $\pm$ 4.3 m/sec. The $\pm$ 4.3 m/sec margin represents the standard deviation in mean velocity from the photographs.

The data were also reduced by averaging 512 spectrum analyzer sweeps over a 28 second period and photographing the results at 30 second intervals. The results of this method of analysis is plotted as a function of time in Figure 3-4. The mean effluent velocity measured in this manner was 46.9 $\pm$ 2.4 m/sec for the time period 14:30 to 14:45 on 28 August 1974.

The velocity distribution of the effluents venting from the smoke stack was very broad. The averaged spectrum analyzer data indicated a 73.2 $\pm$ 5.8 m/sec velocity spread between the -3 dB distribution points.

3.2.3 TAPE #2, RUN #2

Tape #2, Run #2 was recorded between 16:10 and 16:30 on

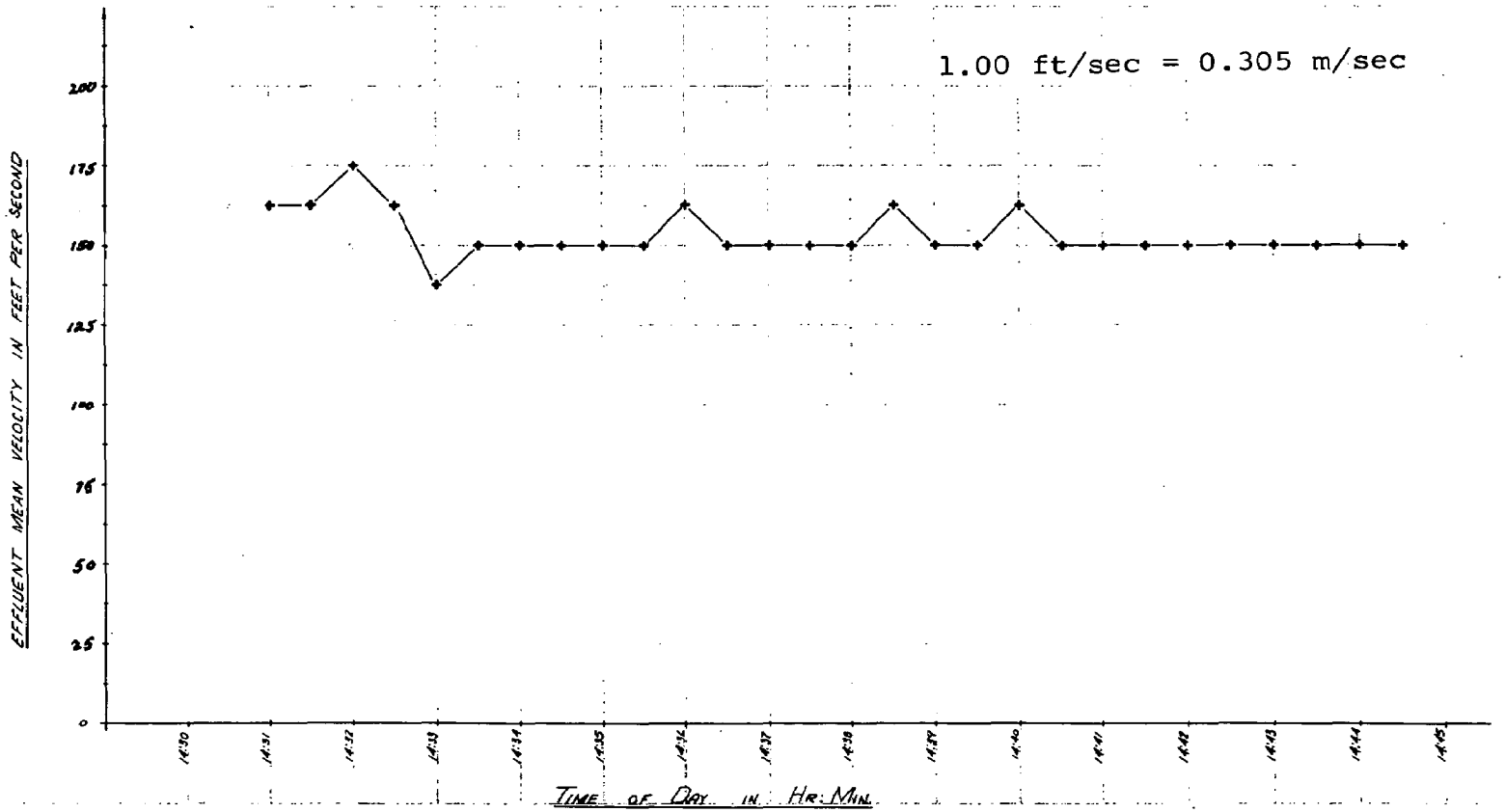

Figure 3-4. Tape #2 Run #1
Duke Power
28 August 1974
0.3 m Above Stack

28 Second Average

28 August 1974. The laser beam was positioned approximately 0.3 m above the number six smoke stack. The laser beam was scanned at approximately 23 cm spacings across the top of the stack. Approximately 1 minute of data were collected at each profile position. The power load during this run was constant at 140 MW.

The data from this run were reduced by means of 2 second composite photographs. Approximately 4 photographs were taken at each profile position. The velocity profile evaluated from 2 second composite photographs is shown in Figure 3-5.

The data were also reduced by averaging 128 spectrum analyzer sweeps over a 7 second period and photographing the results at approximately 10 second intervals. The profile determined from this method of analysis is shown in Figure 3-6.

A comparison of the profiles made in the two different processing methods is shown in Figure 3-7. In general, the two profiles are similar. The profile made with 2 second composite photographs indicated slightly higher effluent velocities.

3.2.4 TAPE #3, RUN #1

Tape #3, Run #1 was recorded between 22:00 and 22:41 on 29 August 1974. The laser beam was positioned above the center of the number six smoke stack. The laser beam was not moved during the run. The power load during this run was reduced from 140 MW to 80 MW. Unfortunately the data run was terminated by a tape recorder failure when the power load was at 100 MW.

The data from this run were reduced by means of 2 second duration composite photographs. The mean effluent velocity during various power load conditions was determined by averaging between 5 and 7 composite photographs. The results are plotted as a function of power load conditions in Figure 3-8.

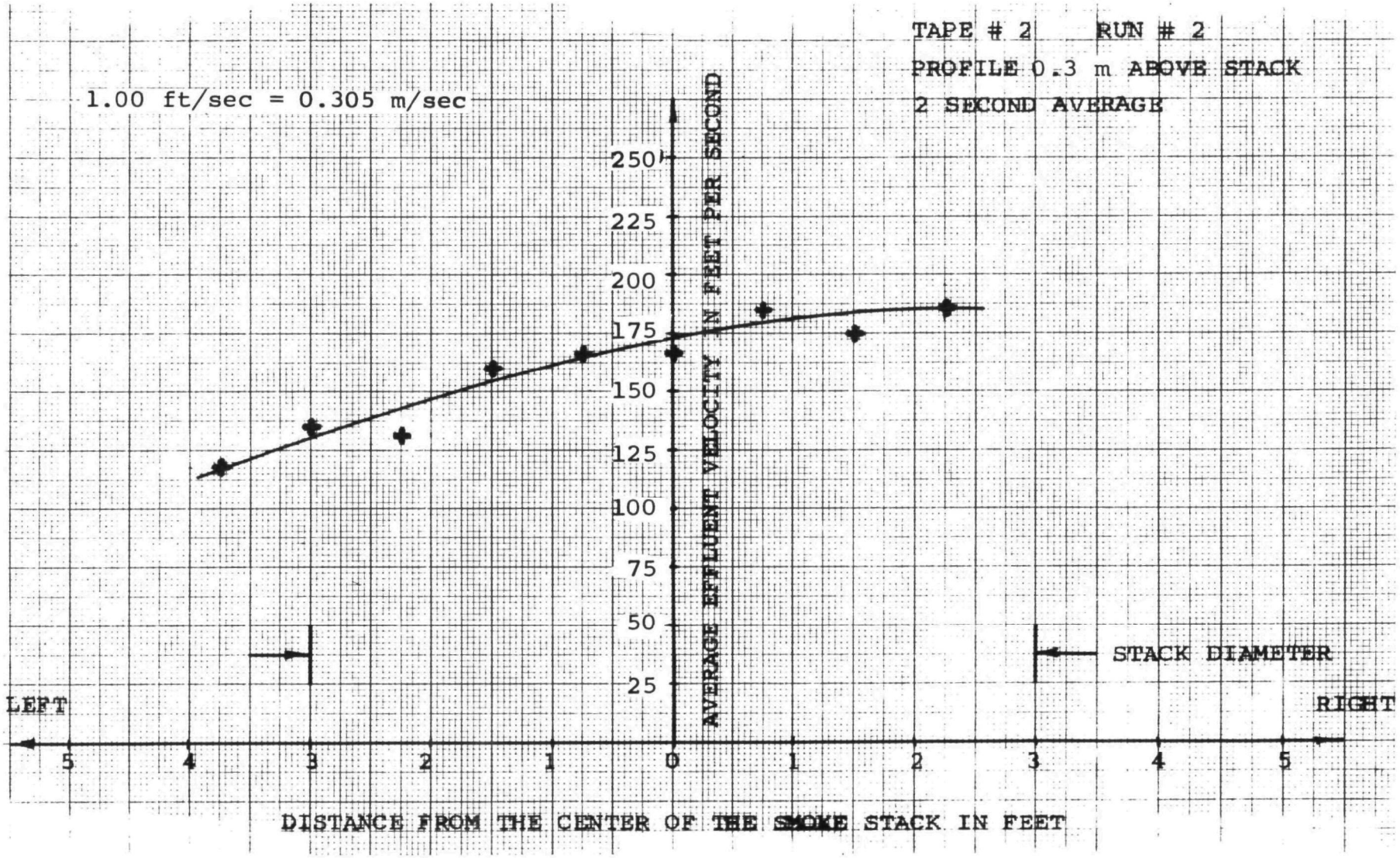

Figure 3-5. The Average Velocity of Effluents from a Smoke Stack as a Function of the Distance from the Center of the Stack

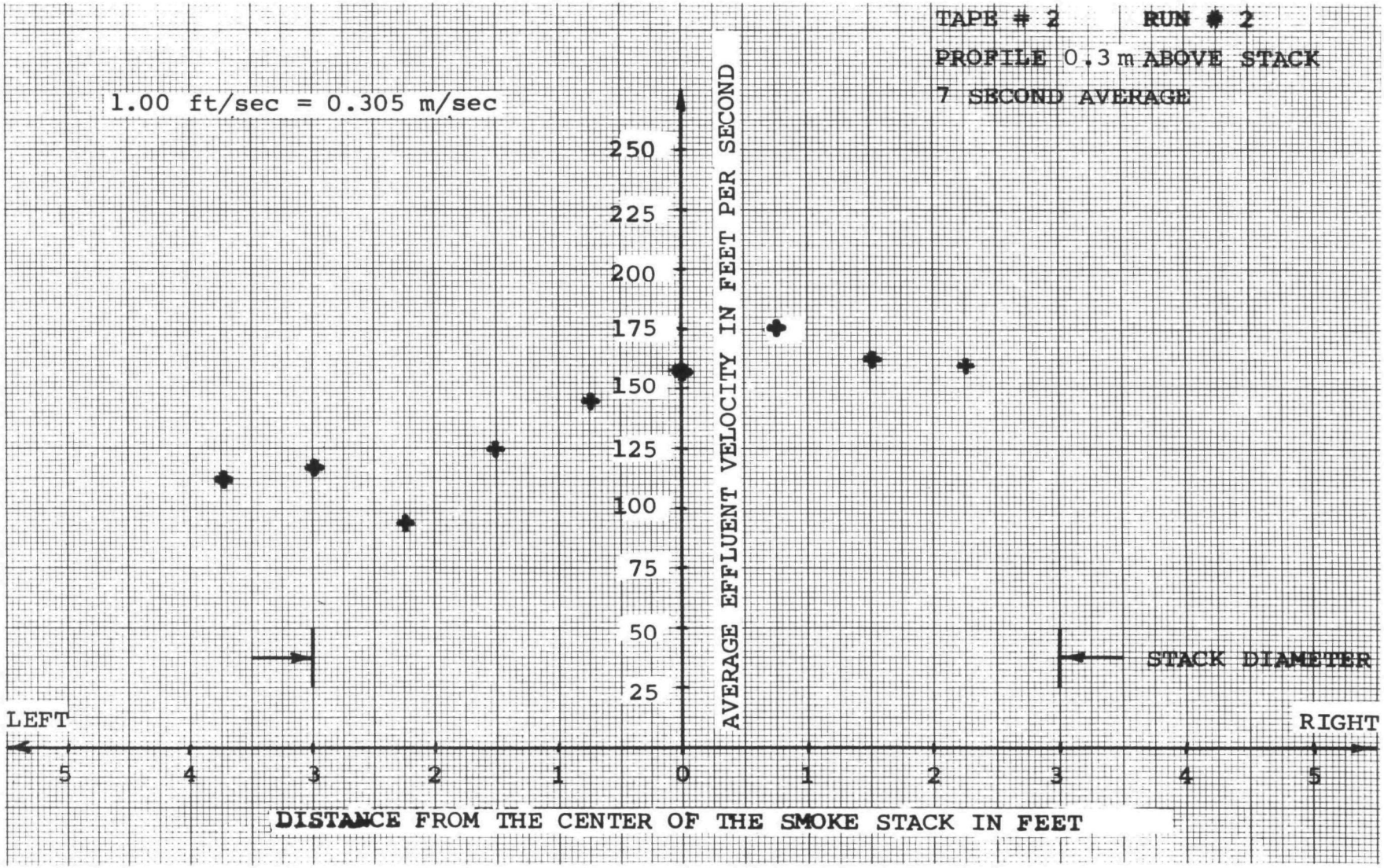

Figure 3-6. The Average Velocity of Effluents from a Smoke Stack as a Function of the Distance from the Center of the Stack

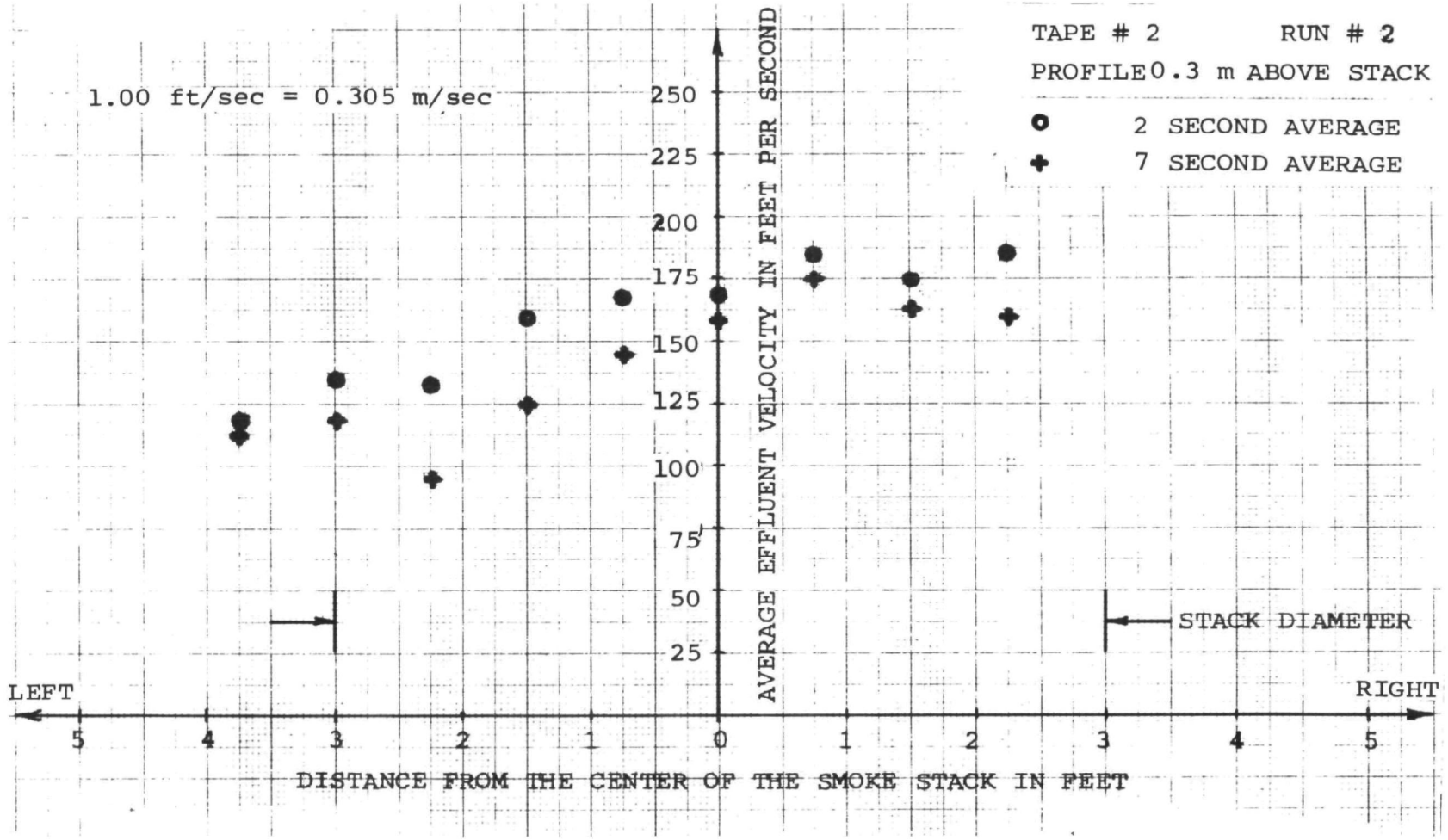

Figure 3-7. A Comparison of the 2 Second and 7 Second Average Effluent Velocity Profile Data

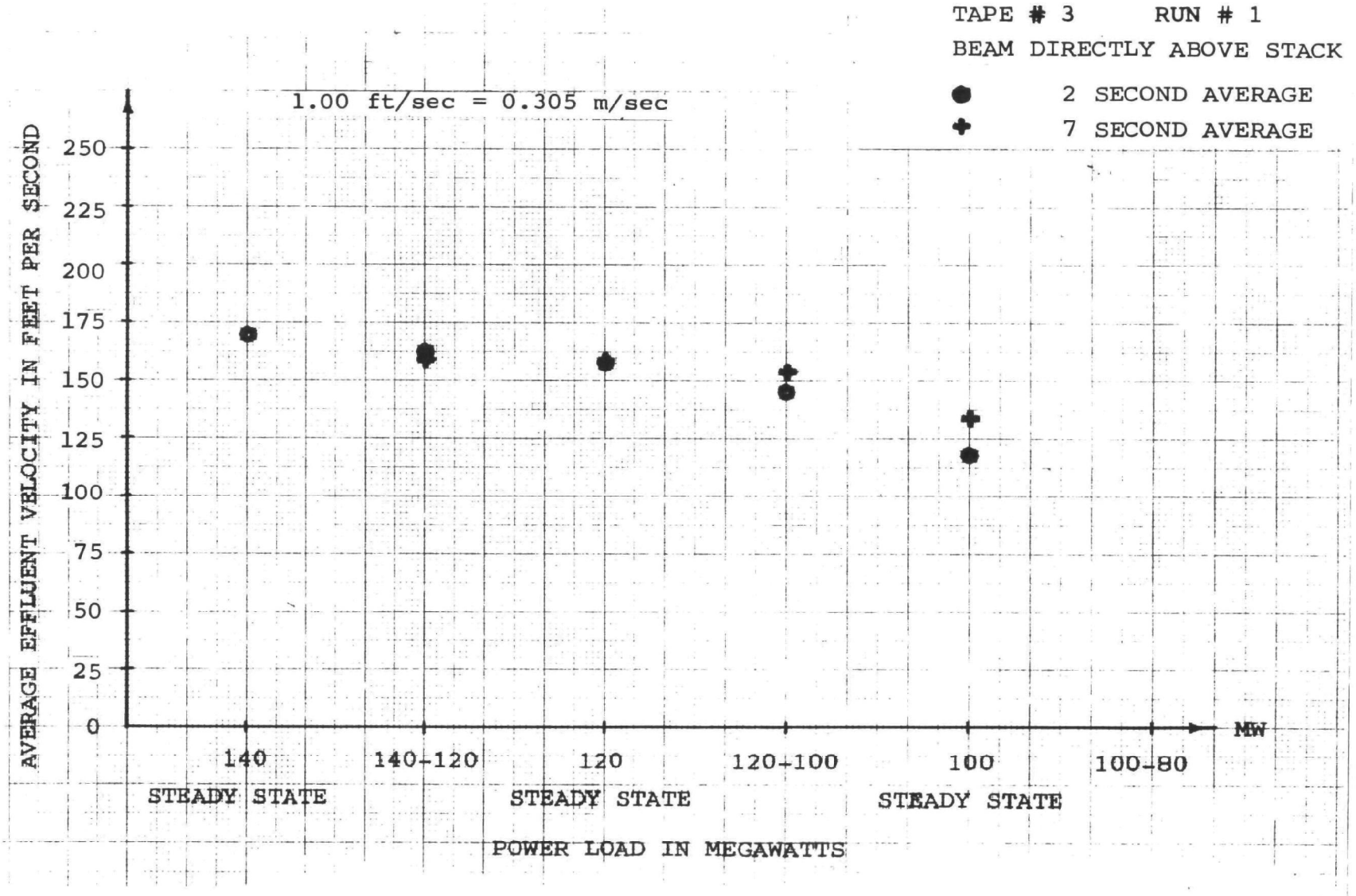

Figure 3-8. Comparison of the 2 Second and 7 Second Averaged Velocity Data for the Power Load Reduction

The data were also reduced by averaging 128 spectrum analyzer sweeps over a 7 second period and photographing the results every 30 seconds. The results of this method of analysis are plotted as a function of time in Figure 3-9. The mean velocity for each power load condition was evaluated by averaging the results of the 7 second average photographs. The results are plotted in Figure 3-8 as a comparison to the 2 second composite photographic data.

3.2.5 TAPE #4, RUNS #1&2

Tape #4, Runs #1&2 was recorded between 12:37 and 12:40 on 29 August 1974. The laser beam was positioned directly above the center of the number six smoke stack. The laser beam was not moved during the run.

The data from this run were reduced by means of 2 second duration composite photographs. The mean effluent velocity measured by averaging 16 composite photographs was 46.9 $\pm$ 7.9 m/sec. The $\pm$ 7.9 m/sec margin represents the standard deviation in velocity from the photographs.

The data were also reduced by averaging 512 spectrum analyzer sweeps over a 28 second period and photographing the results at 30 second intervals. The results of this method of analysis are plotted as a function of time in Figure 3-10. The mean effluent velocity measured in this manner was 54.9 $\pm$ 4.3 m/sec for the time period 12:17 to 12:40 on 29 August 1974.

The velocity distribution of the effluents venting from the smoke stack was very broad. The averaged spectrum analyzer data indicated a 76.2 $\pm$ 6.4 m/sec velocity spread between the -3 dB distribution points.

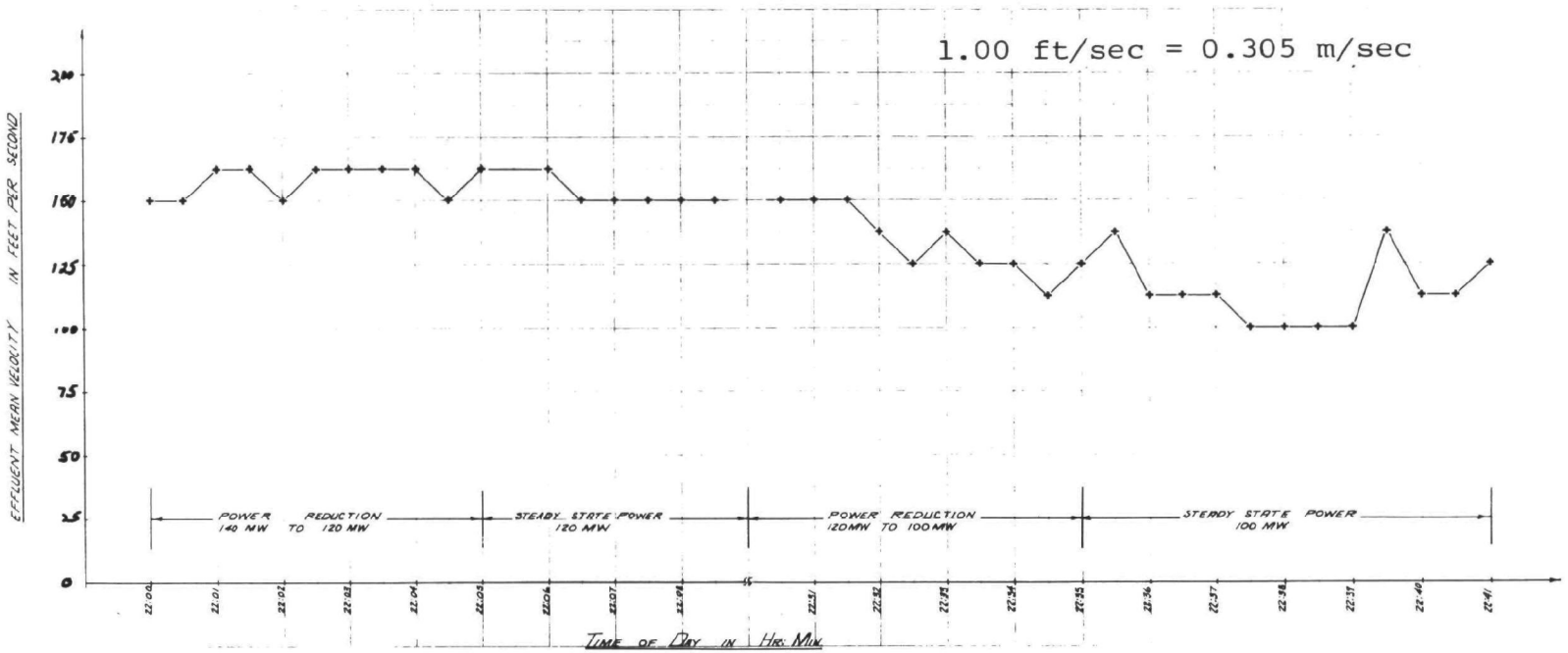

Figure 3-9. Tape #3 Run #1
Duke Power
28 August 1974
Power Reduction

28 Second Average

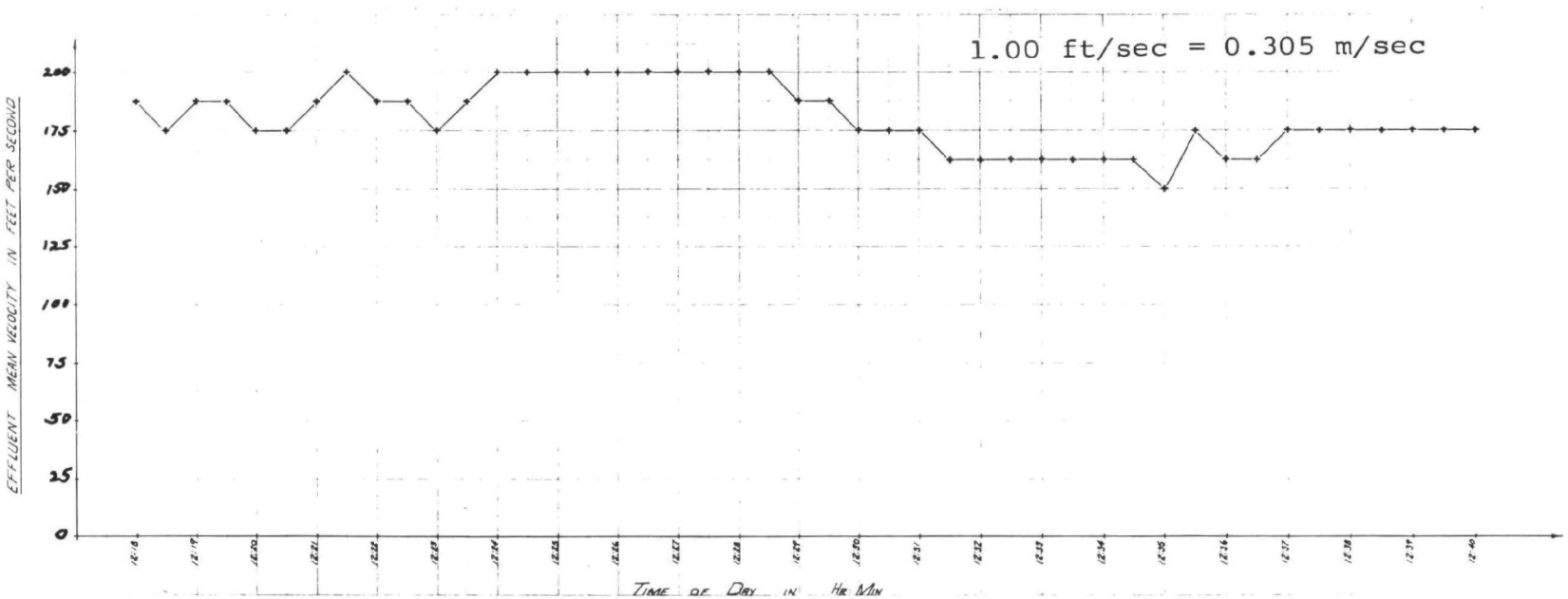

Figure 3-10. Tape #4 Run #1 & 2
Duke Power
29 August 1974
Directly Above Stack

28 Second Average

3.2.6 TAPE #5, RUN #1

Tape #5, Run #1 was recorded between 14:05 and 14:27 on 29 August 1974. The laser beam was positioned directly above the center of the number six smoke stack. The laser beam was not moved during the run.

The data were reduced by averaging 512 spectrum analyzer sweeps over a 28 second period and photographing the results at 30 second intervals. The results of this method of analysis are plotted as a function of time in Figure 3-11. The mean effluent velocity measured in this manner was 48.8 $\pm$ 8.8 m/sec for the time period 14:05 to 14:27 on 29 August 1974.

The velocity distribution of the effluents venting from the smoke stack was very broad. The averaged spectrum analyzer data indicated a 66.4 $\pm$ 7.0 m/sec velocity spread between the -3 dB distribution points.

3.2.7 TAPE #6, RUN #1

Tape #6, Run #1 was recorded between 14:50 and 14:55 on 29 August 1974. The laser beam was positioned directly above the center of the number six smoke stack. The laser beam was not moved during the run.

The data from this run were reduced by means of 2 second duration composite photographs. The mean effluent velocity measured by averaging 9 composite photographs was 53.6 $\pm$ 5.5 m/sec. The $\pm$ 5.5 m/sec margin represents the standard deviation in velocity from the photographs.

The data were also reduced by averaging 512 spectrum analyzer sweeps over a 28 second period and photographing the results at 30 second intervals. The results of this method of analysis are plotted as a function of time in Figure 3-12. The mean effluent

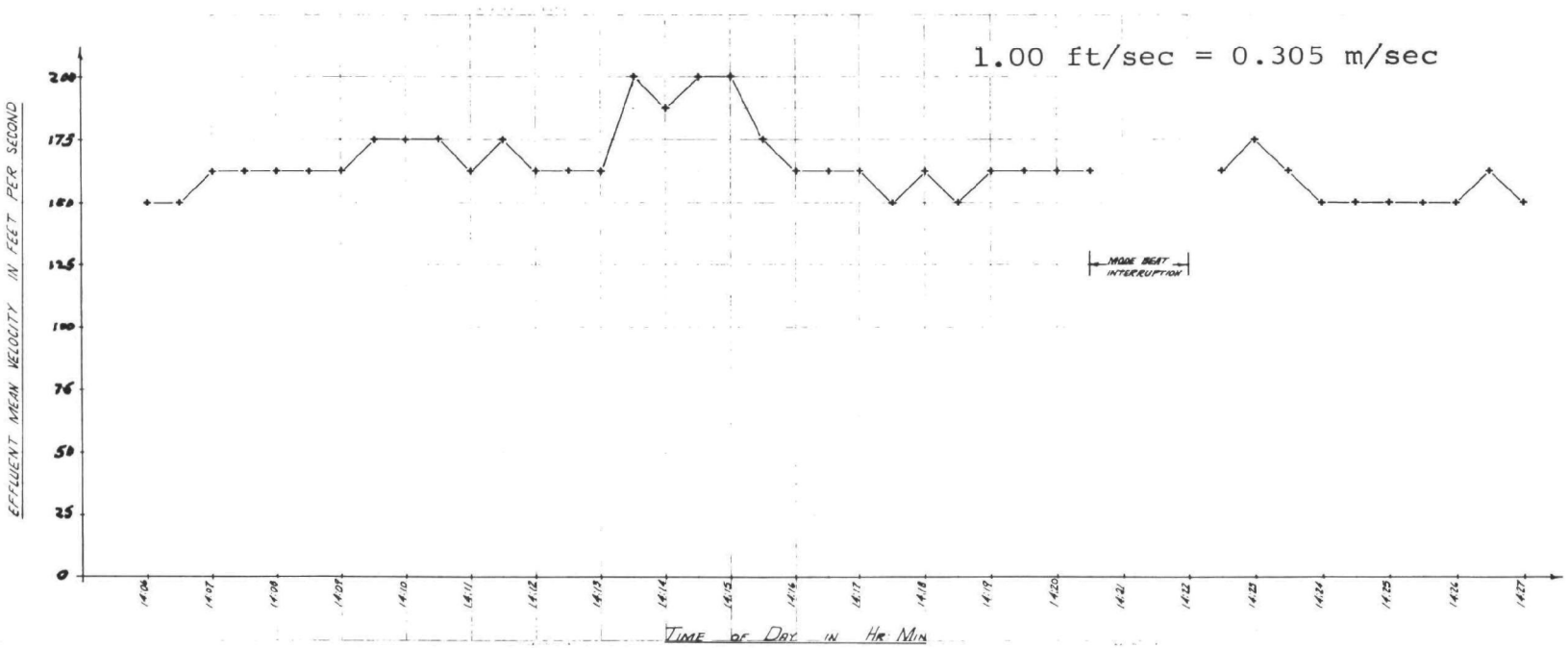

Figure 3-11. Tape #5 Run #1
Duke Power
29 August 1974
Directly Above Stack
28 Second Average

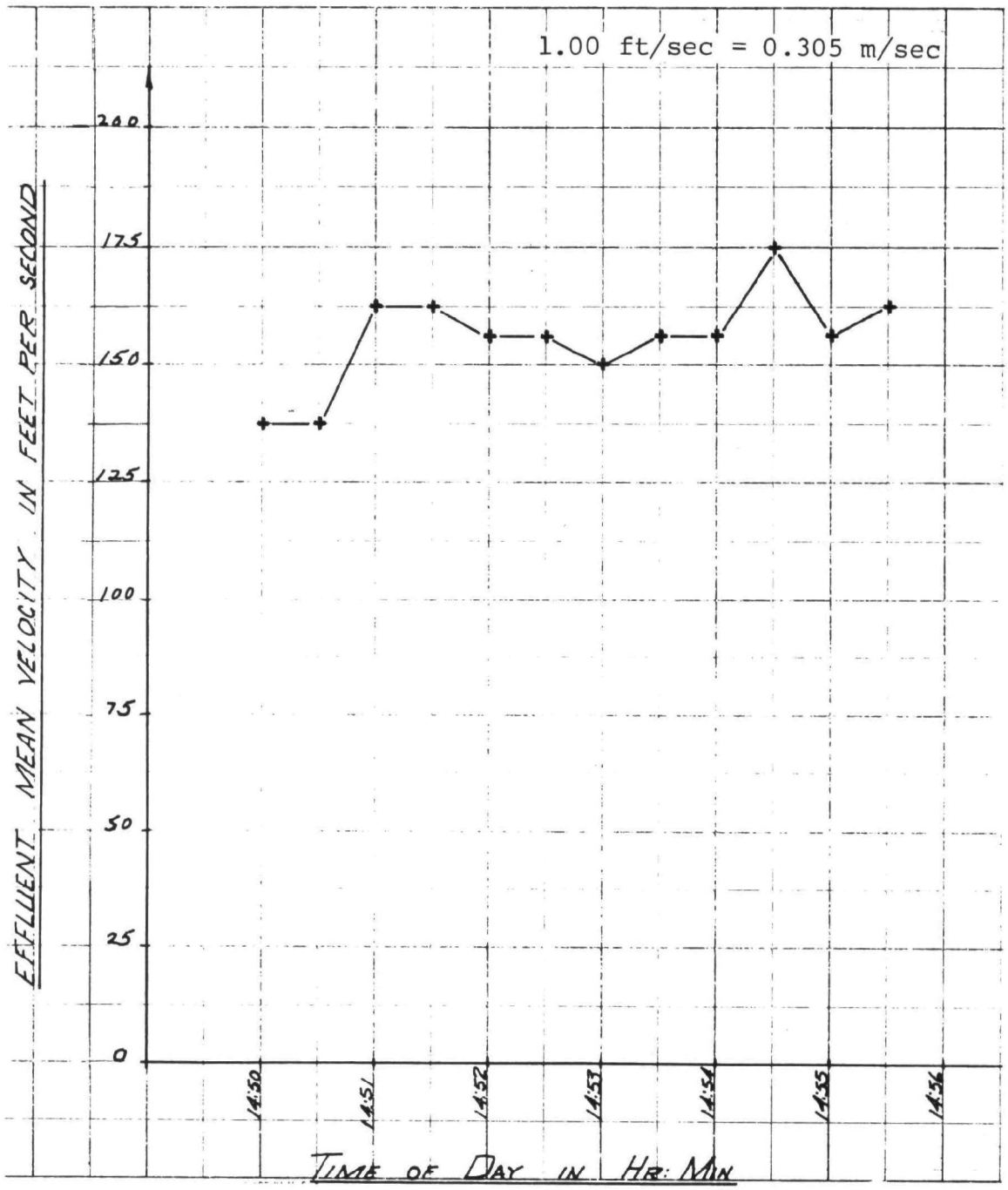

Figure 3-12. Tape #6 Run #1
Duke Power
29 August 1974
Directly Above Stack
28 Second Average

velocity measured in this manner was 47.5 ± 3.0 m/sec for the time period 14:50 to 14:55 on 29 August 1974.

The velocity distribution of the effluents venting from the smoke stack was very broad. The averaged spectrum analyzer data indicated a 85.6 ± 4.0 m/sec velocity spread between the -3 dB distribution points.

3.2.8 TAPE #6, RUN #2

Tape #6, Run #2 was recorded between 15:05 and 15:38 on 29 August 1974. The laser beam was positioned directly above the number six smoke stack. The laser beam was scanned at approximately 26 cm spacings across the top of the stack. Approximately 1 minute of data was collected at each profile position.

The data from this run were reduced by means of 2 second composite photographs. Approximately 4 photographs were taken at each profile position. The velocity profile evaluated from 2 second composite photographs is shown in Figure 3-13.

The data were also reduced by averaging 128 spectrum analyzer sweeps over a 7 second period and photographing the results at approximately 10 second intervals. The profile determined from this method of analysis is shown in Figure 3-14.

A comparison of the profiles made in the two different processing methods is shown in Figure 3-15. In general, the two profiles are quite similar.

3.2.9 TAPE #7, RUN #1

Tape #7, Run #1 was recorded between 15:59 and 16:27 on 29 August 1974. The laser beam was positioned approximately 1.8 m above the number six smoke stack. The laser beam was scanned at approximately 26 cm spacings across the top of the stack.

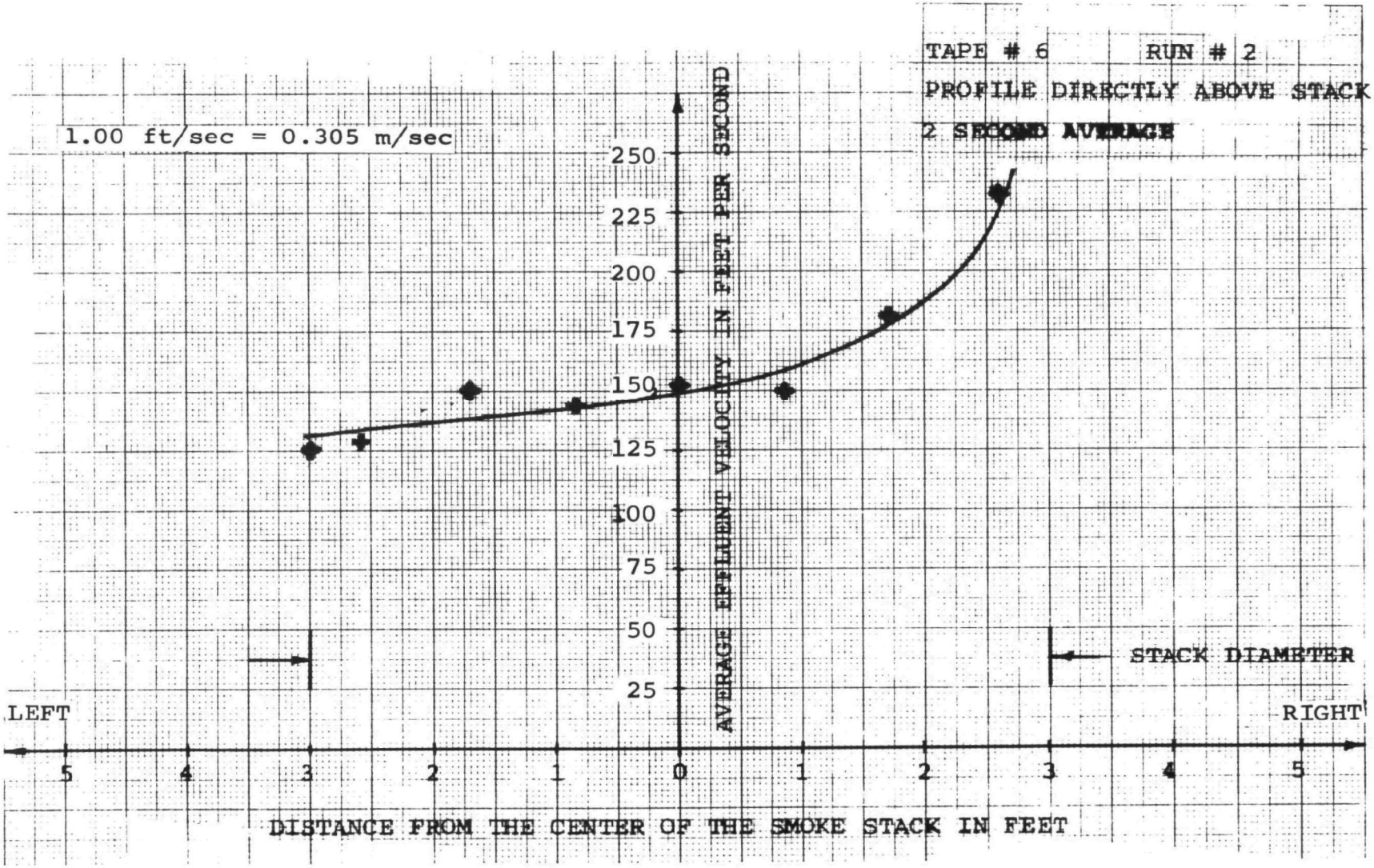

Figure 3-13. The Average Velocity of Effluents from a Smoke Stack as a Function of the Distance from the Center of the Stack

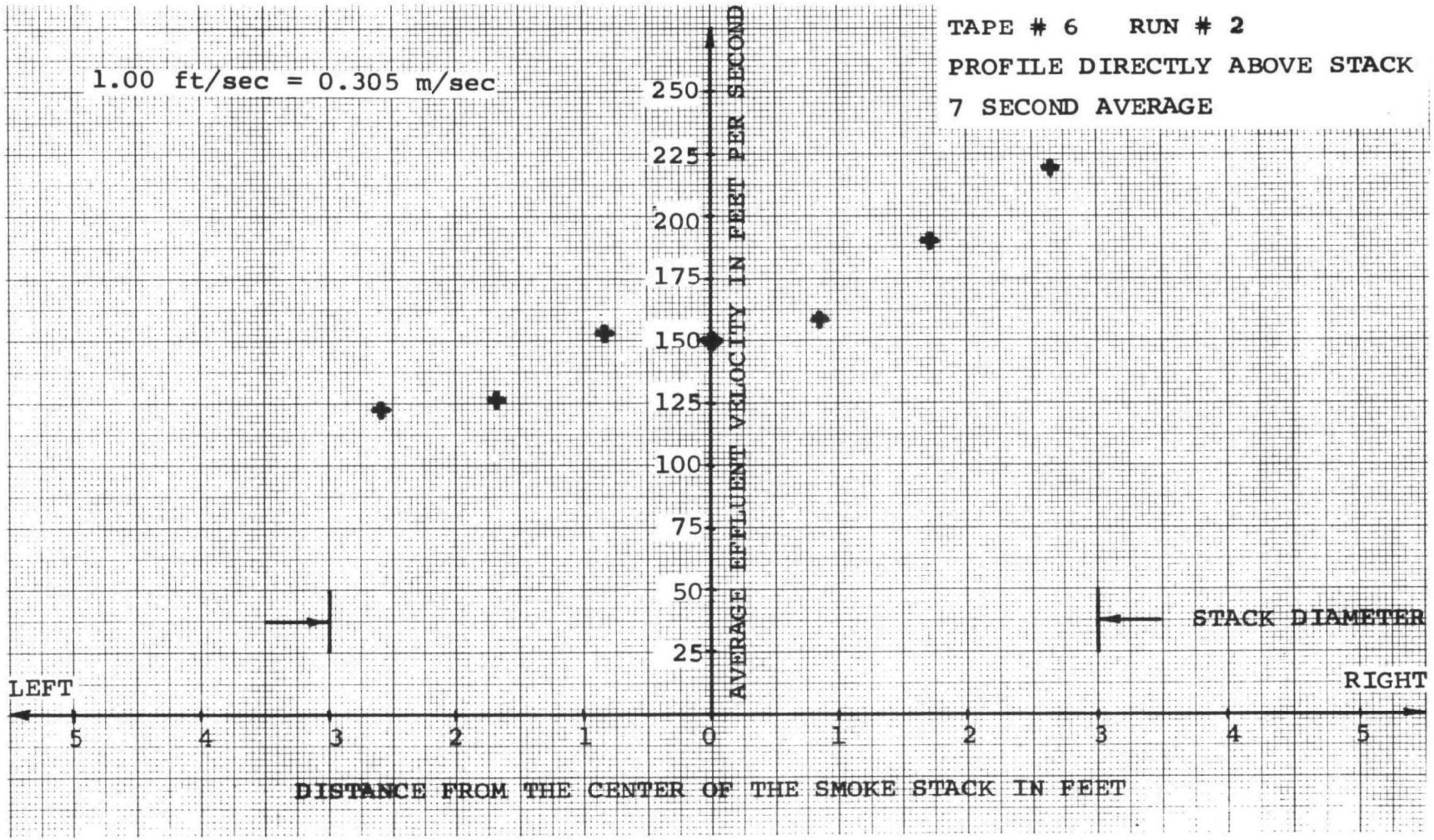

Figure 3-14. The Average Velocity of Effluents from a Smoke Stack as a Function of the Distance from the Center of the Stack

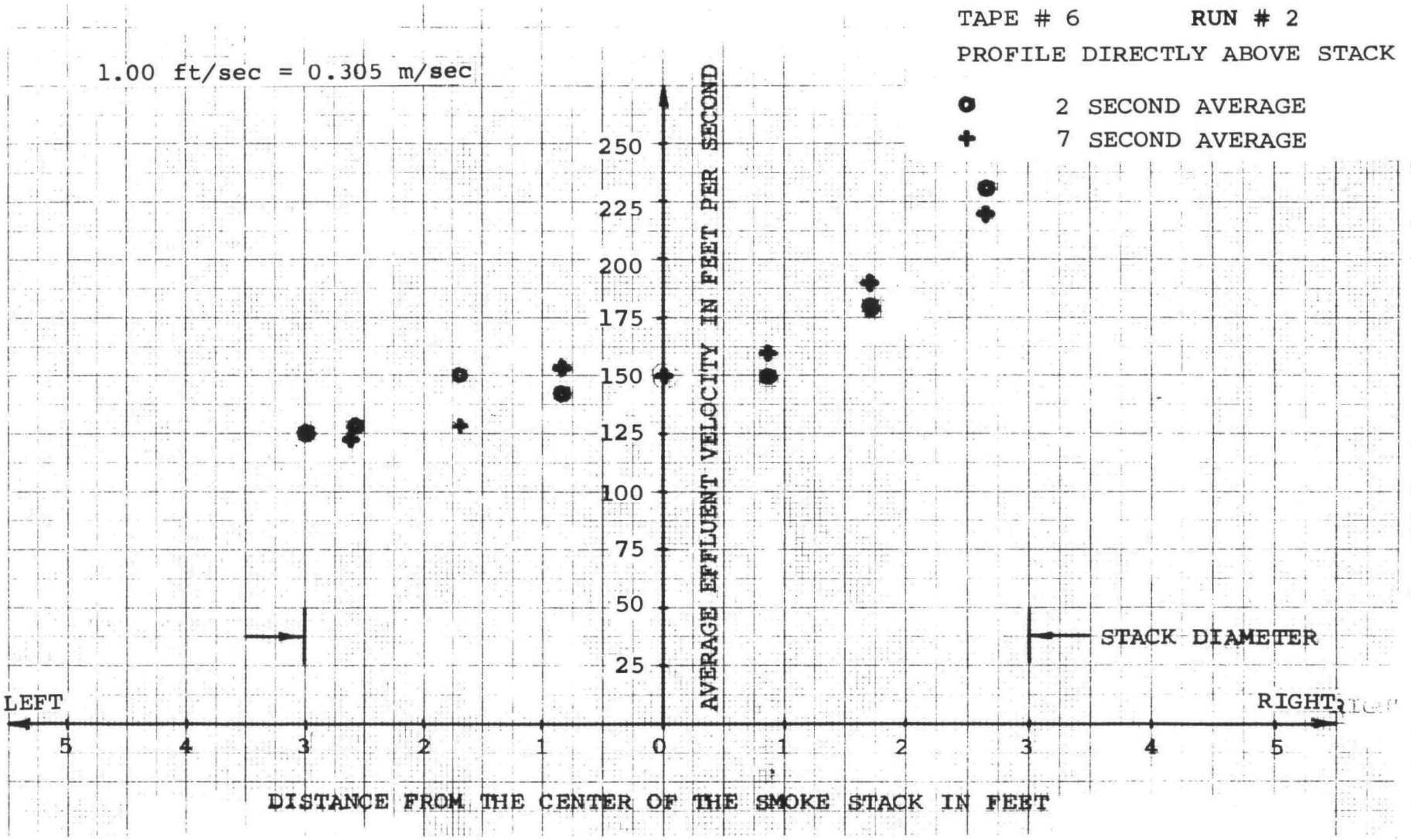

Figure 3-15. A Comparison of the 2 Second and 7 Second Average Effluent Velocity Profile Data

Approximately 1 minute of data was collected at each profile position.

The data from this run were reduced by means of 2 second composite photographs. Approximately 4 photographs were taken at each profile position. The velocity profile evaluated from 2 second composite photographs is shown in Figure 3-16.

The data were also reduced by averaging 128 spectrum analyzer sweeps over a 7 second period and photographing the results at approximately 10 second intervals. The profile determined from this method of analysis is shown in Figure 3-17.

A comparison of the profiles made in the two different processing methods is shown in Figure 3-18. In general, the two profiles are similar.

It is apparent that the turbulence which occurs in the mixing region above the smoke stack produces received signals with widely varying Doppler shifts. The resulting effluent velocity profile at 2.8 m above the stack lip was a distribution which is difficult to interpret. Clearly further experiments and analysis is required before these data can be interpreted accurately.

3.2.10. TAPE #7, RUN #2

Tape #7, Run #2 was recorded between 16:48 and 17:08 on 29 August 1974. The laser beam was positioned directly above the number six smoke stack. The laser beam was scanned at approximately 26 cm spacings across the top of the stack. Approximately 1 minute of data was collected at each profile position.

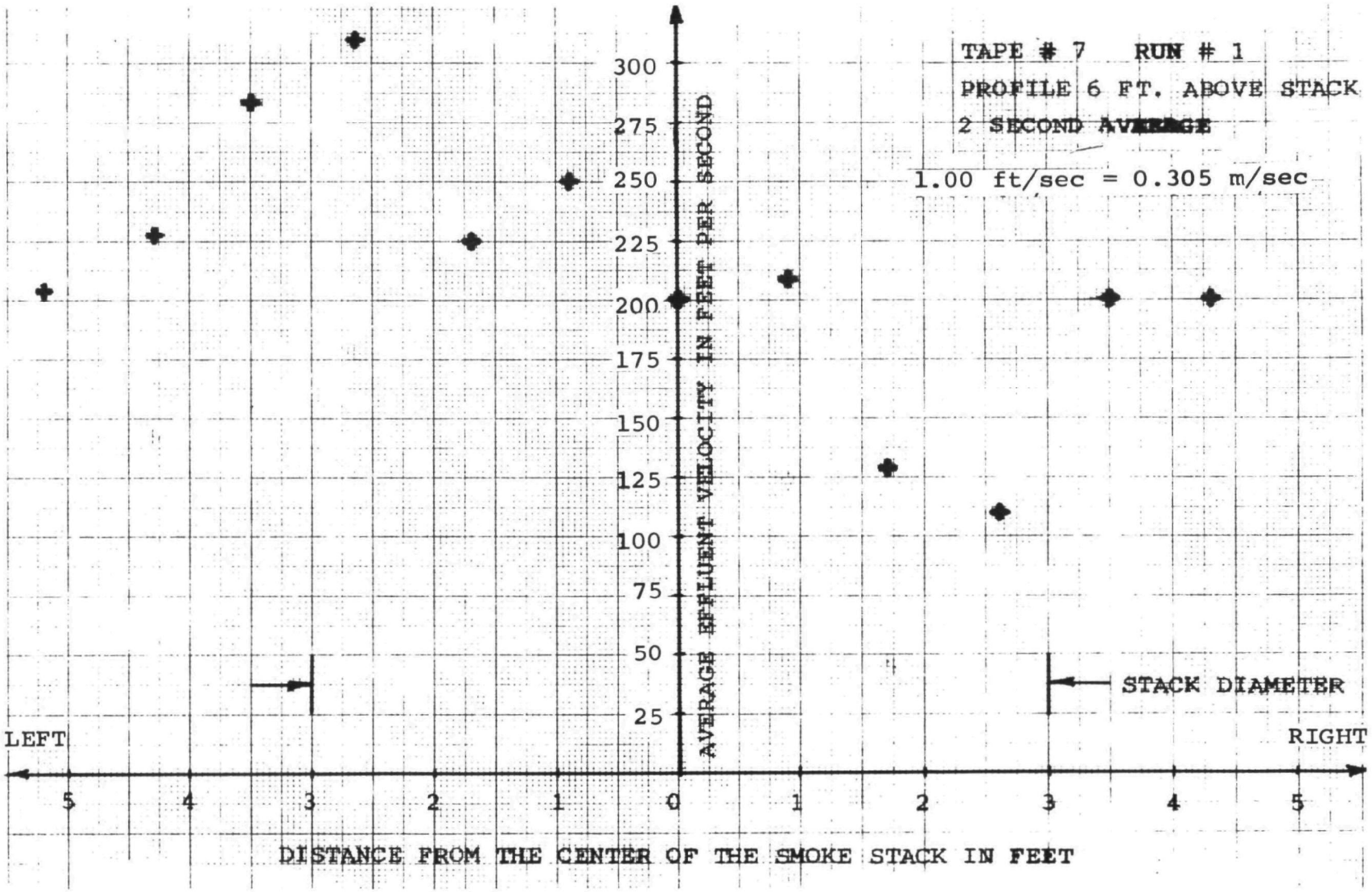

Figure 3-16. The Average Velocity of Effluents from a Smoke Stack as a Function of the Distance from the Center of the Stack

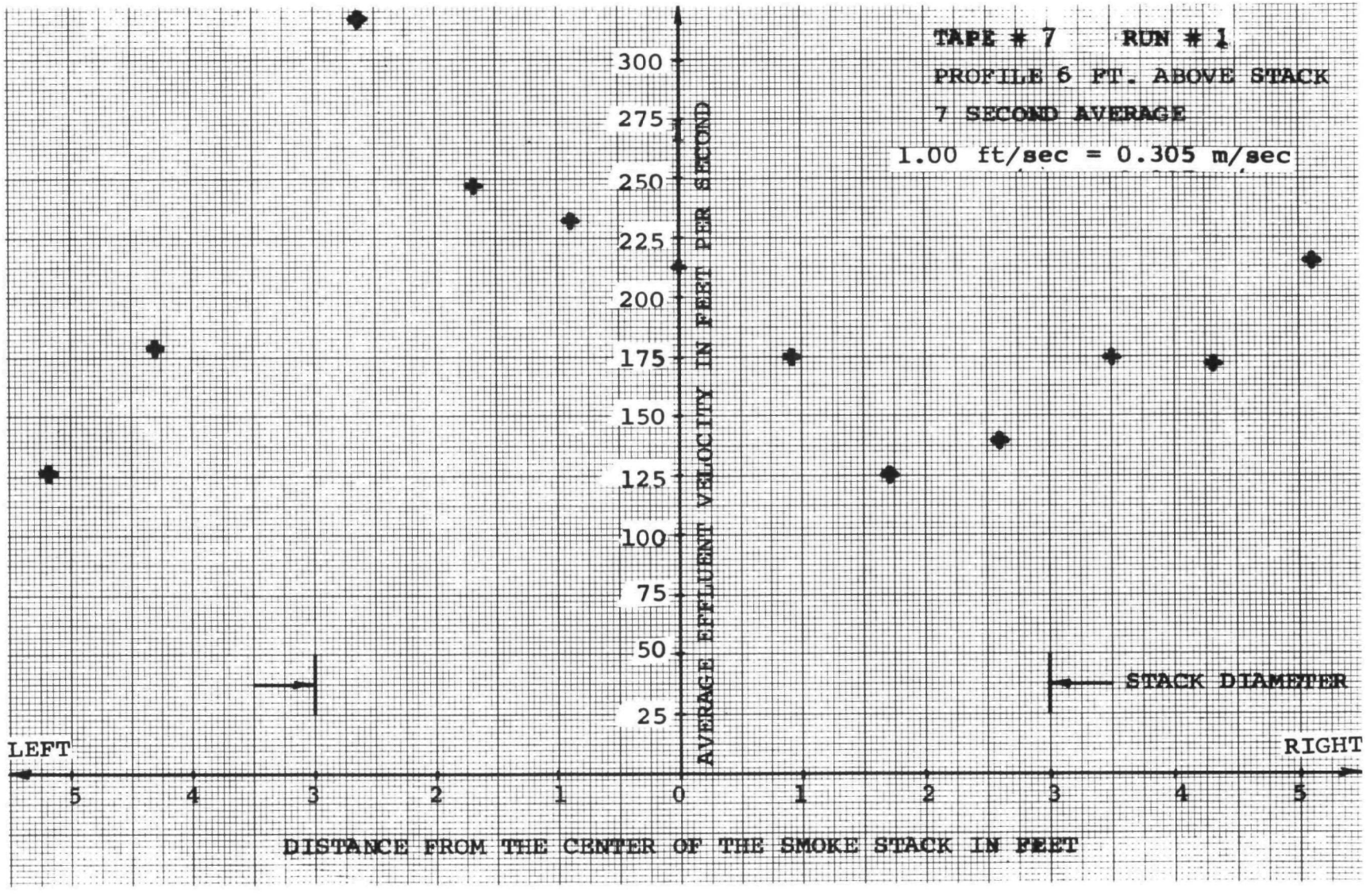

Figure 3-17. The Average Velocity of Effluents from a Smoke Stack as a Function of the Distance from the Center of the Stack

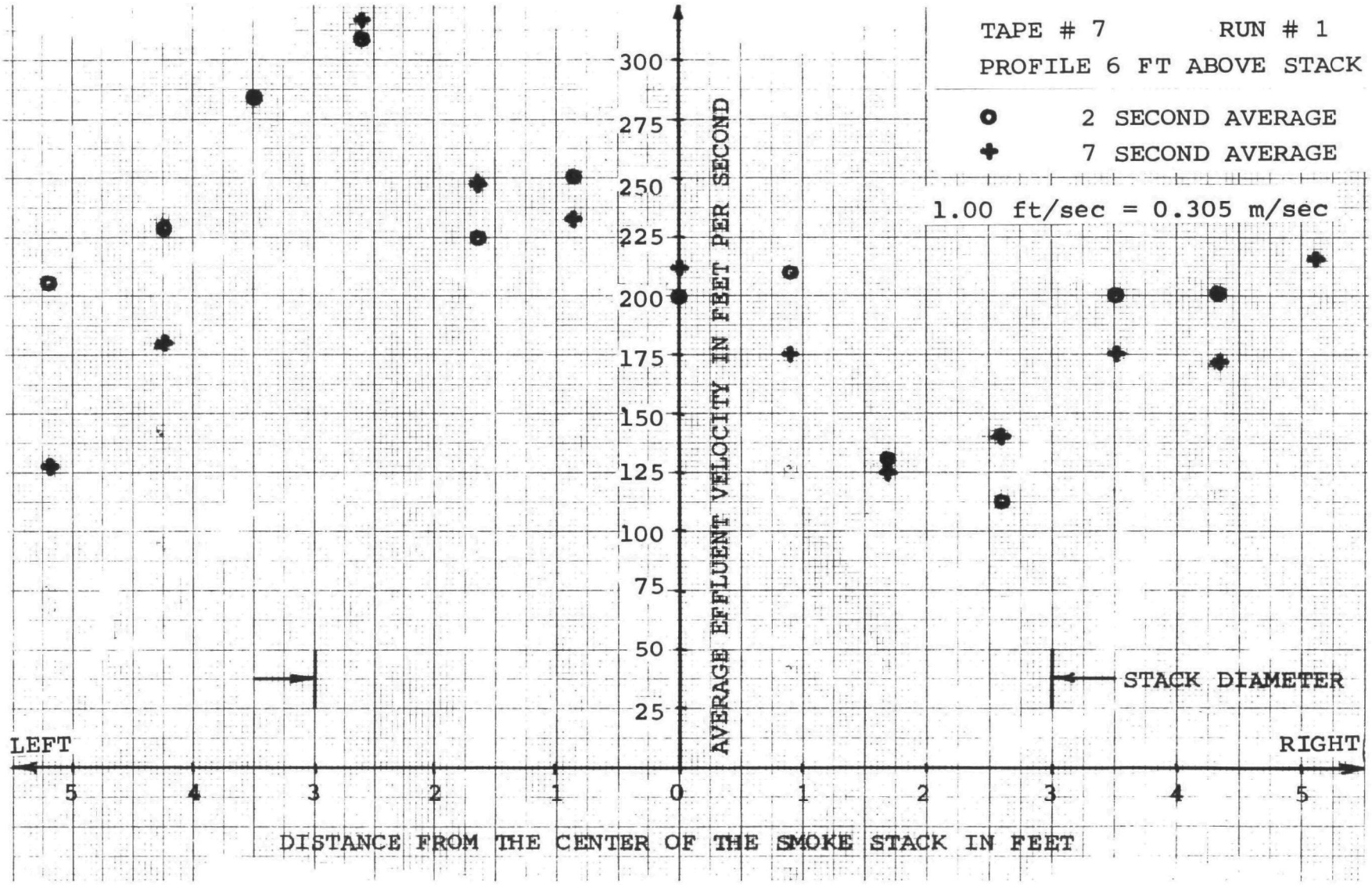

Figure 3-18. A Comparison of the 2 Second and 7 Second Average Effluent Velocity Profile Data

The data from this run were reduced by means of 2 second composite photographs. Approximately 4 photographs were taken at each profile position. The velocity profile evaluated from 2 second composite photographs is shown in Figure 3-19.

The data were also reduced by averaging 128 spectrum analyzer sweeps over a 7 second period and photographing the results at approximately 10 second intervals. The profile determined from this method of analysis is shown in Figure 3-20.

A comparison of the profiles made in the two different processing methods is shown in Figure 3-21. In general, the two profiles are similar. The profile made with 7 second averaged photographs indicates slightly higher effluent velocities.

3.3 CONCLUSIONS ON THE FIRST FIELD TESTS

At the end of the first set of field tests the feasibility of using a Laser Doppler Velocimeter to remotely monitor smoke stack effluents was clearly demonstrated. Comparisons of the in-stack pitot tube velocity data with the Doppler velocity data are shown in Table 3-2. The Doppler velocity data generally exceed the in-stack data by an average of 12%. It is not known whether this error is caused by the miscalibration of either the pitot tube or the LDV, or is the result of the two measurements being carried out at different points on the stack. A significant portion of the error appears to be systematic rather than random, and hence could be removed with more accurate calibration.

During the course of the measurements, it was obvious that changing the number of precipitators in operation did effect the LDV signal intensity. While precise measurements were not made, it appeared that the system SNR increased about 10 dB each time a precipitator was turned off. The implication of this result is that the LDV signal intensity may have the potential of being used as a measure of effluent concentration.

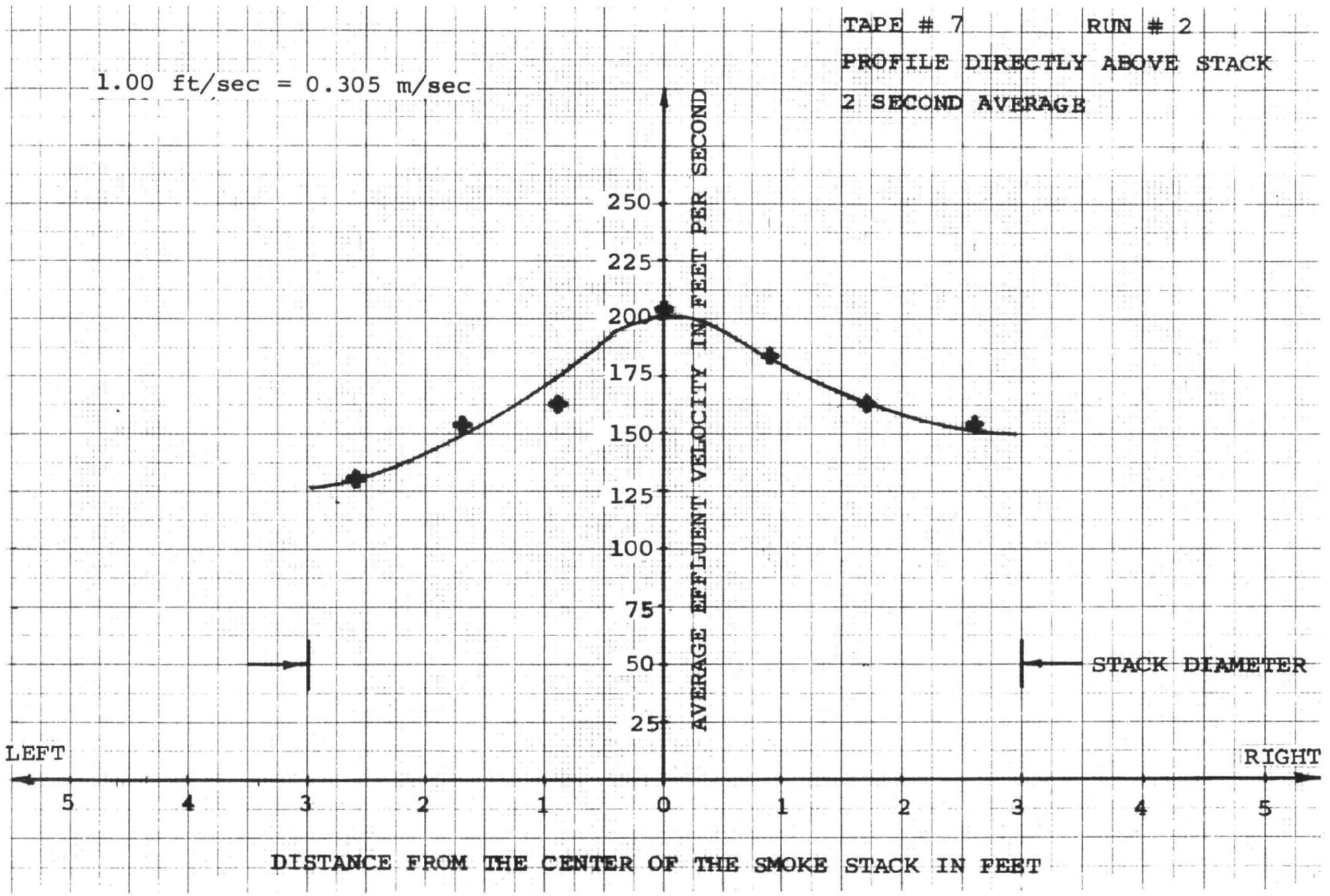

Figure 3-19. The Average Velocity of Effluents from a Smoke Stack as a Function of the Distance from the Center of the Stack

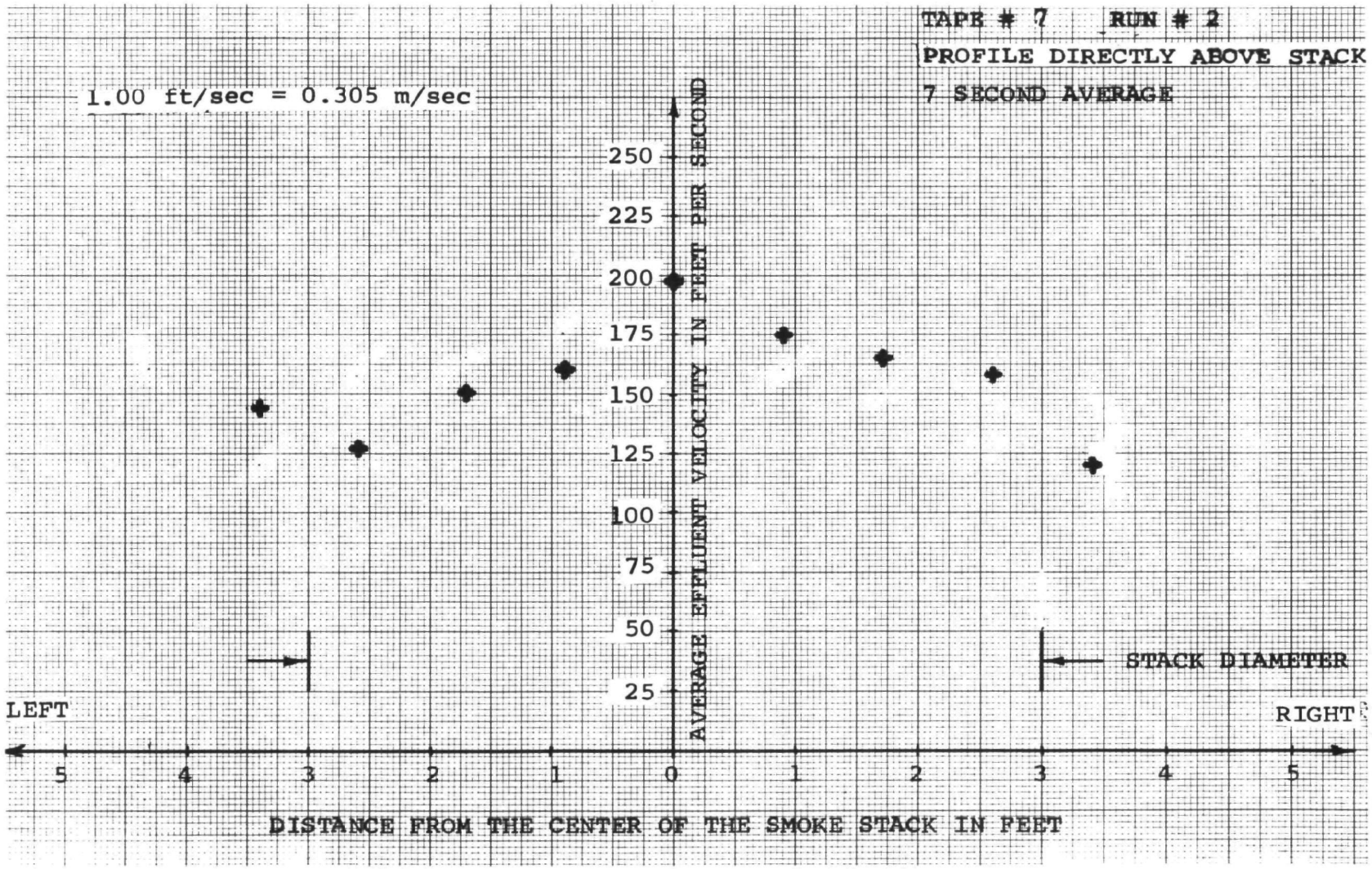

Figure 3-20. The Average Velocity of Effluents from a Smoke Stack as a Function of the Distance from the Center of the Stack

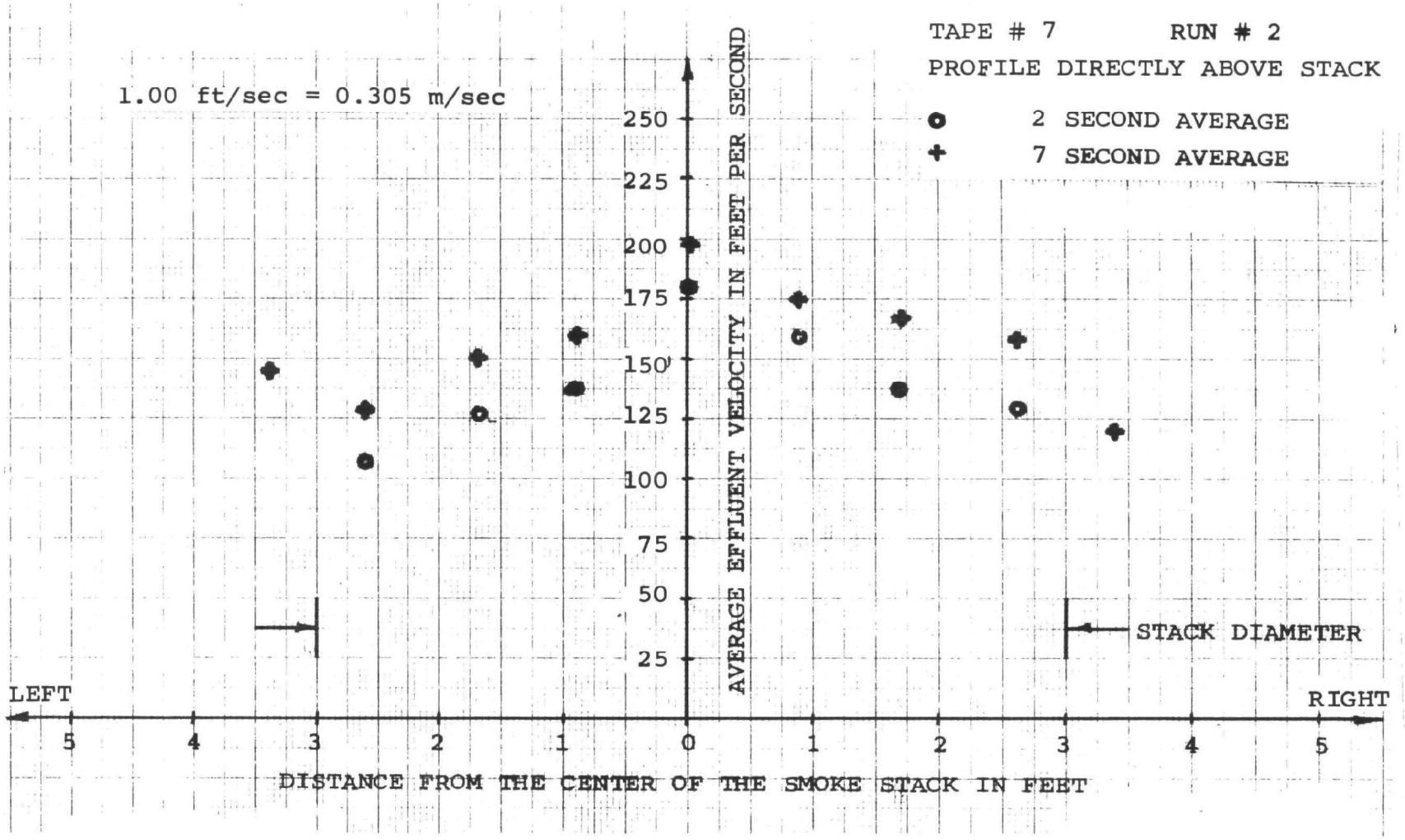

Figure 3-21. A Comparison of the 2 Second and 7 Second Average Effluent Velocity Profile Data

Date	Time	Pitot Tube Velocity V_P (m/sec)	Doppler Velocity V_D (m/sec)	V_D/V_P	Averaged Doppler Velocity, $\bar{V}_D$ (m/sec)	$\bar{V}_D/V_P$
8/28/74	16:20	47.9	53.3	1.11	48.5	1.01
8/28/74	22:05	38.4	47.9	1.25	47.5	1.24
8/28/74	22:35	34.4	36.0	1.05	38.1	1.11
8/29/74	12:15	50.9	-	-	55.2	1.08
Average Ratio =			1.14 ± 0.10		1.11 ± 0.10	
			1.12 ± 0.09			

Table 3-2. A Comparison of Pitot Tube Velocity Data With the Doppler Velocity Data.

V_D data are taken from 2 second composite photographs.

$\bar{V}_D$ data are taken from 7 sec and 28 sec electronically averaged data.

One point which must be emphasized is that the amount of data analyzed in the first test phase represents only a small fraction of the collected data. While the photographic method used appears satisfactory, it is far from ideal. The frequency tracker data was found to be unusable. The tracker was designed to be used with relatively narrow spectral signals. The broad doppler signals widths from the smoke stack effluents were wider than the tracker's discriminator bandwidth. This saturation of the discriminator led to erroneous output signals. As a result, graphs of continuous effluent velocity as a function of time could not be made.

It was apparent that more work needed to be done to investigate turbulence effects and the relationship between LDV signal intensity and effluent concentration. A second set of field tests was scheduled to make these tests on a calibrated LDV system with a suitably modified frequency tracker. The tests and their results are presented in the next section.

SECTION 4

RESULTS OF THE SECOND FIELD TESTS

4.0 INTRODUCTION

After the first field tests were completed, the scope of the program was expanded to include measurements (1) to investigate the feasibility of obtaining mass flow data from the laser doppler velocimeter, (2) to determine the effluent backscatter coefficient as a function of effluent opacity, (3) to produce exit velocity profiles with decreased separation between measurement points, (4) to study the effect of turbulence on the LDV signal spectrum, and (5) to obtain additional measurements of effluent exit velocity for various in-stack velocities and laser elevation angles.

In order to carry out these tasks, certain modifications were made to the LDV system. The modifications included the use of a modified Mach-Zehnder interferometer; a liquid nitrogen cooled, lead tin telluride detector; a frequency/intencity tracker suited to wide bandwidth, rapidly fluctuating, Doppler spectra; and the addition of a time-code generator.

Field tests were carried out at Duke Power's River Bend Steam Station during the week of 12 - 19 January 1975. Approximately 4 hours of data were recorded on magnetic tape for later analysis. This data included runs made at 8^{o}, 20^{o}, 28^{o}, and 37^{o} elevation angles, high resolution velocity profiles at 0 m, 0.9 m, 1.4 m, and 3.7 m above the lip of the smoke stack, runs to determine the LDV signal strength as a function the opacity of the effluent, and runs to evaluate the effluent velocity as a function of the in-stack velocity.

The system modifications, the second set of field tests, and their results are presented in this section.

4.1 SYSTEM MODIFICATIONS

Four modifications to the system described in Section 2 were

incorporated into the LDV for the second set of field tests. A modified Mach-Zehnder interferometer was installed into the system. An attempt was made to use a liquid nitrogen cooled lead-tin telluride detector. Most importantly a frequency/intensity tracker was incorporated to provide continuous voltage outputs proportional to the frequency and intensity of the received doppler IF signals. Finally, a time code generator was used to obtain better time referencing. These system modifications are discussed below.

4.1.1 THE MODIFIED MACH-ZEHNDER INTERFEROMETER

The modified Mach-Zehnder interferometer is a polarized configuration which reduces the inherent 6 dB loss of the conventional Mach-Zehnder interferometer to approximately 1 dB. The construction and operation of the modified Mach-Zehnder interferometer is basically similar to that of the Mach-Zehnder interferometer used in the first field tests and described in Section 2. In order to eliminate the need for independently maintaining alignment of the various mirrors and beamsplitters, the interferometer was constructed from a precision machined block of solid invar. The result was an interferometer which was mechanically ridig and thermally stable.

4.1.2 THE LEAD TIN TELLURIDE DETECTOR

An attempt was made to incorporate a liquid nitrogen cooled lead tin telluride (PbSnTe) detector into the system to avoid having to work with liquid helium in the field. A PbSnTe detector was obtained from Raytheon's Special Microwave Devices Operation and tested to see if it could replace the copper doped germanium detector used in the first field tests.

The PbSnTe photodetectors are junction devices whose frequency response is limited by the capacitance of the junction. In order to maximize the frequency response, the detector area is kept small and the devices are generally used with transimpedance amplifiers. The problem with small area detectors is that they are difficult to get shot noise limited. They tend to saturate or overheat before

sufficient local oscillator power can be applied to produce shot noise limited operation. This problem was observed with this PbSnTe detector.

The detector size was 0.1 x 0.1 mm. By increasing the local oscillator power on the chip, signal-to-noise ratios approached within 8 dB of the results from a Ge:Cu detector. The PbSnTe detector could not be made shot noise limited because of saturation and thermal runaway problems. Nevertheless it was thought that the detector would perform well enough to be used for the detection of smoke stack effluents. Because of the degraded performance, the PbSnTe detector was used a backup, rather than a replacement, for the liquid helium cooled Ge:Cu detector. The measurements made during the second field tests used the Ge:Cu detector.

4.1.3 THE FREQUENCY/INTENSITY TRACKER

In order to obtain continuous monitoring of both the velocity of the effluents and the intensity of the LDV backscatter signals, a frequency/intensity tracker was incorporated into the system. This tracker had the capability of following rapidly fluctuating, wide bandwidth, doppler IF signals. Furthermore, since the tracker operated off the vertical output of a spectrum analyzer, rather than the raw, high frequency, doppler signals, the tracker could be used with tape recorded spectrum analyzer signals. The ability to use a low frequency (30 kHz) FM tape recorder in analyzing megahertz frequency signals has several important advantages with regard to signal processing.

The tracker was used in conjunction with a H.P. 141T/8553B/8552B spectrum analyzer. It could track the frequency and intensity of signals in the 0 - 100 MHz range. When sufficient signal-to-noise ratios were available(typically 5 dB in 100 kHz bandwidths), the tracker could follow signals as small as -100 dBm.

The tracker worked by detecting the frequency component which has the peak amplitude. The tracker also integrated the received signal between preset frequency limits to determine a total received signal strength. The preset limits were used to remove spurious signals due to ground winds and spectrum analyzer frequency markers. The effects of noise were averaged out of the tracker's intensity channel by setting the integrated noise level to zero.

The outputs from both the frequency and intensity tracker channels were equipped with low pass filters having variable time constants. This time constant could be controlled to provide signal averaging over periods from 10 msec to 2000 sec. Typically, 2 sec averaging time constants were used in reducing the data.

In order to check out the frequency/intensity tracker, it was used with data taped on the first field tests. The results of a CW run with the laser beam just above the smoke stack lip is shown in Figure 4-1. The top trace is the relative integrated signal strength as a function of time. The spiking behavior is real and is the result of a rapping cycle on the electrostatic precipitators used to knock off ashes and other particulate matter. The bottom trace is the effluent exit velocity plotted as a function of time. Short term fluctuations are visible but the exit velocity remains fairly constant on a long-term basis. This chart was made from data recorded on Tape #4 on 29 August 1974.

The results of a velocity profile run are shown in Figure 4-3. This chart was made from data recorded on Tape #7 - Run #2 on 29 August 1974. It shows the exit velocity distribution across the lip of the smoke stack. It should be noted that the position of the laser beam above the stack was moved in 26 cm jumps. Hence, the spatial resolution of the profile is not very good. It does prove the usefulness of the tracker however.

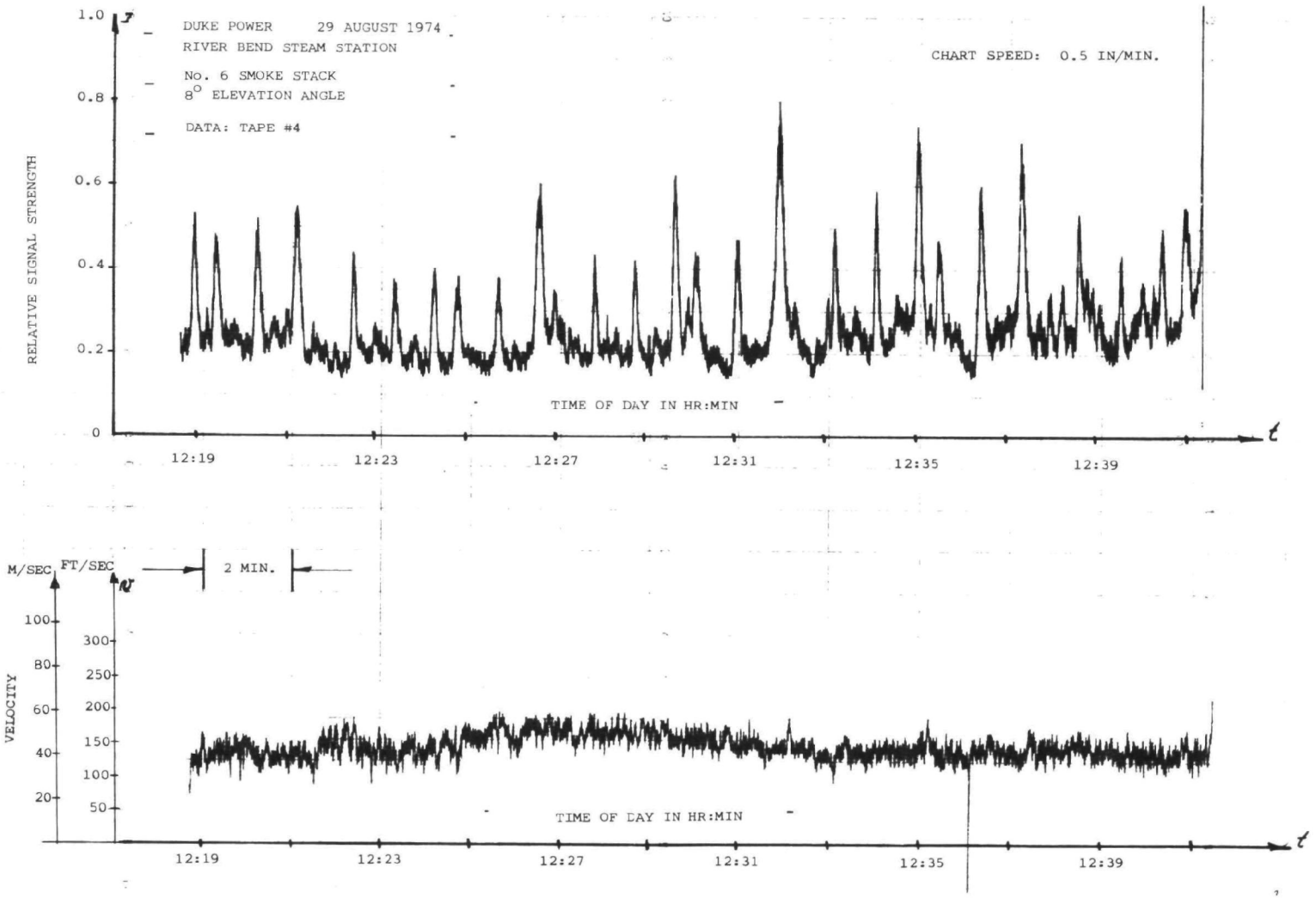

Figure 4-1. Tracker Outputs of Integrated Signal Intensity and Effluent Exit Velocity as a Function of Time.

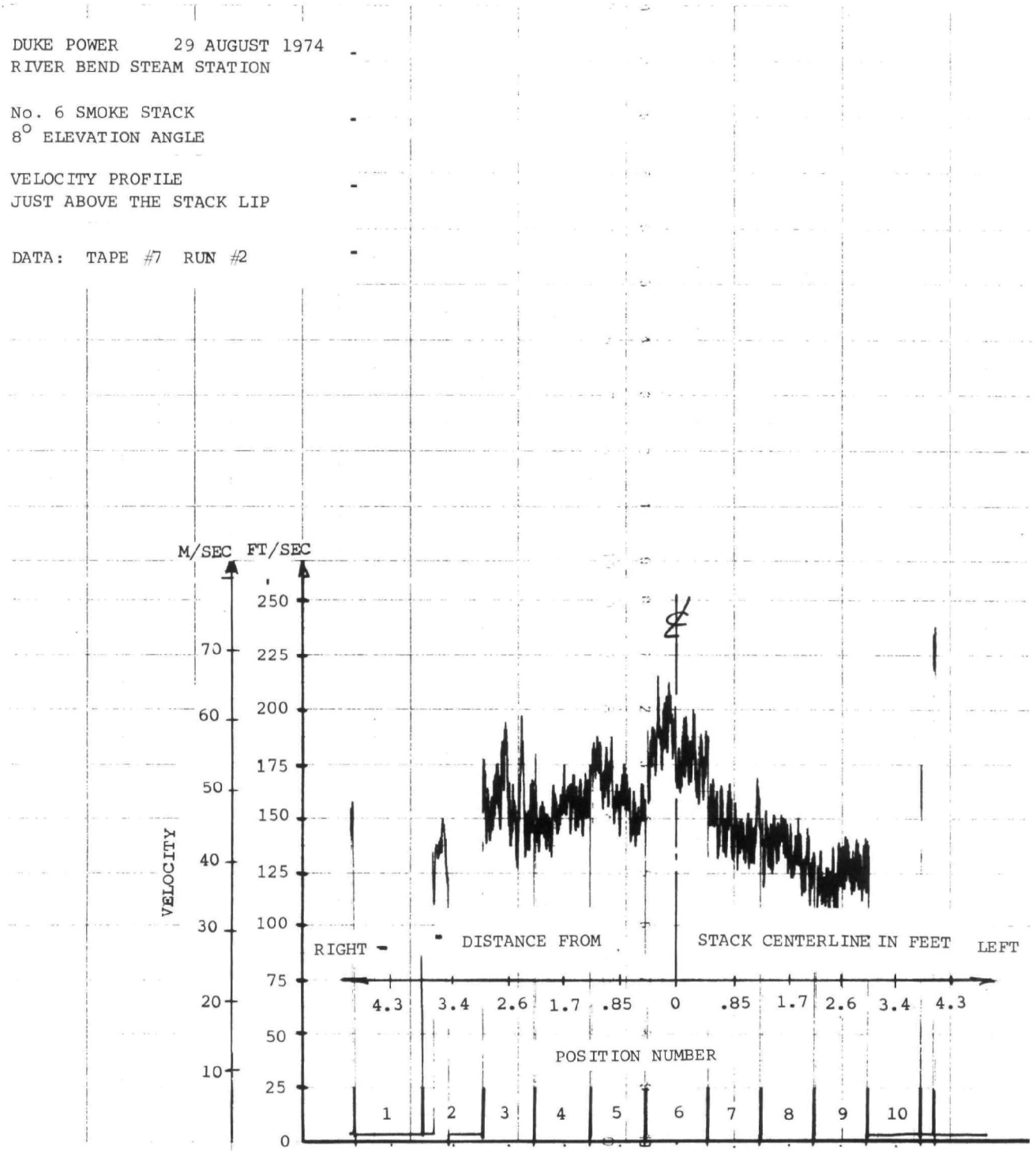

Figure 4-2. Tracker Output Showing Effluent Exit Velocity Profile Across the Smoke Stack Lip.

4.1.4 THE TIME CODE GENERATOR

A time code generator was incorporated into the LDV system to provide an accurate time reference for the measurements. This generator was synchronized with the power plant clock and was recorded with all measurements during the second field tests. The time code playback allowed easy correlation of the LDV data with the in-stack data.

The incorporation of the frequency/intensity tracker and time code generator resulted in slight changes from the LDV configuration (shown in Figure 2-1) of the first field tests. The block diagram of the LDV system used in the second set of effluent measurements is shown in Figure 4-3.

4.2 THE SECOND FIELD TESTS

The LDV system was located at Duke Power's River Bend Steam Station in Mt. Holly, North Carolina during the week of 12 - 19 January 1975 for a second set of smoke stack effluent measurements. The system was set up as shown in Figure 3-1 at a slant range of 400m from the number six smoke stack. The elevation angle to the stack lip was 8^{o}.

The primary direction of the first field tests was to prove the feasibility of remote effluent velocity measurement with an LDV. The second set of tests were oriented toward collecting data to determine: (1) effluent exit velocities as a function of in-stack velocity conditions, (2) correlation of effluent backscatter signal strength with cross-stack optical transmission, (3) the value of the effluent backscatter coefficient at 10.6 μm, (4) high resolution profiles of the effluent exit velocities at various heights above the stack lip, and (5) the effect of plume turbulence on the backscattered Doppler spectra.

The measurement of the effluent backscatter coefficient requires an intensity calibrated LDV. For this purpose, a known Doppler reflector was placed on the power plant roof. A known reflectivity

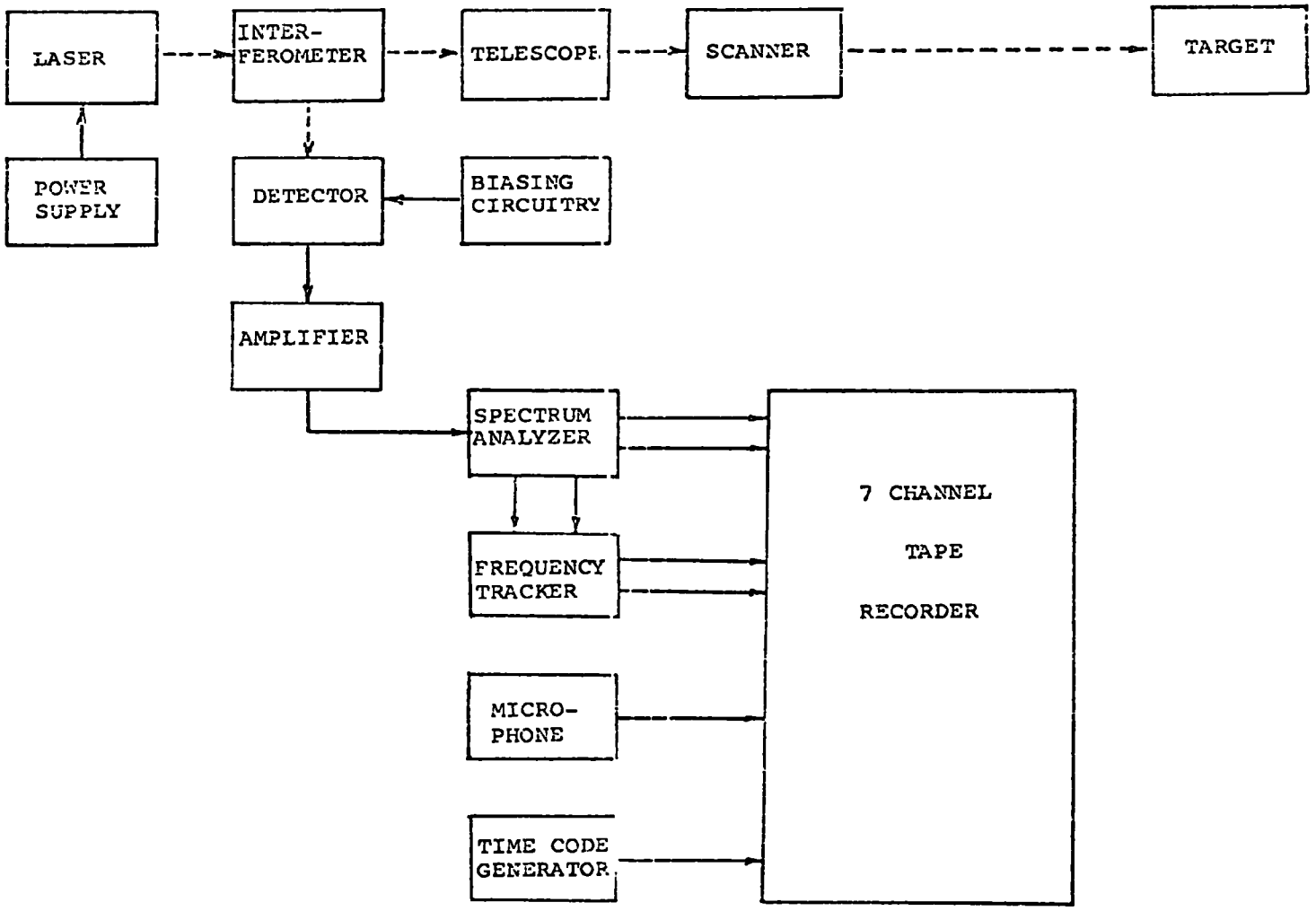

Figure 4-3. Block Diagram of LDV System for Second Field Tests.

allowed the calculation of the LDV system's overall efficiency.

The EPA contracted with Environmental Science and Engineering, Inc. to perform in-stack pitot-tube velocity measurements at the same time as the remote LDV velocity measurements were being made. The in-stack monitoring performed according to EPA reference method No. 2 was done through sampling ports located about 1.6m above the base of the smoke stack as shown in Figure 4-4. The in-stack monitoring included not only pitot-tube velocity transverses but also cross-stack optical transmission as measured on a Lear Seigler Model RM-4 transmissometer.

The constriction of the smoke stack at the top from 2.94m to 1.96m causes an increase in velocity. The gas velocity measured at the base must be multiplied by a factor of 2.32 in order to obtain an estimate of the exit velocity. The use of such a factor assumes that there is no significant cooling or pressure change of the exhaust gases between the sampling ports and the stack exit, which was later experimentally confirmed.

The turbulence measurements required Doppler data at various elevation angles through the smoke stack plume. A relay mirror was placed at various points on top of the electrostatic precipitators as shown in Figure 4-4 to obtain elevation angles between 20° and 40°.

Twelve data runs were made during the second field tests. These data runs included: (1) five high resolution velocity profiles at heights above the stack lip from 2 cm to 3.7 m, (2) four continuous runs through the center of the plume at elevation angles from 8° to 37°, (3) two precipitator variation runs to evaluate the LDV signal intensity as a function of cross-stack optical transmission, and (4) one run during changing power plant load condition. Most of these runs were calibrated to allow evaluation of the backscatter coefficient. The data runs are summarized in Table 4-1 and described in detail in the following sections.

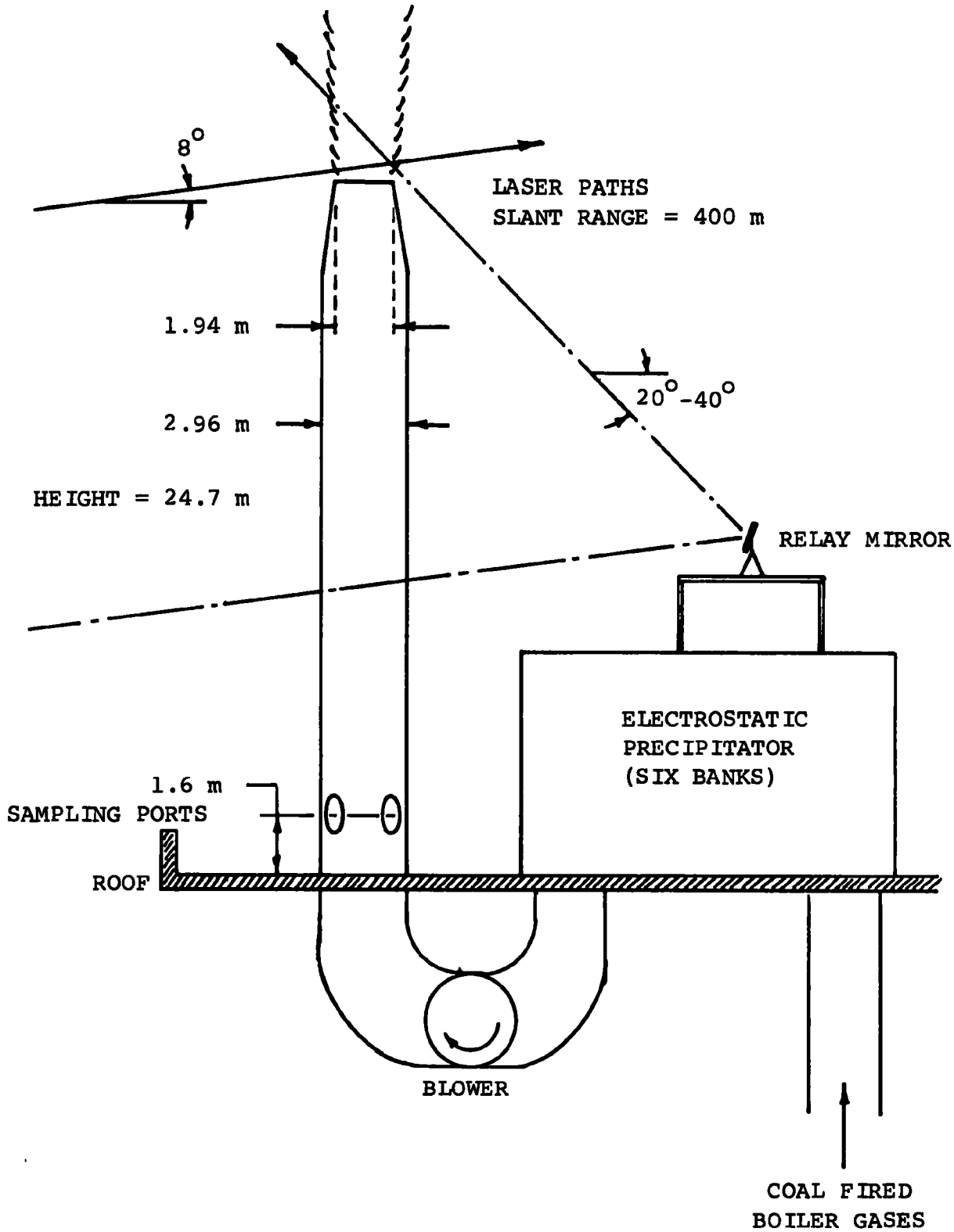

Figure 4-4. Smoke Stack LDV Geometry.

TABLE 4-1

Summary of Data Tapes from the Second Field Tests

Tape	Time	Date	Subject
1	11:13 to 11:34	1/16/75	CW Run - 8° elevation angle - just above lip of stack.
2	12:27 to 12:42	1/16/75	CW Run - 20° elevation angle - just above lip of stack.
3	15:55 to 16:48	1/16/75	Precipitator Run: 7 combinations - 20° elevation angle - just above lip of stack.
4	17:39 to 18:06	1/16/75	Velocity profile - 8° elevation angle- just above lip of stack.
5	9:38 to 13:49	1/17/75	Load change: 83 - 137 MW - 8° and 20° elevation angles - just above lip of stack.
6	15:20 to 15:59	1/17/75	Precipitator run: 4 combinations - 20° elevation angle - just above lip of stack.
7	16:42 to 16:55	1/17/75	CW run - 28° elevation angle - just above lip of stack.
8	17:16 to 17:31	1/17/75	CW run - 37° elevation angle - just above lip of stack.
9	7:40 to 9:00	1/18/75	Velocity profile - 8° elevation angle 0.9 m above lip of stack.
10	9:15 to 10:00	1/18/75	Velocity profile - 8° elevation angle just above lip of stack.
11	10:00 to 10:30	1/18/75	Velocity profile - 8° elevation angle 1.4 m above lip of stack.
12	10:30 to 11:30	1/18/75	Velocity profile - 8° elevation angle 3.7 m above lip of stack.

4.2.1 TAPE #1: 8° CW RUN

Tape #1 was recorded between 11:13 and 11:34 on 16 January 1975. It was a CW run in the sense that all operating conditions remained unchanged during the course of the run. The laser beam was passed directly through the smoke stack plume, just above the lip of the stack. No relay mirrors were used, and the laser beam elevation angle was 8° above horizontal. The power load was constant at about 92 MW. The cross-stack optical transmission was steady at 96%.

An in-stack effluent velocity measurement was made between 11:30 and 12:00. An exit velocity of 33.5 m/sec was calculated from this measurement. The effluent velocity measured remotely with the LDV for the time interval 11:13 to 11:34 is shown in the lower trace of Figure 4-5. The mean exit velocity measured by the LDV was approximately 29.0 m/sec.

The upper trace in Figure 4-5 shows the relative integrated signal strength received by the LDV during the time interval from 11:13 to 11:34.

The data displayed in Figure 4-5 were processed through the frequency/intensity tracker using a 2 sec averaging time constant. The tracker follows the Doppler frequency component with the peak spectral amplitude and integrates all frequency components to give a total integrated signal strength.

4.2.2 TAPE #2: 20° CW RUN

Tape #2 was recorded between 12:27 and 12:42 on 16 January 1975. Like Tape #1, it also was a CW run. A relay mirror on top of a platform on the electrostatic precipitators was used to direct the laser beam through the smoke stack plume. The laser beam passed just above the lip of the stack at an elevation angle of 20° above horizontal. The power load varied slightly from 91 MW at the start of the run, to 96 MW at 12:34, to 92 MW at the end of the run. The cross-stack optical transmission also varied slightly increasing from around 87.5% at the start of the run to 91% at the end of the run.

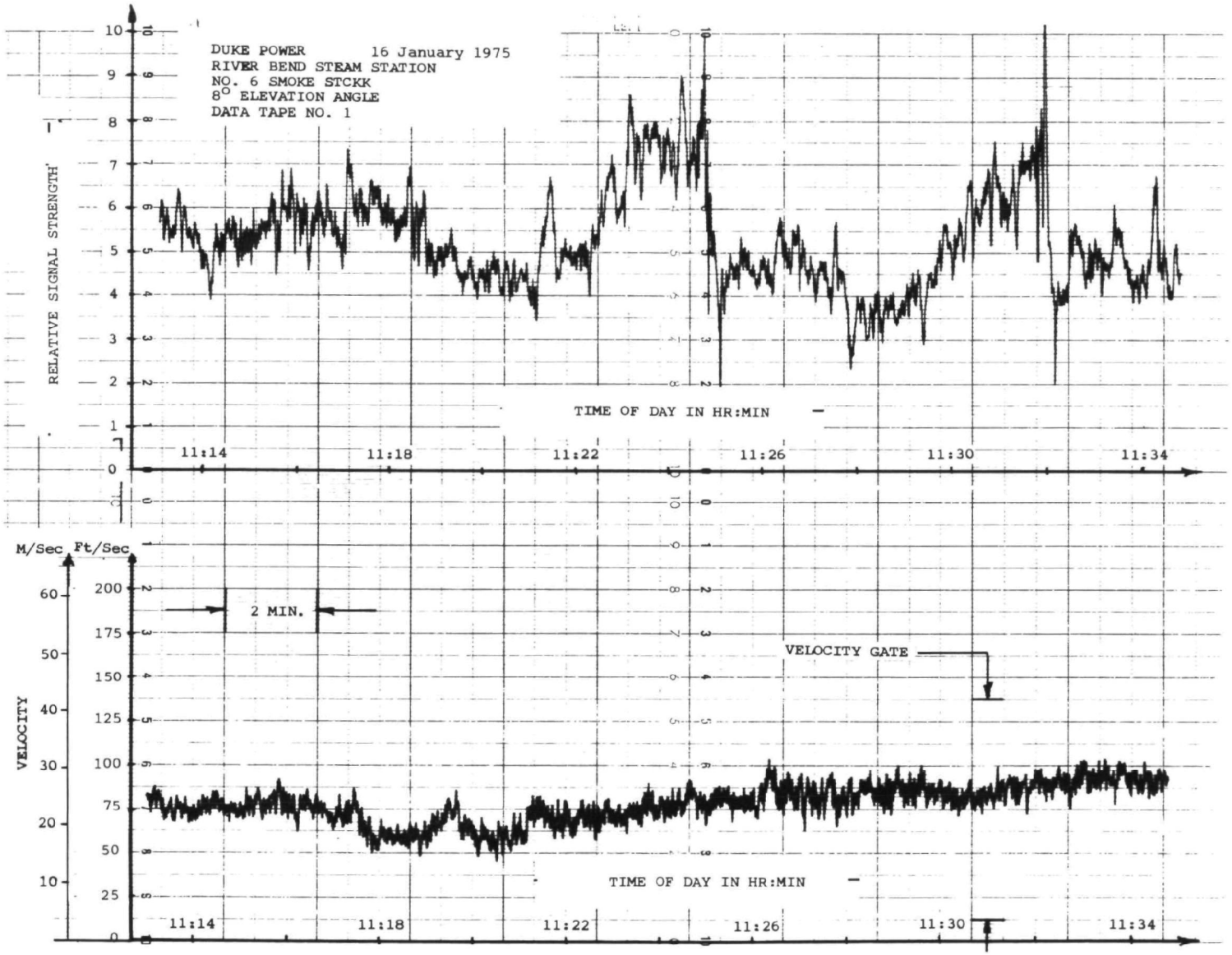

Figure 4-5. The Strength and Frequency of Effluent Signals as a Function of Time for Tape #1: 8° CW Run.

An in-stack effluent velocity measurement was made between 12:15 and 12:45. A mistake was made with the pitot line connections during this measurement. However, an exit velocity of 31.7 m/sec was estimated. The effluent exit velocity measured remotely with the LDV for the time interval 12:27 to 12:42 is shown in the lower trace of Figure 4-6. The mean exit velocity measured by the LDV was approximately 26.5 m/sec.

The upper trace of Figure 4-6 shows the relative integrated signal strength received by the LDV during the time interval from 12:27 to 12:42.

The data displayed in Figure 4-6 were processed through the frequency/intensity tracker using a 2 sec averaging time constant.

4.2.3 TAPE #3: 20° PRECIPITATOR RUN

Tape #3 was recorded between 15:55 and 16:48 on 16 January 1975. In this run various combinations of precipitator banks were turned on and off to vary the effluent particle content. The last three banks of electrostatic precipitators (notated: A, B, and C; A being the last bank) downstream were switched off in various combinations to obtain seven levels of cross-stack optical transmission from 60% to 98.5%. A relay mirror was used to direct the laser beam through the smoke stack plume. The laser beam passed just above the lip of the stack at an elevation angle of 20° above horizontal. The power load was constant at 83 MW.

An in-stack effluent velocity measurement was made between 15:45 and 16:10. A mistake was made with the pitot line connections during this measurement. However, an exit velocity of 30.5 m/sec was estimated. The effluent exit velocity, measured remotely with the LDV at various times during the interval from 15:55 to 16:48, is shown in the lower trace of Figure 4-7. The mean exit velocity measured by the LDV was about 27.4 m/sec.

The upper trace of Figure 4-7 indicates the variation of received signal intensity from the LDV as a function of the electro-

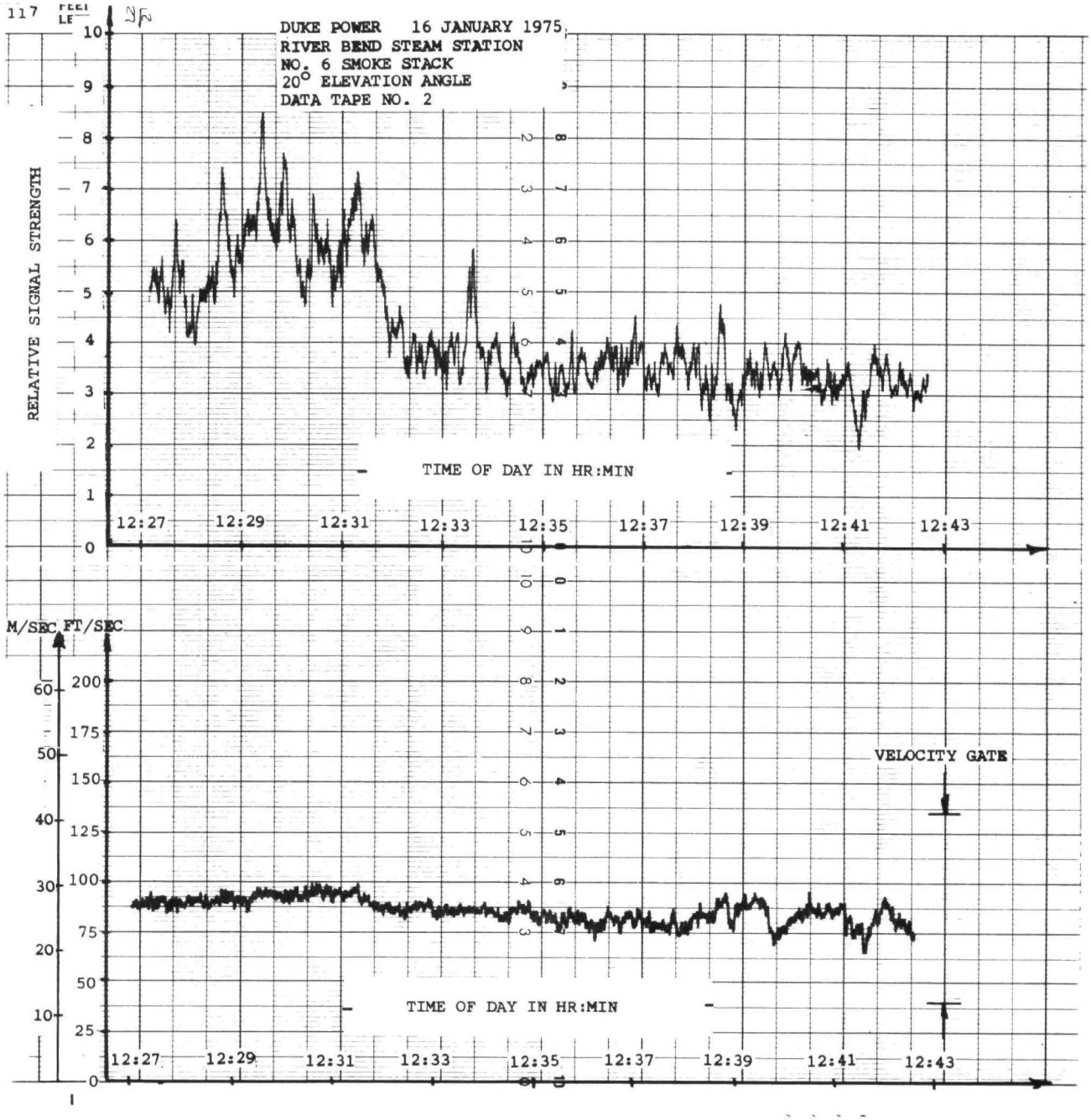

Figure 4-6. The Strength and Frequency of Effluent Signals as a Function of Time for Tape #2: 20° CW Run.

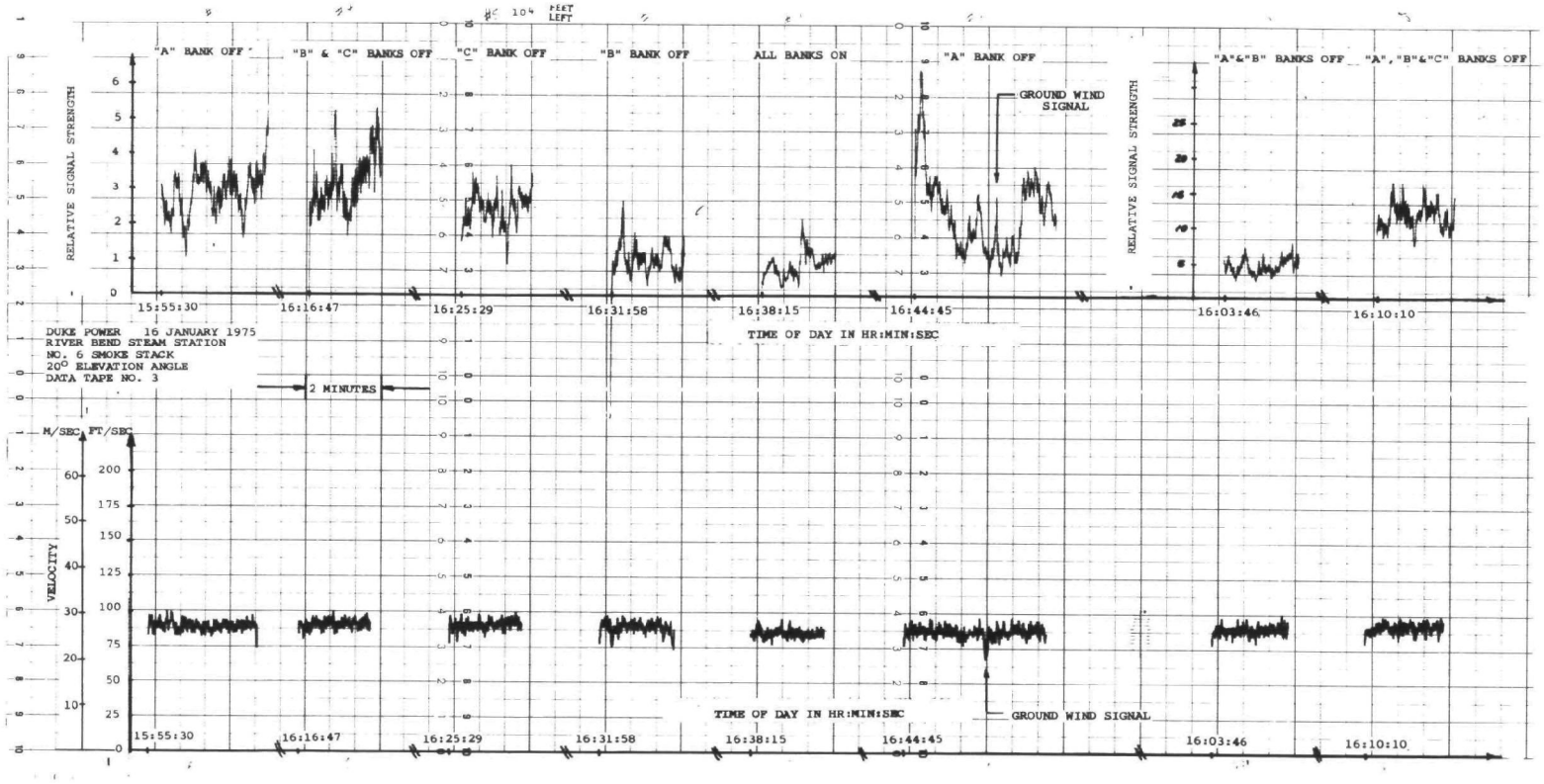

Figure 4-7. The Strength and Frequency of Effluent Signals as a Function of Time for Tape #3: 20° CW Run.

static precipitators in use on the smoke stack.

The data displayed in Figure 4-7 were processed through the frequency/intensity tracker using a 2 sec averaging time constant.

4.2.4 TAPE #4: 8^{o} VELOCITY PROFILE

Tape #4 was recorded between 17:39 and 18:06 on 16 January 1975. Tape #4 was a high resolution profile of the exit velocity distribution across the top of the smoke stack. The laser beam was scanned across the top of the stack just above the stack lip. No relay mirrors were used, and the laser beam elevation angle was 8^{o} above horizontal. The power load during the profile was fairly constant at 83 to 84 MW. The cross-stack optical transmission was steady at 94%.

An in-stack effluent velocity measurement was made between 17:30 and 17:50. A mean exit velocity of 28.4 m/sec was calculated from this measurement. The velocity of effluents was measured at 10 cm intervals across the top of the smoke stack using the LDV. The velocity profile obtained from this remote measurement is shown in the lower trace of Figure 4-8. The exit velocities can be seen to vary between 23 to 30 m/sec across the stack.

The top trace of Figure 4-8 shows the total integrated signal strength received by the LDV as a function of the position of the laser beam above the smoke stack.

The data displayed in Figure 4-8 were obtained by taking one minute duration samples at discrete positions separated by 10 cm and processing them through the frequency/intensity tracker using a 2 sec. averaging time constant.

4.2.5 TAPE #5: VELOCITY VARIATION BY POWER LOAD CHANGE

Tape #5 was recorded between 9:38 and 13:49 on 17 January 1975. This tape was made during a period of changing electrical power load on the generating unit exhausting gases through the number six smoke stack. The power load decreased from 135 MW to 83 MW in four steps and then increased to 137 MW in four steps. Two sets of Doppler

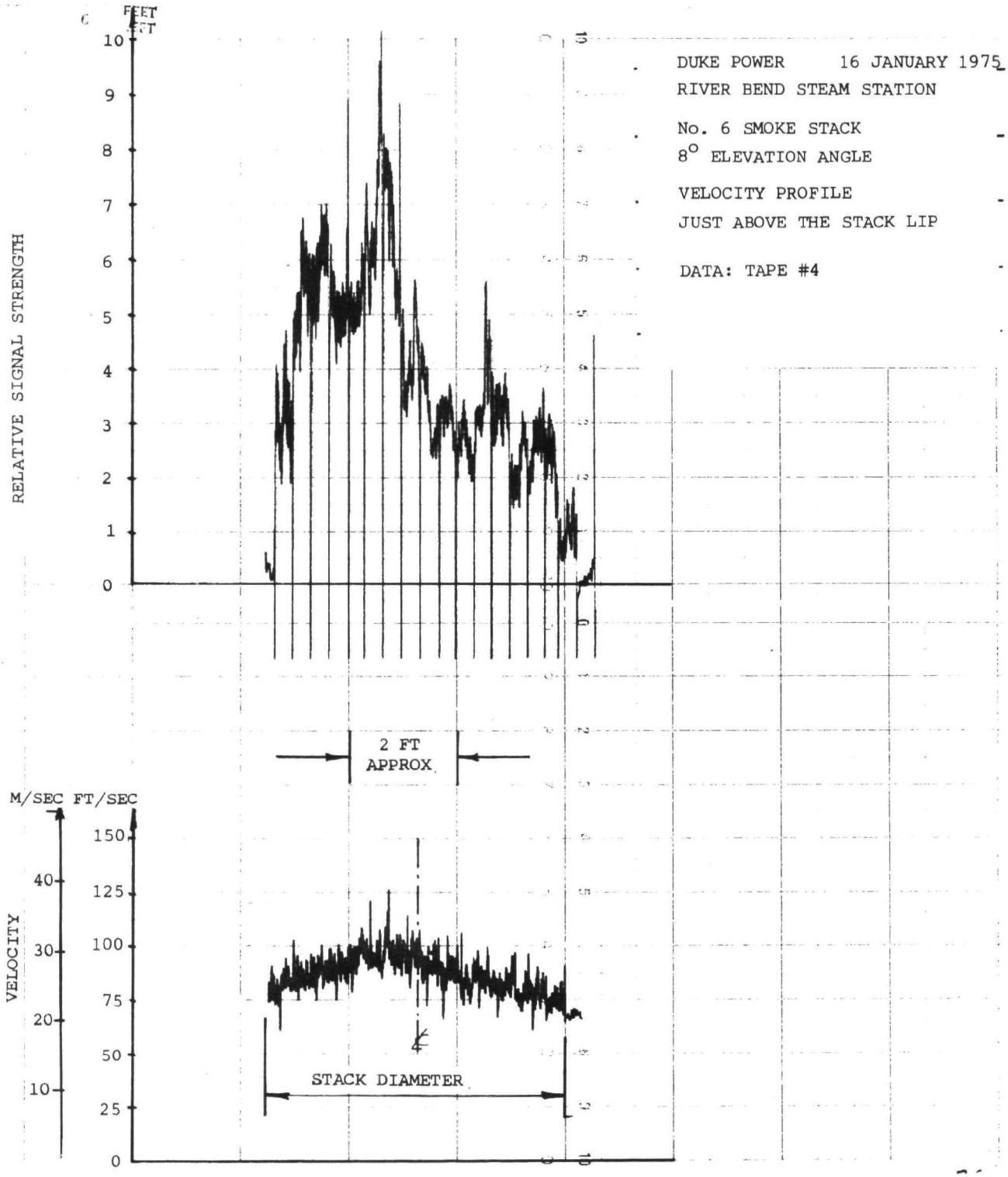

Figure 4-8. The Strength and Frequency of Effluent Signals as a Function of the Position above the Smoke Stack Lip from Tape #4: 8° Velocity Profile.

measurements were made: one at an 8° elevation angle, the other at a 20° elevation angle. The laser beam was passed directly through the smoke stack plume just above the lip of the stack to get an 8° elevation angle. A relay mirror on top of a platform on the electrostatic precipitators was used to redirect the laser beam through the plume at a 20° elevation angle. The cross-stack optical transmission changed during this run from 91% at the start to 98% at 11:00 to 81% at the end of the run. This transmission variation was due to both the load conditions and the number of precipitators in use.

In-stack effluent velocity measurements were made at each load level. The effluent velocity was measured remotely with the LDV at each load level. The velocity data for the 8° elevation angle Doppler measurements are shown in Figure 4-9. The velocity data for the 20° elevation angle Doppler measurements are shown in Figure 4-10. The data in Figures 4-9 and 4-10 were processed through the frequency tracker with a 2 sec time constant. The results of the in-stack and remote Doppler velocity data are summarized in Table 4-2.

4.2.6 TAPE #6: 20° PRECIPITATOR RUN

Tape #6 was recorded between 15:20 and 15:59 on 17 January 1975. As in Tape #3, various combinations of precipitator banks were turned on and off to vary the effluent particle content (and size distribution). The last three banks of electrostatic precipitators (notated: A, B, and C; A being the last bank) were switched off in various combinations to obtain four levels of cross-static optical transmission from 49% to 94%. A relay mirror was used to direct the laser beam through the smoke stack plume. The laser beam passed just above the lip of the stack at an elevation angle of 20° above horizontal. The power load was constant during the run at 131 MW.

An in-stack effluent velocity measurement was made between 15:15 and 15:30. A mean exit velocity of 41.4 m/sec was calculated from this measurement. The effluent velocity, measured remotely with the LDV at various times between 15:20 and 15:59, is shown in the lower trace

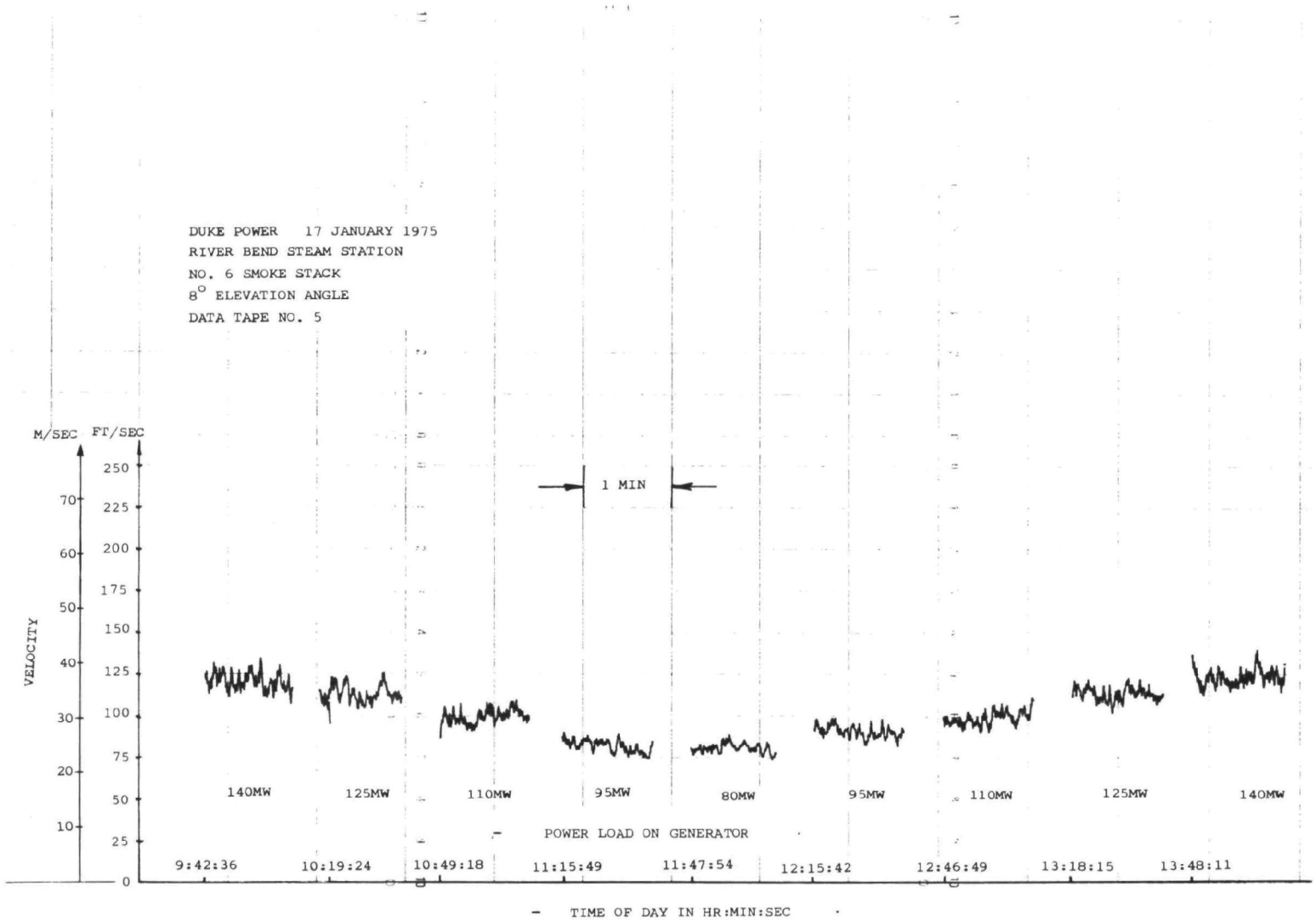

Figure 4-9. The Frequency of Effluent Signals as a Function of Time for Tape #5: 8° Power Load Change.

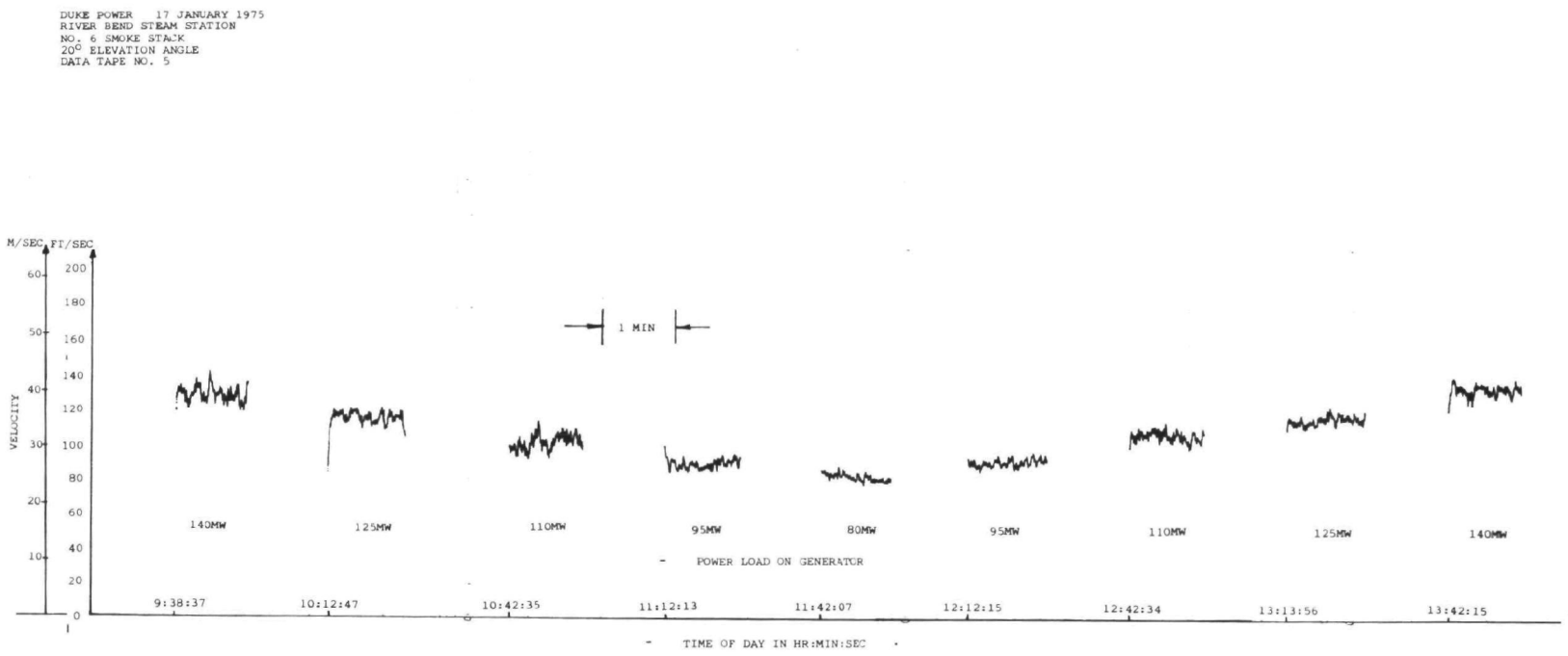

Figure 4-10. The Frequency of Effluent Signals as a Function of Time for Tape #5: 20° Power Load Change.

TABLE 4-2

Comparison of In-Stack and LDV Velocity Measurements

For Tape #5 on 17 January 1975

Time (Hr:Min)	Load (MW)	Pitot Exit Velocity, V_P (m/sec)	8^o Elevation Angle		20^o Elevation Angle	
			Doppler Exit Velocity, V_D (m/sec)	V_P/V_D	Doppler Exit Velocity, V_D (m/sec)	V_P/V_D
9:45	135	44.5	36.6	1.22	39.6	1.12
10:15	124	41.4	34.1	1.17	35.9	1.08
10:45	111	35.9	30.5	1.18	31.4	1.15
11:15	96	32.6	25.3	1.29	27.4	1.19
11:45	83	26.6	24.4	1.09	25.3	1.05
12:15	97	31.1	27.4	1.13	28.1	1.11
12:45	109	35.9	30.5	1.18	32.6	1.10
13:15	122	39.3	34.4	1.14	36.2	1.08
13:45	137	44.5	38.1	1.17	41.2	1.08

of Figure 4-11. The mean exit velocity measured by the LDV was about 38.1 m/sec.

The upper trace of Figure 4-11 shows the relative integrated signal strength received by the LDV as a function of the electrostatic precipitators in use on the stack.

The data displayed in Figure 4-11 were processed through the frequency/intensity tracker using a 2 sec averaging time constant.

4.2.7 TAPE #7: 28° CW RUN

Tape #7 was recorded between 16:42 and 16:55 on 17 January 1975. Like Tapes #1 and 2, it was a CW run. A relay mirror on top of the electrostatic precipitators was used to direct the laser beam through the smoke stack plume. The beam passed just above the lip of the stack at an elevation angle of 28° above horizontal. The power load was constant at 131 MW throughout the run. The cross-stack optical transmission was steady at 87%.

An in-stack effluent velocity measurement was made between 16:30 and 16:45. An exit velocity of 43.3 m/sec was calculated from this measurement. The effluent velocity, measured remotely with the LDV during the time interval from 16:42 - 16:55, is shown in the lower trace of Figure 4-12. The mean exit velocity measured by the LDV was about 35.7 m/sec.

The upper trace in Figure 4-12 shows the relative integrated signal strength received by the LDV during the time interval from 16:42 to 16:55.

The data displayed in Figure 4-12 were processed through the frequency/intensity tracker using a 2 sec averaging time constant.

4.2.8 TAPE #8: 37° CW RUN

Tape #8 was recorded between 17:16 and 17:31 on 17 January 1975. It was a CW run similar to Tape #7. A relay mirror on top of the electrostatic precipitators was used to direct the laser beam through the smoke stack plume. The laser beam passed just above the lip of

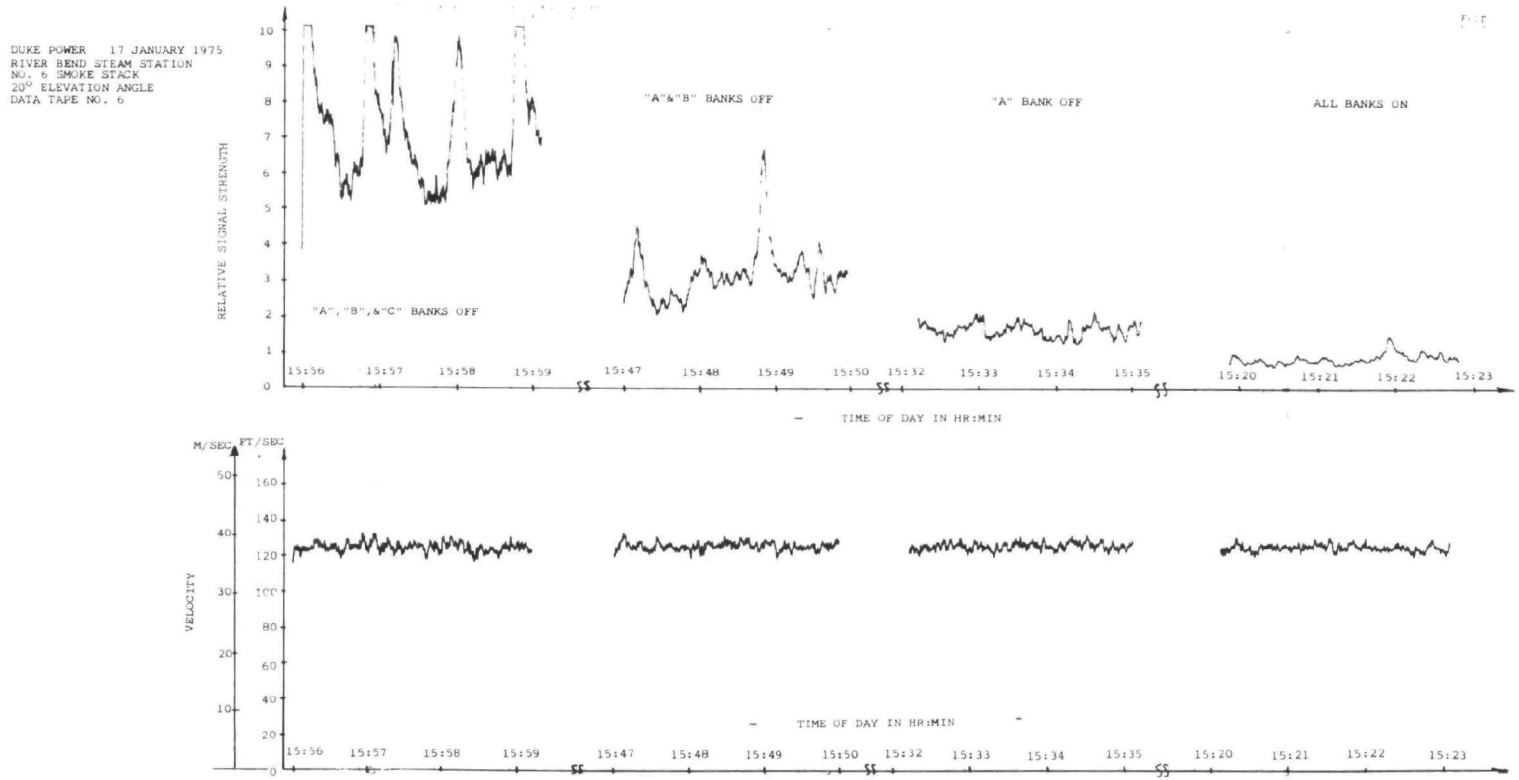

Figure 4-11. The Strength and Frequency of Effluent Signals as a Function of Time for Tape #6: 20° CW Run.

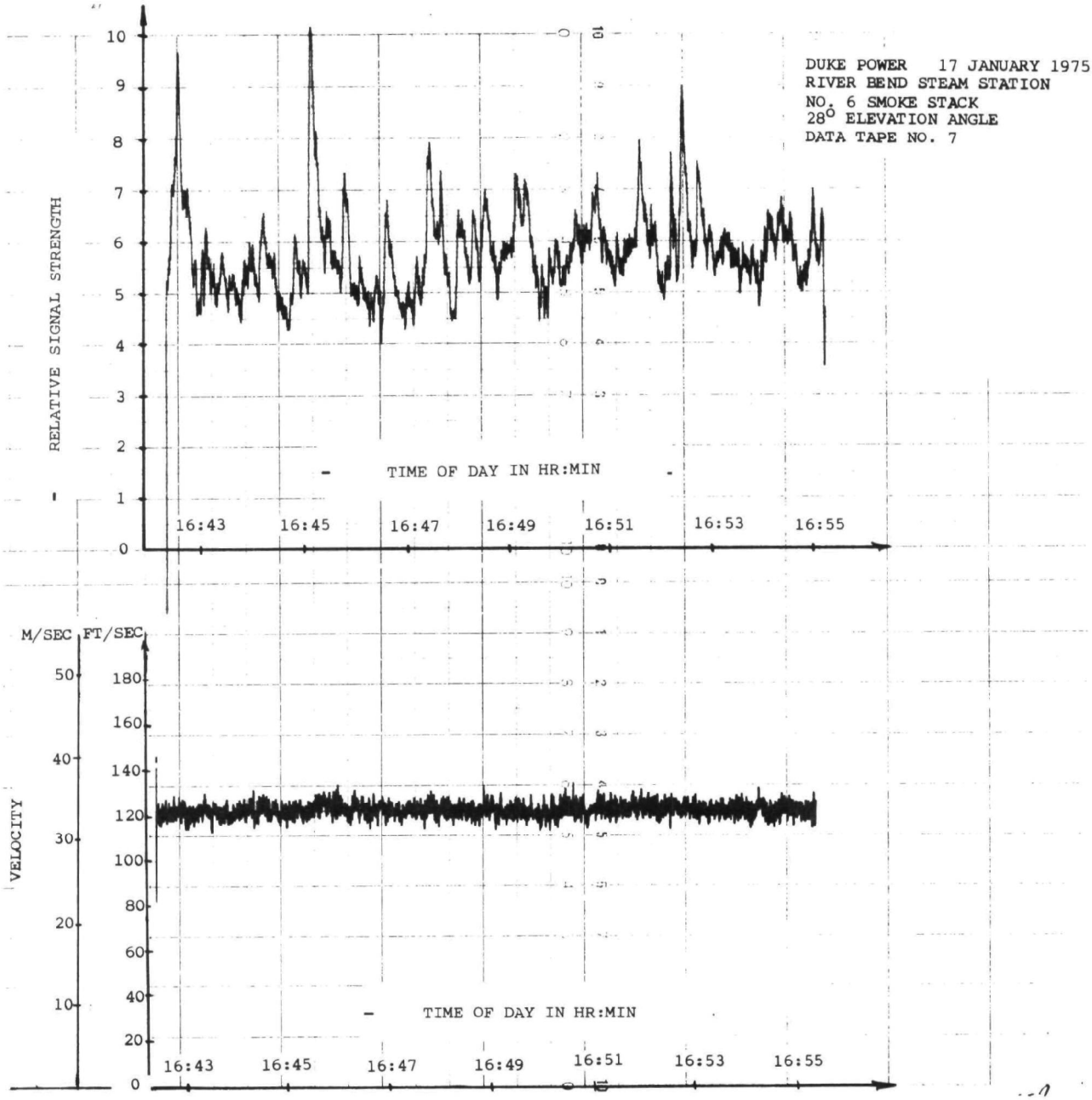

Figure 4-12. The Strength and Frequency of Effluent Signals as a Function of Time for Tape #7: 28° CW Run.

the stack at an elevation angle of 37° above horizontal. The power load was constant at 131 MW throughout the run. The cross-stack optical transmission was steady at 87%.

No in-stack effluent velocity measurement was made during the run. However, conditions were stable after the previous measurement which was taken during the time interval from 16:30 to 16:45. An exit velocity of 43.3 m/sec was calculated from this measurement. The effluent velocity, measured remotely with the LDV during the time interval from 17:16 to 17:31, is shown in the lower trace of Figure 4-13. The mean exit velocity measured by the LDV was about 38.1 m/sec.

The upper trace in Figure 4-13 shows the relative integrated signal strength received by the LDV during the time interval from 17:16 to 17:31.

The data displayed in Figure 4-13 were processed through the frequency/intensity tracker using a 2 sec averaging time constant.

4.2.9 TAPES #9, 10, 11, and 12: 8° VELOCITY PROFILES

Tapes #9, 10, 11, and 12 were recorded between 7:40 and 11:30 on 18 January 1975. These runs were high resolution profiles of the exit velocity distribution across the top of the smoke stack. The laser beam was scanned across the top of the stack at heights from 0 to 3.7 m above the lip. No power load data were collected for these runs. The cross-stack optical transmission increased gradually from 90 to 94% during the course of the runs.

Three in-stack effluent velocity measurements were made while the profiles were in progress. The mean exit velocity was calculated to have the values of 36.9 m/sec during the time interval from 8:15 to 8:30, 36.3 m/sec between 9:00 and 9:15, and 36.9 m/sec from 10:00 to 10:15. The velocity of the effluents was measured at 10 cm intervals across the top of the smoke stack using the LDV. Profiles were made at heights of 2 cm, 0.9 m, 1.4 m, and 3.7 m above the lip of the stack. The velocity profiles obtained by these remote measurements are shown in Figure 4-14. The variation of the profiles with increasing height

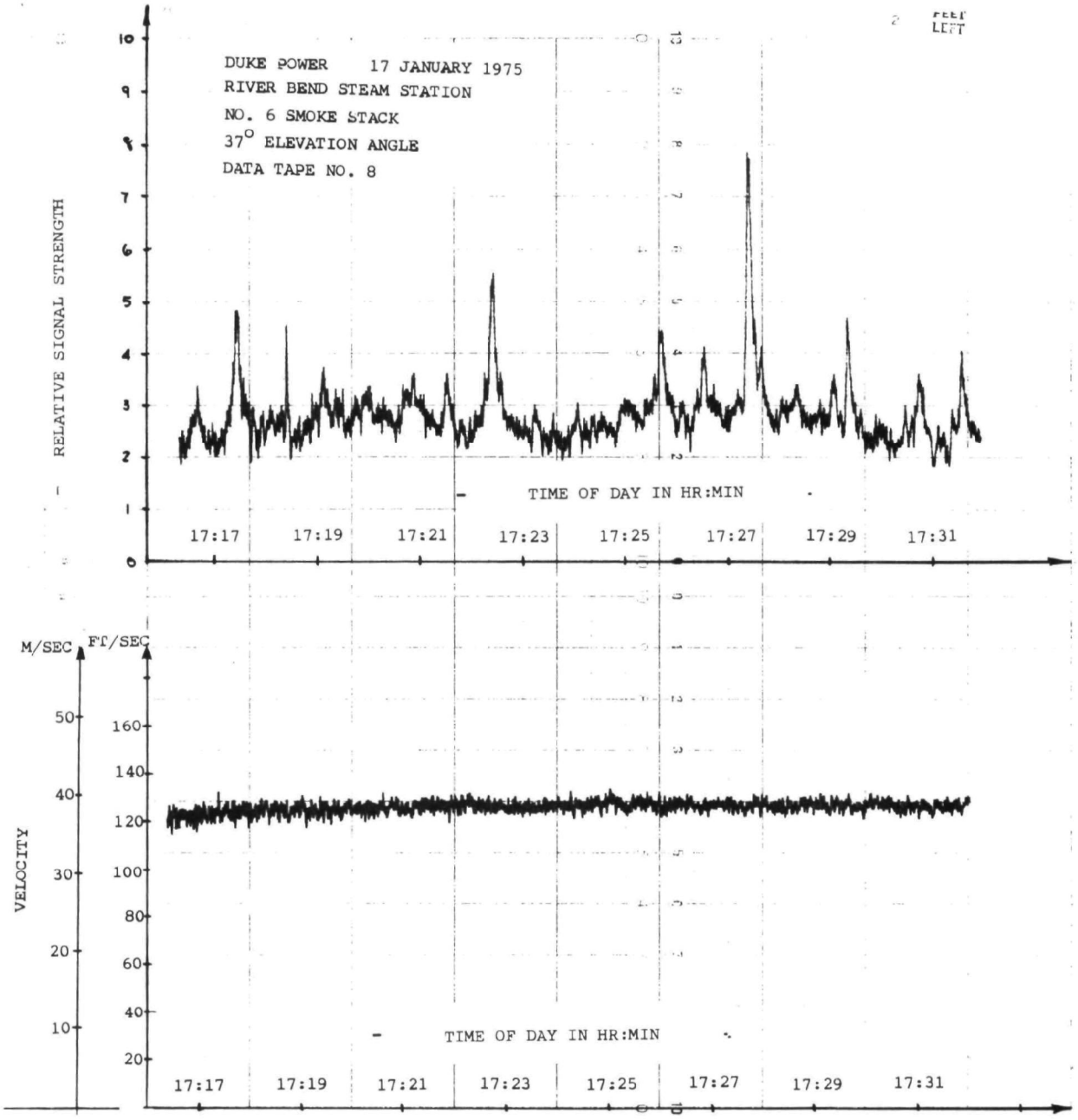

Figure 4-13. The Strength and Frequency of Effluent Signals as a Function of Time for Tape #8: 37° CW Run.

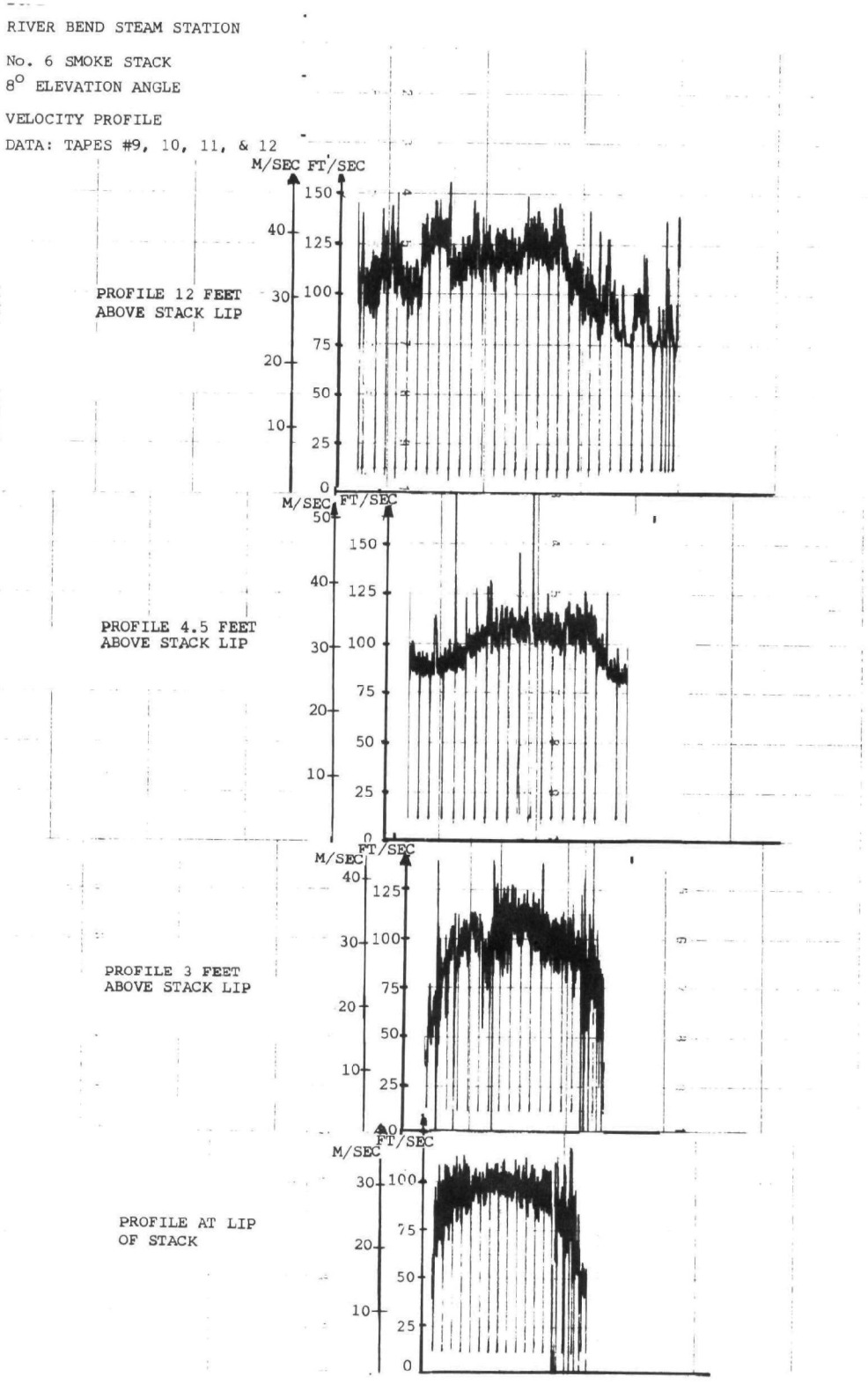

Figure 4-14. The Frequency of Effluent Signals as a Function of the Position and Height Above the Smoke Stack Lip from Tapes #9, 10, 11, and 12: 8° Velocity Profiles.

is considerable. Velocities range from 15 m/sec at the edges to greater than 38 m/sec at points in the middle. The data displayed in Figure 4-14 were obtained by taking one minute duration samples at discrete positions 10 cm apart and processing them through the frequency tracker using a 2 sec averaging time constant.

4.3 DATA ANALYSIS

The twelve tapes were analyzed to determine: (1) the degree of agreement between LDV and pitot tube measurements of smoke stack effluent exit velocities, (2) the correlation of effluent backscatter signal strength with the cross-stack optical transmission, (3) the range of values of the effluent backscatter coefficient at 10.6 μm, and (4) the effects of plume turbulence on the backscattered Doppler spectra. The analyses are discussed in detail below.

4.3.1 LDV AND PITOT TUBE VELOCITY MEASUREMENTS

Tapes #1, 3, 5, 6, 7, and 8 were used to determine the degree of agreement between LDV and pitot-tube measurements of smoke stack exit velocity. During each of these runs, the power load was steady at a value between 83 MW and 137 MW and both remote and in-stack effluent velocity measurements were made.

The results of this analysis are tabulated in Table 4-3 and shown graphically in Figure 4-15. It appears that the effluent exit velocity from a power plant smoke stack is a linear function of the power load on the generating unit exhausting gases through the stack. A linear least squares fit to the remote LDV velocity data is shown in Figure 4-15 by the solid line. It indicates that the exit velocity can be found from the equation:

$$v\ (\text{m/sec}) = 0.26\ \text{load}\ (\text{MW}) + 3.05 \qquad (4\text{-}1)$$

TABLE 4-3

Velocity vs. Load Data

16 - 17 January 1975

Load MW	Pitot Velocity (m/sec)	Doppler Velocity (m/sec)	Tape	Percentage (V_P/V_D) x 100			
				8°	20°	28°	37°
83	26.6	24.4	5	109			
83	26.6	25.3	5		105		
83	30.5	27.4	3		111		
92	33.5	29.0	1	116			
96	32.6	25.3	5	129			
96	32.6	27.4	5		119		
97	31.1	27.4	5	113			
97	31.1	28.0	5		111		
109	36.0	30.5	5	118			
109	36.0	32.6	5		110		
111	36.0	30.5	5	118			
111	36.0	31.4	5		115		
122	39.3	34.4	5	114			
122	39.3	36.3	5		108		
124	41.5	34.1	5	121			
124	41.5	36.0	5		115		
130	41.5	38.1	6		109		
130	43.3	35.7	7			121	
130	43.3*	38.1	8				114
135	44.5	36.6	5	122			
135	44.5	39.6	5		112		
137	44.5	38.1	5	117			
137	44.5	41.1	5		108		
Velocity Ratio = $\overline{V_P/V_D}$				1.177	1.112	1.21	1.14
Standard Deviation = $\sigma(V_P/V_D)$				0.055	0.040	-	-

Total Ratio: 1.14 ± 0.056

Linear Fit: Pitot $v = 0.31L + 2.38$ $\sigma = 1.10$ m/sec

Doppler $v = 0.26L + 3.05$ $\sigma = 1.40$ m/sec

* Same as Tape #7

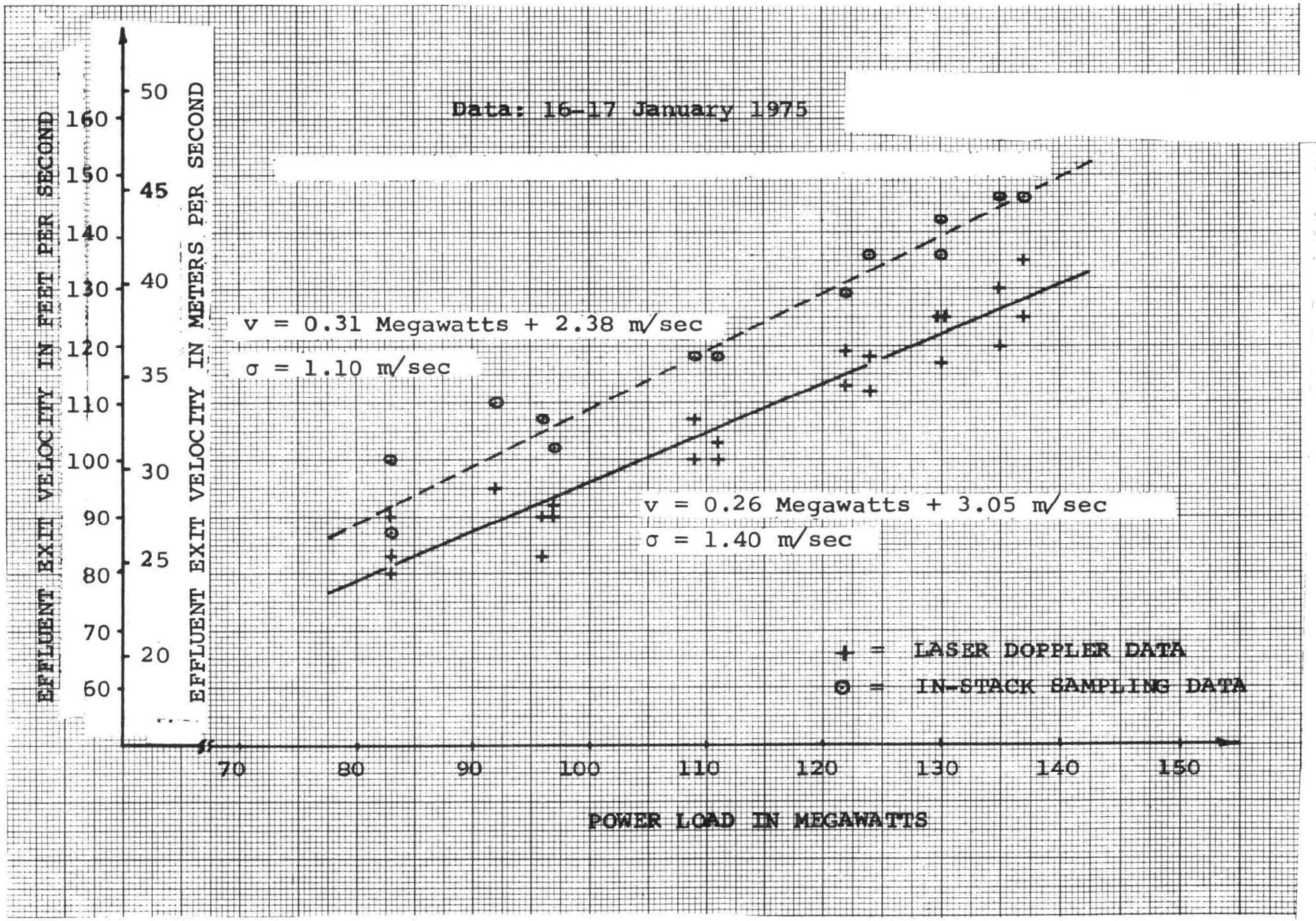

Figure 4-15. Effluent Exit Velocity as a Function of Power Load.

The standard deviation of the Doppler data from this equation is 1.40 m/sec, which indicates that the linear equation provides a good approximation for estimation of the exit velocity.

The in-stack velocity measurements yielded exit velocities which averaged 14% higher than the LDV measured velocities. The results is shown in Figure 4-16 where the LDV velocity data is plotted against the pitot-tube velocity data. A linear least squares fit to the pitot tube data indicated that exit velocity as a function of load followed the equation:

$$v\ (m/sec) = 0.31\ megawatts + 2.38 \qquad (4\text{-}2)$$

The standard deviation of the pitot-tube data from this equation is 1.10 m/sec again indicating that a good fit was made.

The cause for the 14% discrepancy between the remote and in-stack velocity data is not known. A number of possible causes are: (1) error in measuring the LDV's elevation angles, (2) miscalibration of the pitot tube used on the in-stack measurements, (3) erroneous correction factor used in calculating the gas exit velocity from the in-stack velocity, and/or (4) unaccounted for factors such as compression or thermal cooling of gases in the stack. In any event the discrepancy appears to be the result of a systematic error rather than a random error. If such an error can be accounted for, the LDV should be able to make remote smoke stack effluent velocity measurements accurate to about 1.5 m/sec or less.

4.3.2 SIGNAL STRENGTH AS A FUNCTION OF CROSS-STACK TRANSMISSION

Tapes #3 and 6 were used to determine the relationship between the LDV's received signal strength backscattered from the smoke stack effluents and the cross-stack optical transmission as measured on a Lear Seigler RM-4 transmissometer. During these runs the electrostatic precipitator banks on the stack were turned on and off in various combinations to change the cross-stack optical transmission. It was assumed that both absorption and single scattering determined the optical transmission across the stack. Since the attenuation coefficient is proportional to particle concentration, the optical transmission should obey the relationship:

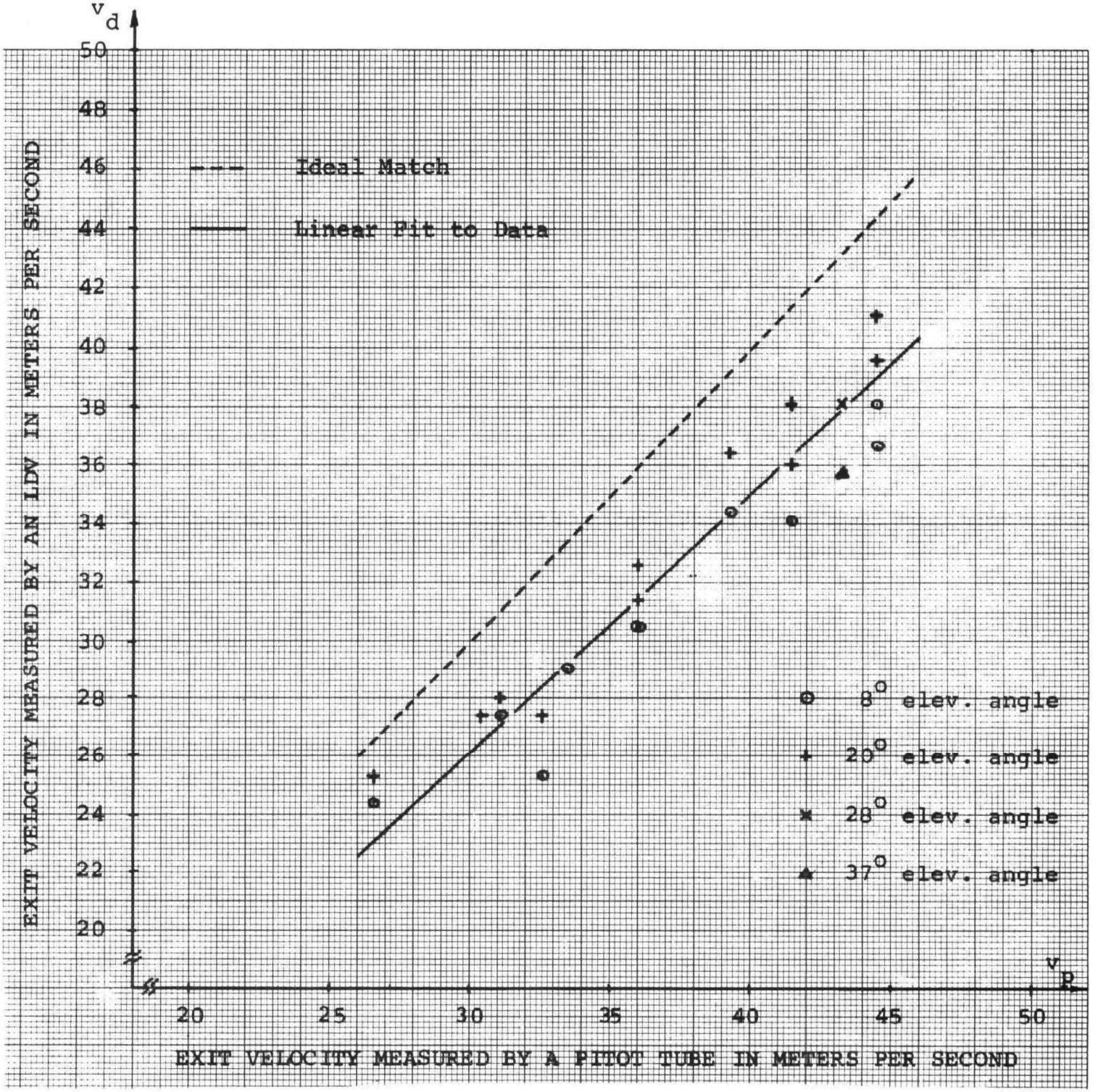

Figure 4-16. Effluent Exit Velocity Measured by a Laser Doppler Velocimeter as a Function of the Exit Velocity Measured by an In-Stack Pitot Tube.

$$T = \exp\left[-\alpha(N)L_s\right] \qquad (4\text{-}3)$$

where T is the optical transmission, L_s is stack diameter, and $\alpha(N)$ is the attenuation coefficient and is linearly proportional to the particle concentration, N.

Unfortunately varying the number of precipitators in use also changes the effluent particle size distribution as well as the particle concentration. This result is shown in Table 4-4. The precipitators tend to remove the larger particles from the smoke stack effluents. The scattering at 10.6-μm from these particles is described by Mie theory. The Mie scattering functions depend on two parameters: the index of refraction of the particle and a size parameter, μ, given by the equation:

$$\mu = \frac{2\pi r}{\lambda} \qquad (4\text{-}4)$$

where r is the particle radius and λ is the wavelength. The Mie scattering functions for the stack are very difficult to evaluate since they require exact knowledge of the size distribution and chemical distribution of the effluent. It was hoped, however, that a qualitative rather than an exact quantitative correlation would exist between transmission in the visible and scattering at 10.6 μm.

In order to determine the relationship between the backscattered signal strength and the cross-stack optical transmission, the total integrated signal strength taken from the intensity tracker was plotted as a function of the attenuation coefficient measured in the visible. Assuming that there is no compression of the exhaust gases through the stack constriction, the attenuation coefficient at the stack exit has the same value as the in-stack attenuation coefficient described in Equation (4-3). The data from two different runs is tabulated in Table 4-5 and is shown graphically in Figure 4-17, where the relative integrated signal strength is plotted as a function of the optical attenuation coefficient. The solid line in the figure represents a least squares linear fit to the data points. The apparent linearity of the graph in Figure 4-17 indicates a linear

TABLE 4-4

Smoke Stack Effluent Particle Concentration and Emission Data. Data Taken from Environmental Science and Engineering, Inc. Measurements Under EPA Contract No. 68-02-0232, Task No. 45, Sub-task No. 3, 26 - 30 August 1974.

Date	Time (Hr:Min)	Load (MW)	Exit Velocity (m/sec)	Opacity (%)	Precipitators Off	Emission (kg/hr)	Particle Size (μm)	Percent Collected
8/28/74	16:50 - 19:55	140	48.3	~ 5	Unknown	18	> 8.42	0
							8.42 - 5.03	3.57
							5.03 - 3.47	2.23
							3.47 - 1.89	0.44
							1.89 - 1.25	1.79
							< 1.25	91.97
8/29/74	11:15 - 14:30	140	51.5	30	Unknown	99.5	> 5.77	24.34
							5.77 - 3.43	14.44
							3.43 - 2.63	8.87
							2.63 - 1.27	2.26
							1.27 - 0.83	3.13
							< 0.83	46.96

TABLE 4-5

Relative Integrated Doppler Signal Strength as a Function of Cross-Stack Transmission and the Optical Attenuation Coefficient. Data from Tape #3, 16 January 1975 and Tape #6, 17 January 1975.

Precipitator Conditions	Cross-Stack Optical Transmission (%)	Optical Attenuation Coefficient (m^{-1})	Relative Integrated Signal Strength
A Bank off 15:56 16 January 1975	94	2.09×10^{-2}	0.180
A & B Banks off 16:04 16 January 1975	82.5	6.50×10^{-2}	0.299
A, B, & C Banks off 16:10 16 January 1975	60	1.73×10^{-1}	0.718
B & C Banks off 16:17 16 January 1975	93.5	2.27×10^{-2}	0.191
C Bank off 16:25 16 January 1975	94	2.09×10^{-2}	0.150
B Bank off 16:32 16 January 1975	97	1.03×10^{-2}	0.066
No Banks off 16:38 16 January 1975	98.5	5.11×10^{-3}	0.060
A Bank off 16:45 16 January 1975	94	2.09×10^{-2}	0.120
No Banks off 15:20 - 15:23 17 January 1975	93.5	2.27×10^{-2}	0.129
A Bank off 15:32 - 15:35 17 January 1975	89	3.94×10^{-2}	0.243
A & B Banks off 15:47 - 15:50 17 January 1975	74	1.02×10^{-1}	0.457
A, B, & C Banks off 15:56 - 15:59 17 January 1975	49	2.41×10^{-1}	1.000

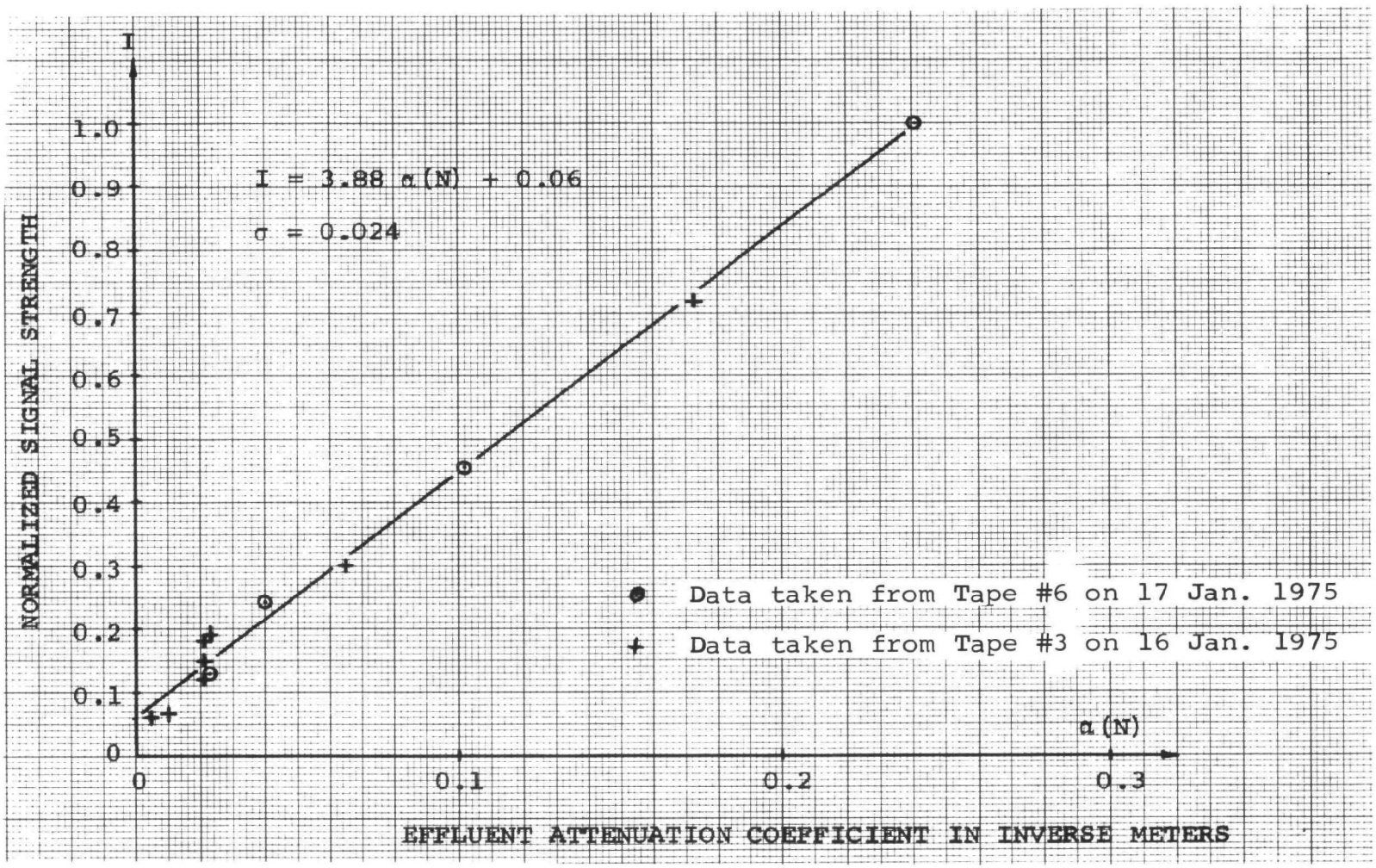

Figure 4-17. Relative Integrated Doppler Signal Strength as a Function of the Effluent Attenuation Coefficient.

relationship between the received backscattered signal at 10.6 μm and effluent particle concentration. However, a clarifying point must be made on this point. The intensity tracker integrates the signals from the spectrum analyzer between preset frequency limits. The spectrum analyzer was set to give a linear display. For a heterodyne system, a linear spectrum analyzer output provides a signal output which is proportional to the received signal's electric field strength rather than optical power. The signal strength plotted in Figure 4-17 is an integrated electric field strength. Because of the integration, there is no simple relationship between the integrated electric field strength and total received optical power.

If a good amplitude calibration can be established for the LDV, and the smoke stack under test, it appears that the total received signal strength measured by the LDV could be used to conveniently determine the optical transmission through the smoke stack plume. If sufficient information on particulate concentration and optical transmission is available,[7] the LDV could be used to measure smoke stack effluent particle concentrations.

4.3.3 THE EFFLUENT BACKSCATTER COEFFICIENT

Estimates of the backscatter coefficient can be made using theoretical analysis or a variety of experimental techniques. Evaluation of the effluent backscatter coefficient by theoretical analysis is very difficult since determination of the Mie scattering functions requires exact knowledge of the size distribution and chemical composition of the effluent.

With regard to evaluation of the backscatter coefficient by experimental techniques, the experimentation should be carried out at the wavelength of interest since the backscatter coefficient can vary with wavelength. One technique is to calibrate the system making the measurements, so that the signal amplitude can be related to the backscatter coefficient. According to Sonnenschein and Horrigan[1] the signal-to-noise ratio for a focussed, coaxial, laser heterodyne system which collects scattered radiation from a small length, ΔL, around the focus is given by the equation:

$$SNR = \frac{\eta_s P_T \beta(\pi)}{2h\nu B}\left[\frac{\pi D^2 \Delta L}{4L^2}\right] \qquad (4\text{-}5)$$

where

η_s is the system efficiency,

P_T is optical power output of the laser,

$\beta(\pi)$ is the backscatter coefficient,

D is the receiver optics diameter,

L is the range to the target (L equals the focal distance in Equation (4-5),

$h\nu$ is the photon energy of a quanta of laser radiation, and

B is the noise bandwidth.

The use of Equation (4-5) assumes the use of a shot-noise limited photoconductive detector which was the case in the smoke stack effluent measurements. Equation (4-5) can be solved for the backscatter coefficient giving the equation:

$$\beta(\pi) = \frac{8h\nu B\ L^2}{\pi\ \eta_s\ P_T\ D^2\ \Delta L} \cdot SNR \qquad (4\text{-}6)$$

For the smoke stack effluent measurements the bandwidth, B, was fixed by the spectrum analyzer IF filter at 100 kHz; the range, L, to the stack was measured on a laser rangefinder to be 400 m; the 2m stack exit diameter determined the resolution length, ΔL; the receiver optics diameter was 0.3 m; and the photon energy, $h\nu$ for the 10.6-um CO_2 laser was 1.875×10^{-20} Joule. If these values are substituted into Equation (4-6) $\beta(\pi)$ follows the relationship:

$$\beta(\pi) = 4.25 \times 10^{-9}\ \frac{SNR}{\eta_s\ P_T}\ [m^{-1}] \qquad (4\text{-}7)$$

The signal-to-noise ratio, system efficiency, and laser power were measured at various values of cross-stack optical transmission. The results of these measurements are plotted in Figure 4-18. The backscatter coefficient at any level of optical transmission has a wide range of values. This range of values is the result of the rapping cycles in the electrostatic precipitators. The fluctuations are filtered out of the transmissometer readings by averaging over long time intervals. The solid line in Figure 4-18 is a plot of the mean value of the backscatter coefficient as a function of the cross-stack optical transmission.

It was originally hoped that the backscatter coefficient would be a linear function of the effluent particle density. A good indication that such a relationship would not be found was the linear relationship established between the integrated electric field strength output from the intensity tracker and the effluent particle density. Since the heterodyne signal-to-noise ratio is proportional to the received optical power backscattered from the target, it was suspected that the backscatter coefficient would obey a functional relationship of the form:

$$\beta(\pi) = k\left[\alpha(N)L_e\right]^m \qquad (4\text{-}8)$$

where k is a constant; $\alpha(N)$ is the optical attenuation coefficient proportional to effluent particle concentration, N; L_e is exit diameter of the smoke stack; and the exponent m is a constant whose value is approximately 2. In order to confirm this assumption, the backscatter coefficient, $\beta(\pi)$, was plotted as a function of the natural logarithm of the optical transmission at the stack exit on log-log graph paper. The results are shown in Figure 4-19. It appears that the effluent backscatter coefficient at 10.6 μm can be approximated by the equation:

$$\beta(\pi)\ [m^{-1}] = 5.1 \times 10^{-4}\ (-\mathrm{Ln}T_e)^{1.6} \qquad (4\text{-}9)$$

where T_e is the optical transmission at the smoke stack exit.

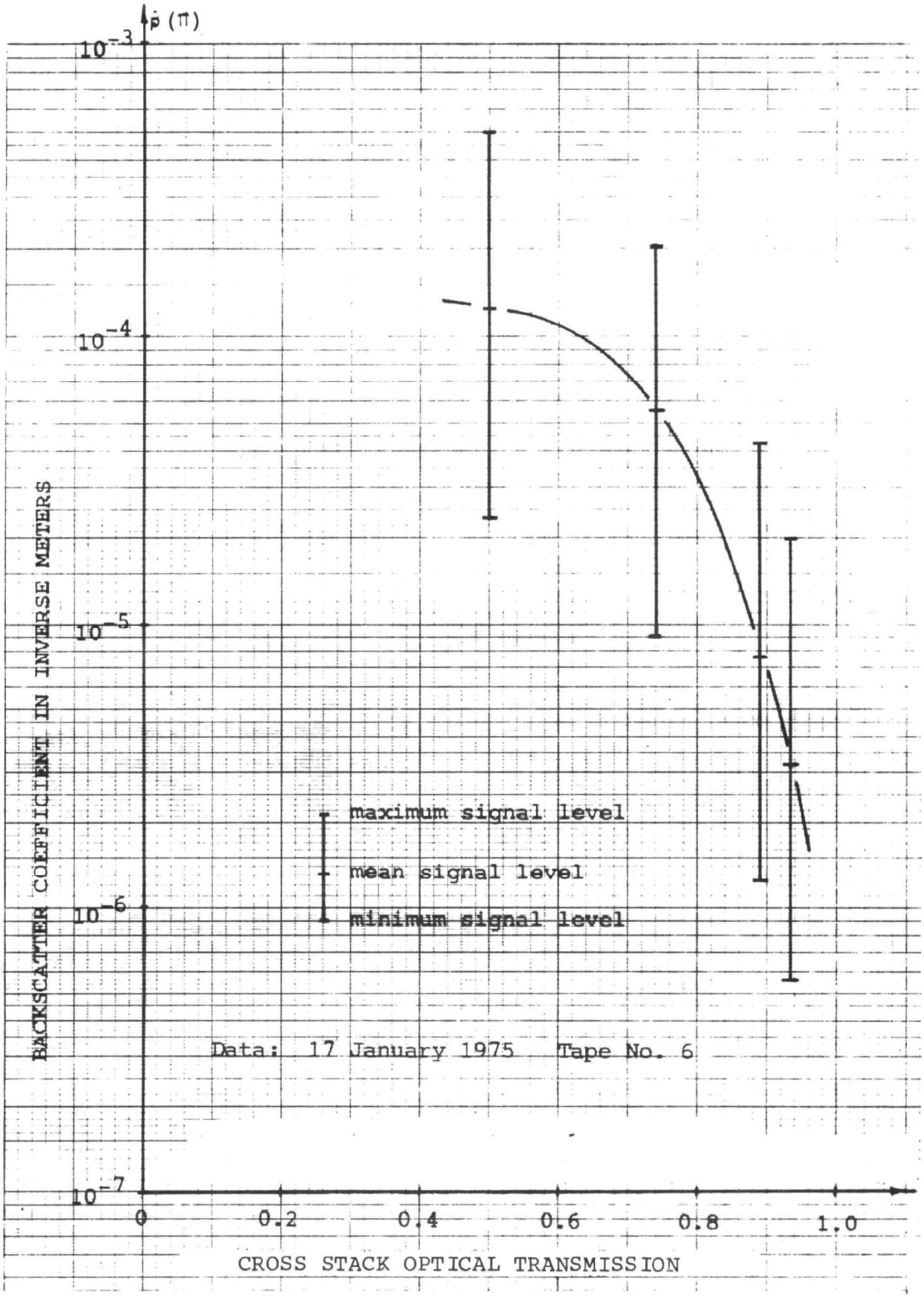

Figure 4-18. Effluent Backscatter Coefficient as a Function of the Cross-Stack Transmission.

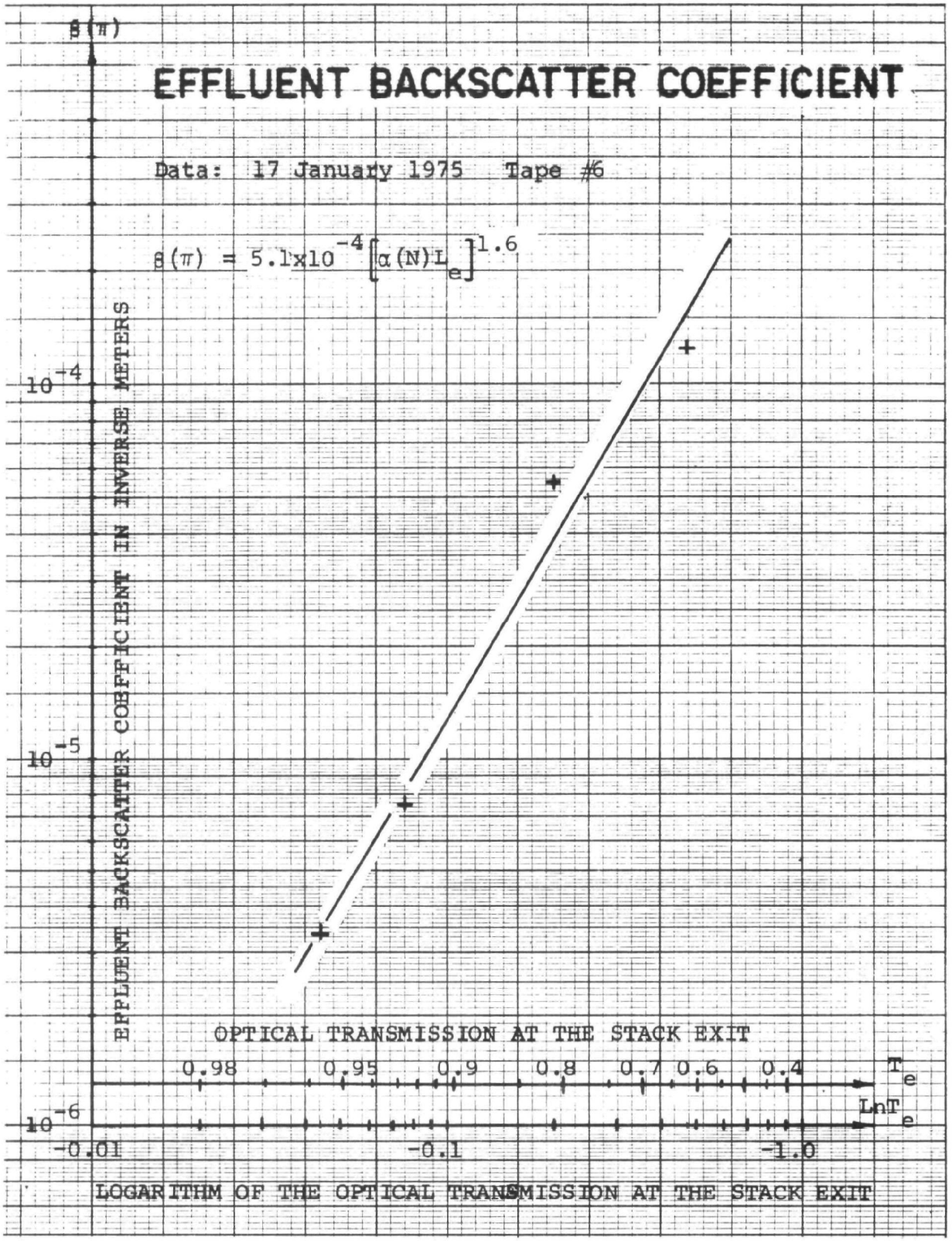

Figure 4-19. The Effluent Backscatter Coefficient Plotted as a Function of the Optical Transmission at the Smoke Stack Exit.

The reason that the backscatter coefficient follows such a relationship is not known. It may be the result of variations in the effluent particles' scattering functions caused by changes in the effluent particle size distribution.

4.3.4 TURBULENCE EFFECTS[6]

A simple model of the smoke stack exhaust velocity profile and the LDV's interaction with it can be used to estimate the effects of velocity spread and turbulence on the Doppler signal. A power law velocity profile of the form

$$u(r) = u_c(1-r/R)^{1/n} \qquad (4\text{-}10)$$

is assumed to describe the velocity in the stack near the sampling ports. In Equation (4-10), u(r) represents the velocity component parallel to the axis of the stack at a radius r from the center line of the stack; u_c is velocity at the center of the stack; and R is the radius of the stack. The value of the exponent n is determined by the Reynold's number for the smoke stack. For large values of Reynold's number the exponent n is approximately equal to 7.[2] The Reynold's number is the criterion for determining if a flow is laminar or turbulent. When the Reynold's number is less than 2100 the flow is laminar; when it is greater than 3100 it is turbulent and n is approximately equal to 7.[3] The Reynold's number is a function of four parameters: average velocity, density, viscosity, and a characteristic dimension of passage such as the tube diameter. The Reynold's number of the smoke stack at Duke Power is in the 30,000 to 40,000 range indicating a turbulent gas flow.[4] The velocity profile inside the stack and below the constriction has a flattened axial velocity profile of the form:

$$u(r) = u_c(1-r/R)^{1/7} \qquad (4\text{-}11)$$

This profile is plotted in the lower distribution of Figure 4-20.

The smoke stack is topped with a converging section 3.05 m in length which reduces the diameter from 2.96 m to 1.94 m. This constriction results in an increase in the average flow velocity by a factor of $(1.52)^2$ (assuming no compression occurs). It also further flattens the velocity profile. Along each streamline Bernoulli's

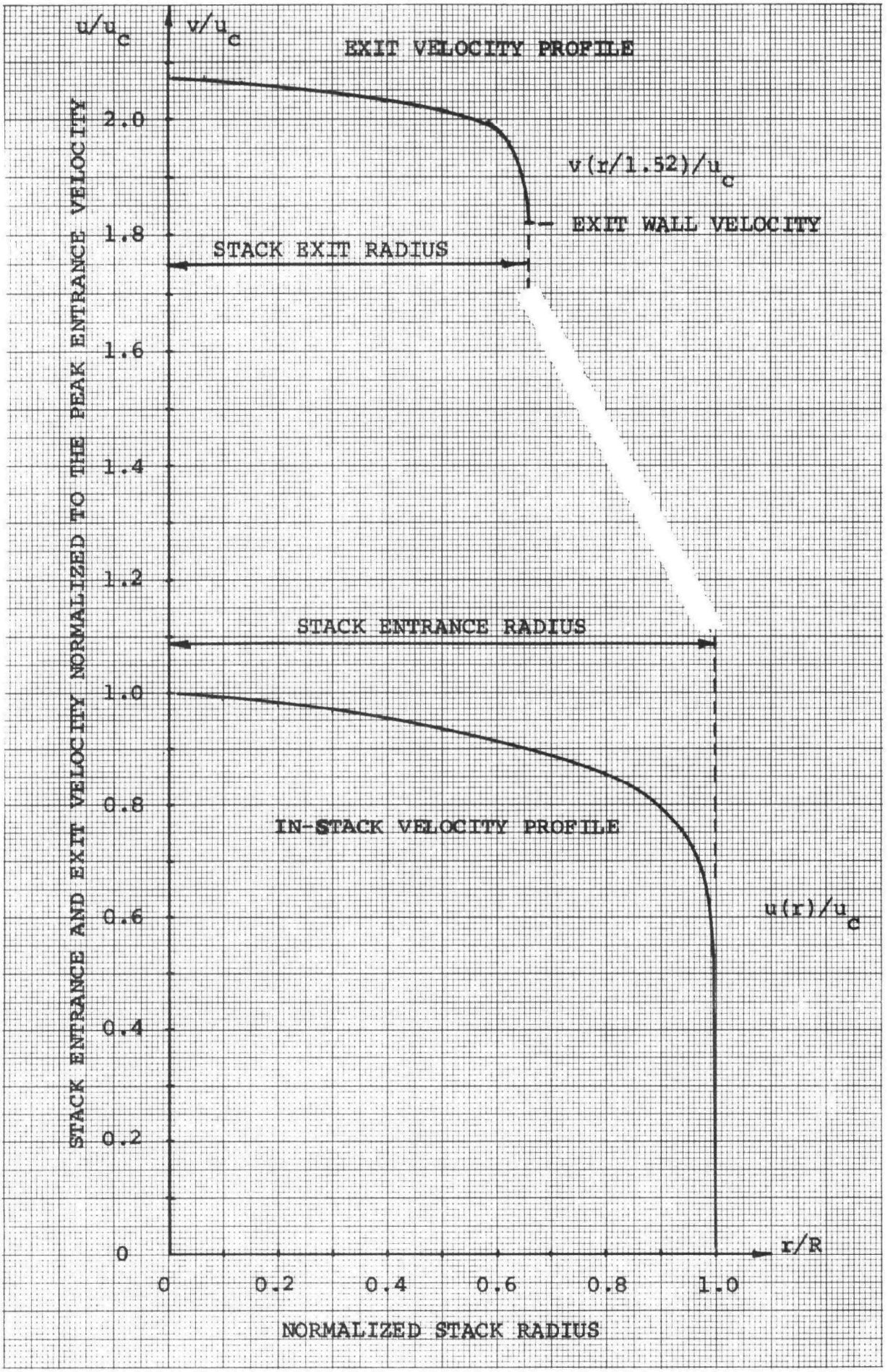

Figure 4-20. Theoretical In-Stack and Exit Velocity Profiles.

equation requires that the exit velocity, v, be related to the entrance velocity, u, according to the formula:

$$v^2 = u^2 + \frac{2}{\rho}(p_1 - p_2) \qquad (4\text{-}12)$$

where ρ is the density of the stack cases and p_1 and p_2 are the respective entrance and exit pressures on the converging section. The pressure term in Equation (4-12) can be estimated by assuming a flat velocity profile in the downstream stack section. Conservation of mass then requires that:

$$2(p_1 - p_2)/\rho \approx \bar{v}^2 - \bar{u}^2 = \bar{u}^2 \left[(\bar{v}/\bar{u})^2 - 1 \right] \qquad (4\text{-}13)$$

where the $\bar{u}$ and $\bar{v}$ are the respective mean entrance and exit velocities. For the Duke Power smoke stack, the mean exit to mean entrance velocity ratio is 2.32 which determines that:

$$2(p_1 - p_2)/\rho \approx 4.41\bar{u}^2 \qquad (4\text{-}14)$$

By substituting Equation (4-14) into Equation (4-12), the exit velocity at a radius r from the stack center line can be found. The exit velocity is given by the equation:

$$v(r/1.52) = \left[u(r)^2 + 4.41\bar{u}^2 \right]^{1/2} \qquad (4\text{-}15)$$

The average flow velocity below the stack construction can be found by averaging Equation (4-11) over the cross-sectional area of the stack. Hence:

$$\bar{u} = \frac{2\pi u_c}{\pi R^2} \int_0^R r(1 - r/R)^{1/7} \, dr = 0.817 \, u_c \qquad (4\text{-}16)$$

By utilizing Equations (4-11), (4-16) and (4-15), the exit velocity distribution can be found to have the form:

$$v(r/1.52) = \bar{u}\left[1.50(1-r/R)^{2/7} + 4.41\right]^{1/2} \qquad (4\text{-}17)$$

The exit velocity distribution is plotted in the upper distribution of Figure 4-22 for comparison to the in-stack distribution. The exit profile is flat except near the exit wall. Even near the wall the exit profile is flatter than entrance profile. These theoretical results are more or less confirmed by the experimentally obtained profiles shown in Figures 4-2, 4-8, and 4-14. Neglecting asymmetries and velocity fluctuations within the profile, the experimental profiles are fairly flat and exhibit the high wall velocities predicted by the simple fluid dynamical model.

The flow out of the stack is turbulent and has fluctuating velocity components in the direction of the flow and perpendicular to the flow. The turbulence velocity in the direction of the flow is assumed to have an RMS velocity, v_x'. The turbulence velocities perpendicular to the flow can be broken up into radial and tangential components with RMS velocities, v_r' and v_ϕ', respectively.

The component of velocity, $v_{||}$, parallel to a laser beam passing through the centerline of the stack dust above the lip at an elevation angle, θ, is given by the equation:

$$v_{||} = (v + v_x') \sin\theta + v_r' \cos\theta \qquad (4\text{-}18)$$

Since the stack exit diameter is much smaller than the LDV's range resolution, the entire distribution of velocities through the stack will be detected. The backscattered radiation will be Doppler shifted by amount:

$$\Delta\nu_D = \frac{2}{\lambda} v_{||} \qquad (4\text{-}19)$$

If the flow and turbulence velocity profiles are assumed to be nearly flat across the stack, the Doppler shift will have a mean frequency:

$$\overline{\Delta\nu_D} = \frac{2}{\lambda} \bar{v} \sin\theta \qquad (4\text{-}20)$$

where the superimposed bar is used to denote an average. The Doppler spectra will have a frequency width, Δf_D, given by the equation:

$$\Delta f_D = \frac{4}{\lambda}\left[\bar{v}_x' \sin\theta + \bar{v}_r' \cos\theta\right] \tag{4-21}$$

By analyzing the Doppler spectra from various elevation angles, estimates can be made for the axial and radial turbulent velocity compoents.

The Doppler spectra from four different elevation angles are shown in Figure 4-21. These spectra were analyzed to determine the mean Doppler frequency, the spectral width, and the ratio of the spectral width to the mean Doppler frequency. These data are tabulated in Table 4-6. In order to determine the turbulence parameters, Equation (4-21) was divided by Equation (4-20) to produce the normalized equation:

$$\frac{\Delta f_D}{\overline{\Delta v}_D} = \frac{2\bar{v}_x'}{\bar{v}} + \frac{2\bar{v}_r'}{\bar{v}} \cot\theta \tag{4-22}$$

The data in Table 4-7 were fitted to Equation (4-29) to obtain estimates for the normalized turbulence velocities, $\bar{v}_x'/\bar{v}$ and $\bar{v}_r'/\bar{v}$. The fit shown in Table 4-7 was obtained with the turbulence values:

$$\bar{v}_x'/\bar{v} = 0.040 \tag{4-23}$$

$$\bar{v}_r'/\bar{v} = 0.057 \tag{4-24}$$

These values of relative turbulence can be compared to previously measured values of relative turbulence intensities. Figure 4-22 shows relative turbulence intensities measured in a fully developed pipe flow with a Reynolds number of 5×10^5. Our fitted values can be seen to have the same range of values as those measured by Laufer.

Undoubtedly the turbulence effects increase with height above the stack lip. A mixing region between the stationary air and effluent gases develops at the lip of the stack and spreads upward

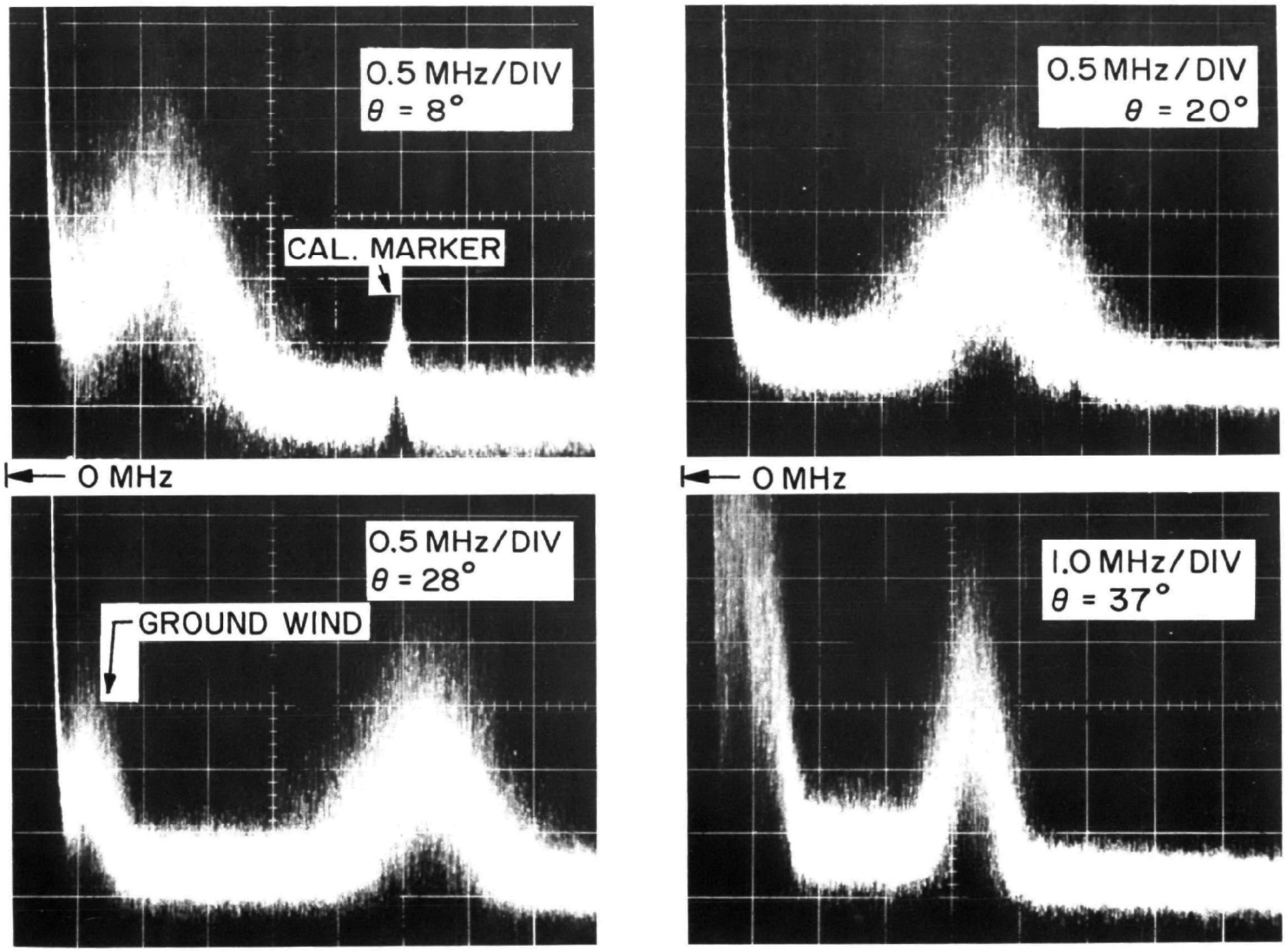

Figure 4-21. Typical Doppler Spectra from Smoke Stack Effluents at Various Laser Elevation Angles.

TABLE 4-6

Data on Doppler Spectra of
Smoke Stack Effluents

θ (Deg)	$\Delta\nu_D$ (MHz)	Δf_D (MHz)	$\Delta f_D/\overline{\Delta\nu}_D$ Experimental	$\Delta f_D/\overline{\Delta\nu}_D$ Fitted Data*
8	1.2	1.06	0.88	0.88
20	2.4	0.99	0.41	0.40
28	3.2	0.96	0.29	0.29
37	4.3	0.95	0.20	0.23

* Fit with $\overline{v}_x'/\overline{v} = 0.040$ and $\overline{v}_r'/\overline{v} = 0.057$

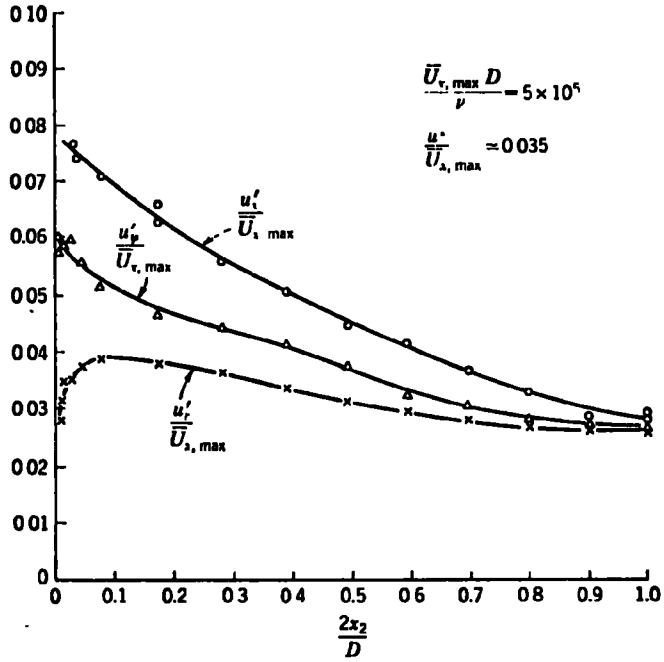

Figure 4-22. Relative Turbulence Intensities in Pipe Flow. (Laufer, J.; Reprinted from NACA Tech. Repts. 1174, pp. 6 and 7, 1954.)

with an angle of about 3^{o}.[5] This spreading can be observed in the velocitiy profiles shown in Figure 4-14. In the mixing layer the flow velocity is approximately one half the flow velocity at the exit wall. The turbulence velocities in the mixing region can reach 15% of flow velocity at the exit wall.[7] However, the particle concentration in the mixing region is reduced, so that the intensity of returns from this area is diminished. The increased turbulence in the mixing region could broaden the large elevation angle Doppler spectra. If the beam passes close to the lip of the stack, the broadening should not be significant for elevation angles less than 40^{o}.

SECTION 5

SYSTEM ANALYSIS

5.1 INTRODUCTION

A preliminary system analysis for a CO_2 laser heterodyne system to be used for the measurement of the velocity, and possibly particulate mass concentration, of the effluent emerging from smoke stacks of power plants has been performed. This analysis is based upon the theory of laser heterodyning and upon the results of the measurement program described in Section 4. The system to be analyzed is shown in Figure 5-1.

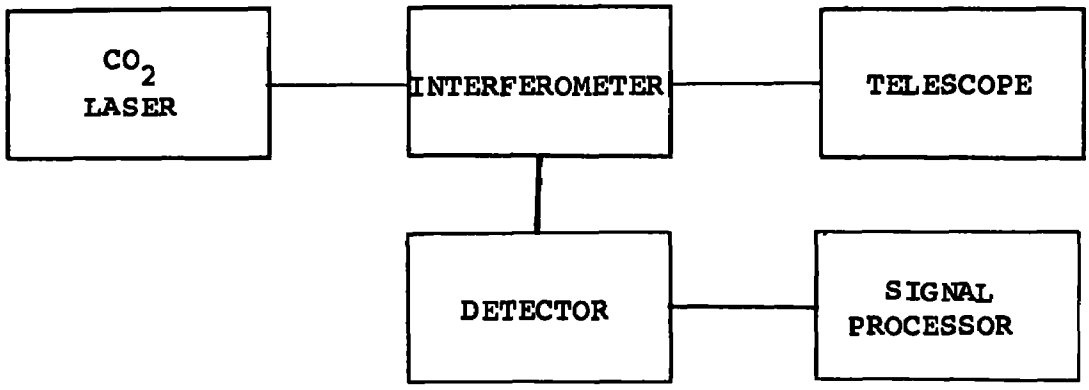

Figure 5-1. System Block Diagram.

5.2 HETERODYNE DETECTION

Radiation from the laser illuminates a moving target, in this case the aerosols emitted from the power plant smoke stack. The laser radiation is scattered by the aerosols, and the scattered radiation has a frequency shifted from the original laser frequency. For the system illustrated in Figure 5-1, where a common transmitting and receiving telescope is used, the frequency shift, $\Delta\nu_D$,

$$\Delta\nu_D = \frac{2v_{\parallel}}{\lambda} \tag{5-1}$$

where

$v_{\parallel}$ = aerosol velocity component parallel to the line connecting transmitter and target

λ = laser wavelength

For a CO_2 laser, the frequency shift is approximately 33 kHz per m/sec of the aerosol velocity component. For a vertical flow,

$$\Delta\nu_D = \frac{2}{\lambda} v \sin\theta \tag{5-2}$$

where

v = magnitude of aerosol velocity

θ = transmitter elevation angle

Radiation collected by the receiving telescope is combined with radiation at the original laser frequency. When this combination illuminates a square law detector, energy at the difference frequency, $\Delta\nu_D$, is obtained. A measurement of this frequency combined with knowledge of the system geometry enables the determination of the magnitude of the aerosol velocity.

5.3 SIGNAL TO NOISE RATIO

The ability of the laser system to measure the difference frequency, and therefore the aerosol velocity, is determined by the system signal to noise ratio. A theoretical derivation of this quantity for a laser heterodyne system against a target that is a collection of aerosols is given in Reference 1. This shows that

$$\frac{S}{N} = \frac{\eta_Q \eta_S P_T \beta(\pi)\lambda}{2h\nu B} \left\{ \tan^{-1}\left[\frac{4\lambda L_2}{\pi D^2} - \frac{\pi D^2}{4\lambda f}\left(1 - \frac{L_2}{f}\right)\right] - \tan^{-1}\left[\frac{4\lambda L_1}{\pi D^2} - \frac{\pi D^2}{4\lambda f}\left(1 - \frac{L_1}{f}\right)\right]\right\} \tag{5-3}$$

where

η_Q = quantum efficiency
η_S = system efficiency
P_T = transmitter power
$\beta(\pi)$ = effluent backscatter coefficient
h = Planck's constant
ν = laser frequency
B = system bandwidth
L_2 = maximum target range
L_1 = minimum target range
f = range to focus of laser beam
D = optics diameter

If the target extent, ΔL,

$$\Delta L = L_2 - L_1 \tag{5-4}$$

is much greater than the mean range, L,

$$L = f >> \Delta L \tag{5-5}$$

then as shown in Reference 1

$$S/N = \frac{\pi \eta_Q \eta_S P_T \beta(\pi) D^2 \Delta L}{8\, h\nu B\, L^2} \tag{5-6}$$

For a photovoltaic detector, the noise is decreased by a factor of two; additionally a more exact calculation shows

$$\frac{S}{N} = \frac{0.4\pi \eta_Q \eta_S P_T \beta(\pi) D^2 \Delta L}{4h\nu B\, L^2} \tag{5-7}$$

It is important to select realistic system parameters that will be valid for a variety of applications. From systems that have been actually constructed,

η_Q = 0.5
η_S = 0.1

Reasonable stack parameters and ranges appear to be

$$250m \leq L \leq 1000m$$
$$\Delta L = 2m$$

and from the results of Section 4, the lowest value of backscatter coefficient and the highest value of bandwidth are

$$\beta(\pi) = 3 \times 10^{-6}\ m^{-1}\ ster^{-1}$$
$$B = 5 \times 10^{5}\ Hz$$

Then

$$\frac{S}{N} = 1.01 \times 10^{7}\ P_T \left(\frac{D}{L}\right)^2 \qquad (5\text{-}8)$$

Plots of equation (5-7) appear in Figure 5-2 through Figure 5-4 , for laser powers of 1 W, 5 W, and 23 W and for ranges of 250 m, 500 m, and 1000 m.

From these curves, a combination of optics sizes and laser powers can be obtained for any given signal-to-noise ratio. A signal-to-noise ratio of approximately ten is desired. For no signal integration, these values are shown in Table 5-1.

TABLE 5-1

Trades Between Power and Optics Size

No Integration

Laser Power (W)	Optics Diameter (cm)		
	L = 250 m	L = 500 m	L = 1000 m
1	25	50	100
5	11	22	44
20	5.5	11	22

The use of a signal processor to integrate the return signal increases system signal-to-noise ratio by approximately the square cost of the number of pulses to be integrated. A processor, similar to the one

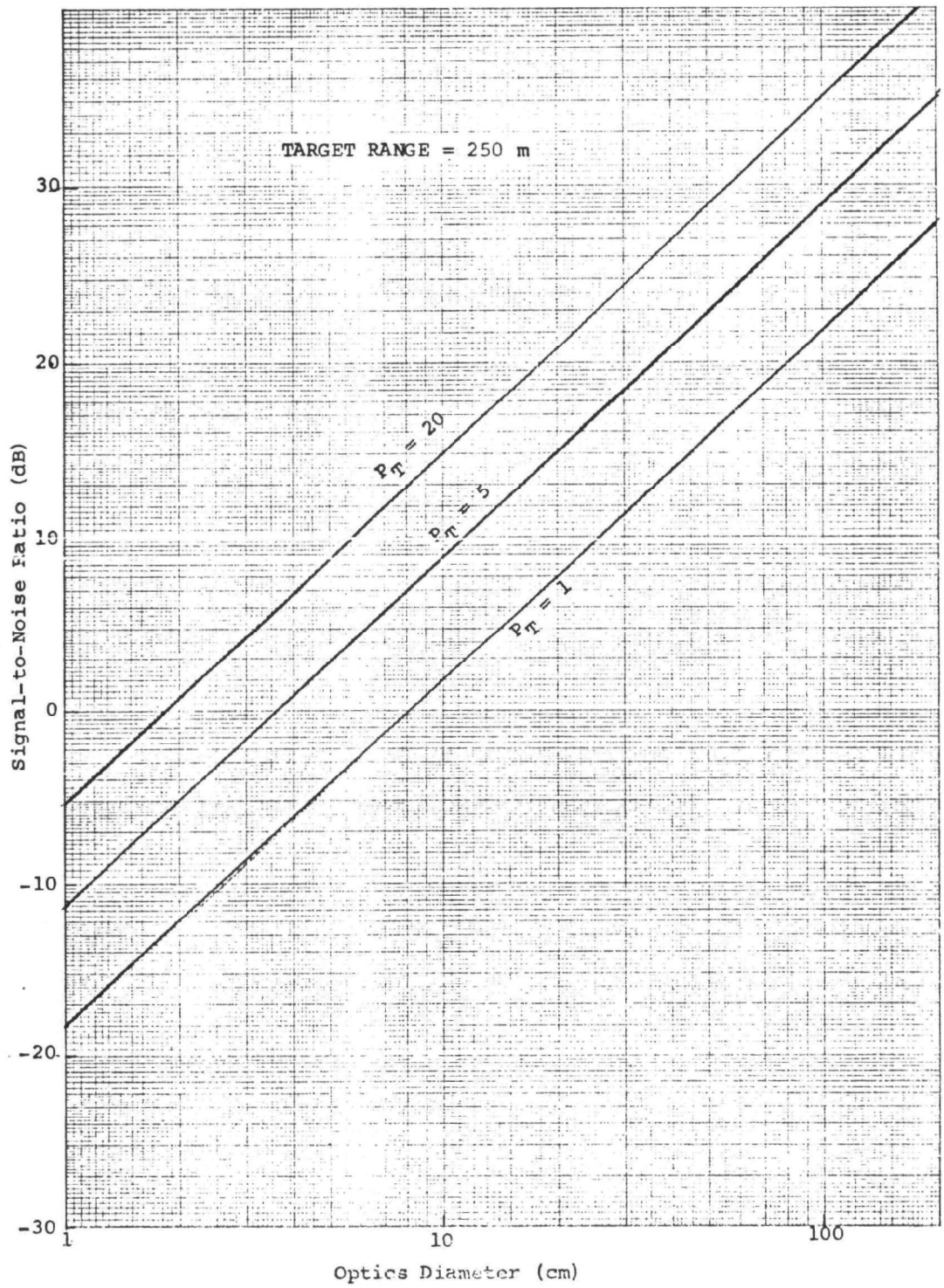

Figure 5-2. System Signal-to-Noise Ratio for Range = 250 m.

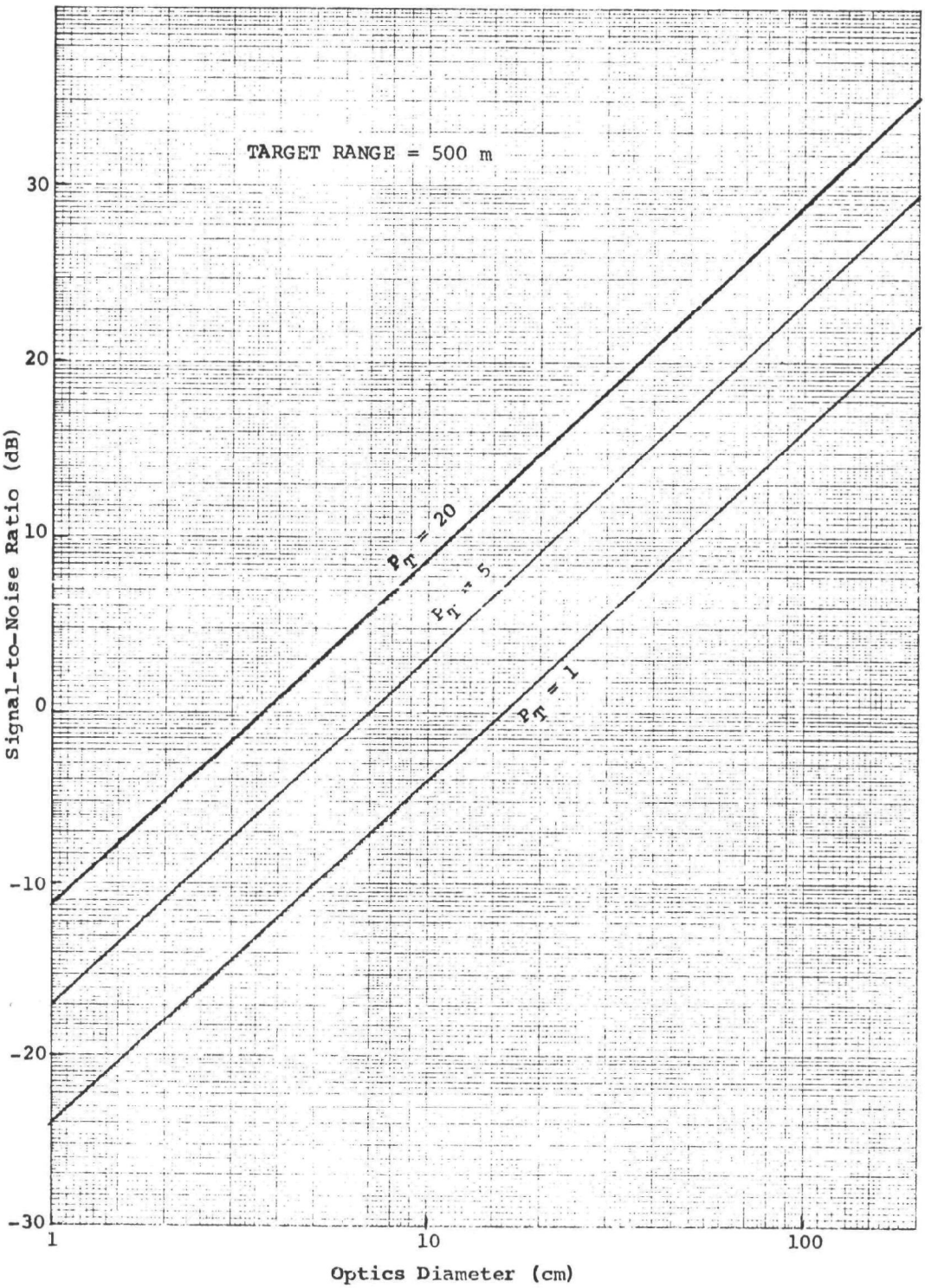

Figure 5-3. System Signal-to-Noise Ratio for Range = 500 m.

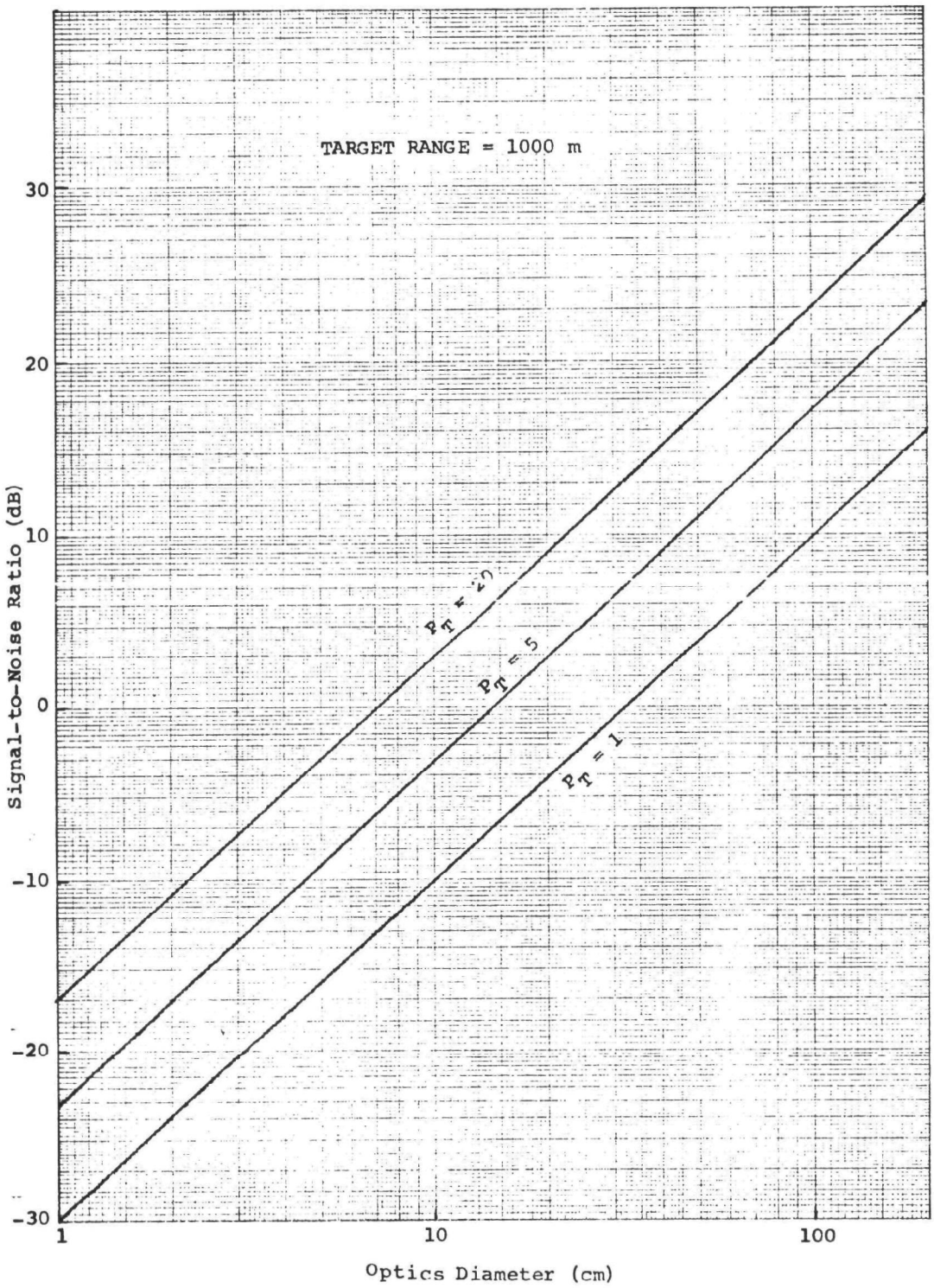

Figure 5-4. System Signal-to-Noise Ratio for Range = 1000 m.

required for this application, has been fabricated by Raytheon Company. It integrates a Doppler spectrum for times of the order of 1 msec and obtains approximately a 10 dB improvement in signal-to-noise ratio. With such a processor, operation can be accomplished with a pre-integration signal-to-noise ratio of one. The trade between laser power and optics diameter for this case is shown in Table 5-2.

TABLE 5-2

Trades Between Power and Optics Size Integration

Laser Power (W)	Optics Diameter (cm)		
	L = 250 m	L = 500 m	L = 1000 m
1	8	16	32
5	3.6	7.2	14
20	1.8	3.6	7.2

Therefore, depending upon choices of laser power, target range, and integration, optics sizes can run from less than 2 cm to 1 m and laser power can vary from 1 W to 20 W.

5.4 BEAM SIZE

The analysis in Section 5.3 assumed that the beam size on target was smaller than the target. In fact, to insure a relatively uniform region of flow, it is reasonable to keep the beam size no greater than one quarter of the stack diameter.

The far field distance of an aperture, d_{FF},

$$d_{FF} = \frac{D^2}{\lambda} \tag{5-8}$$

For ranges less than the far field distance, the optical beam can be focused and will be smaller than the transmitter diameter. For ranges greater than the far field distance, the beam diameter, D_{TAR}

$$D_{TAR} = \frac{R_o \lambda}{D} \qquad (5\text{-}9)$$

For operation at a range of 1000 m, the condition that D_{TAR} be greater than 0.5 m (one-quarter of the stack diameter) requires an optics diameter of 2 cm or greater. Operation at shorter ranges permits the use of smaller optics. Referring to Tables 5-1 and 5-2 shows that this requirement presents no problem.

5.5 BANDWIDTH CONSIDERATIONS

The system must have a bandwidth sufficiently wide to handle all potential Doppler shifts. If a maximum vertical velocity of 45 m/sec at an elevation angle of 45° is assumed, then a maximum system bandwidth of 6 MHz is required. However, since the signal frequency varies with elevation angle and the angle is fixed for a set of measurements, a smaller instantaneous bandwidth, approximately 1 MHz to 2 MHz, can be used. The center frequency of the processor can be tuned as a function of elevation angle.

SECTION 6

CONCLUSIONS

During the course of this program, a CO_2 Laser Doppler Velocimeter was tested against a coal burning power plant equipped with electrostatic precipitators. The purpose of the tests was to prove the feasibility of making remote velocity measurements of the exhaust gases from power plant smoke stacks. Remote effluent velocity measurements were made at a slant range of 400 m from the smoke stack and at elevation angles of 8°, 20°, 28°, and 37° from the horizontal. These measurements were made under a variety of power plant operating conditions, including different exit velocities obtained by varying power plant load conditions from 80 MW to 140 MW, and different particulate concentrations obtained by varying the precipitator operating conditions. In-stack measurements of the flue gas velocity and optical transmission were taken by the EPA for comparison purposes. Ground wind velocities were also measured. These were typically less than 2 m/s and had no effect on the stack exit velocity. The measurement data from the LDV was processed, recorded on magnetic tape, and later analyzed. The following conclusions can be reached as a result of that analysis:

A Laser Doppler Velocimeter has conclusively shown its ability to remotely measure the velocity of effluents from a power plant smoke stack. Velocity data was both selfconsistent, as shown from profile measurements, and in good agreement with pitot tube data. Deviations between the LDV and the pitot tube were of a systematic, rather than a random, nature and are probably associated with a relative miscalibration between the two instruments. A least square fit analysis of the velocity data indicates an accuracy of approximately 1.5 m/sec, although greater accuracy has been obtained in other LDV measurement.

A linear relationship was established between the relative integrated electric field strength received by the LDV and the attenuation coefficient measured in the visible through the smoke stack plume. Since the attenuation coefficient is proportional to particle concentration,[7] it appears that the signal strength received by the LDV can be used to evaluate smoke stack effluent particle concentrations. A good amplitude calibration would have to be established for each smoke stack before such measurements could be made, but an LDV has the potential for making mass emission rate measurements on power plant smoke stacks.

The effluent backscatter coefficient at 10.6-μm was evaluated as a function of the optical transmission through the smoke stack plume. It appears that the effluent backscatter coefficient at 10.6-μm can be approximated by the equation:

$$\beta(\pi)\left[m^{-1}\right] = 5.1 \times 10^{-4}\ (-\mathrm{Ln}T_e)^{1.6} \qquad (6\text{-}2)$$

where T_e is the optical transmission at the smoke stack exit. Based on measurements made during the first field tests an effluent backscatter coefficient of 10^{-4} m^{-1} corresponds to an effluent particle density of approximately 0.2 g/m^3.

It was shown that the turbulent flow in the smoke stack flattens the velocity distribution of the gases in the stack. The converging section at the top of the stack further flattens the velocity profile so that the exit velocity at the wall is 88% of the peak exit velocity at the center. This flattening was observed in the experimentally measured velocity profiles across the top of the smoke stack. The flat exit velocity distribution of the exhaust gases from the stack relaxes the alignment requirements on the LDV.

Estimates were made of the radial and axial turbulent intensity components. These estimates were based on the broadening of the Doppler spectra observed at various elevation angles between 8^o and 37^o. The axial and radial turbulence intensities were found to have the mean relative values:

$$\overline{v}_x'/\overline{v} = 0.040 \qquad (6\text{-}3)$$

$$\overline{v}_r'/\overline{v} = 0.057 \qquad (6\text{-}4)$$

These turbulence components produce a broadening of the Doppler spectra which is relatively independent of elevation angle. The magnitude of the broadening was sufficiently small that suitable effluent velocity measurements could be made at any elevation angle between 8° and 37°.

SECTION 7

REFERENCES

1. C. M. Sonnenschein and F. A. Horrigan, "Signal-to-Noise Relationships for Coaxial Systems that Heterodyne Backscatter from the Atmosphere", Applied Optics, Vol. 10, No. 7, July 1971, pp. 1600 - 1604, (see equation 23).

2. R. B. Bird, W. E. Stewart, and E. N. Lightfoot, Transport Phenomena, John Wiley and Sons, Inc., New York, New York, 1960.

3. J. F. Lee and F. W. Sears, Thermodynamics, Addison-Wesley Publishing Co., Inc., Reading, Massachusetts, 1963, pp. 284 - 287.

4. Private communication from Dr. W. F. Herget, EPA, NERC.

5. H. Tennekes and J. L. Lumley, A First Course in Turbulence, MIT Press, Cambridge, Massachusetts, 1972.

6. The authors would like to acknowledge J. A. L. Thomson's contribution to this section.

7. W. D. Conner, "Measurement of the Opacity and Mass Concentration of Particulate Emissions by Transmissometry", EPA Report No. EPA-650/2-74-128, November 1974.

TECHNICAL REPORT DATA
(Please read Instructions on the reverse before completing)

1. REPORT NO.	2.	3. RECIPIENT'S ACCESSION NO.
EPA-650/2-75-062		

4. TITLE AND SUBTITLE
REMOTE MEASUREMENT OF POWER PLANT SMOKE STACK EFFLUENT VELOCITY

5. REPORT DATE
August 1975

6. PERFORMING ORGANIZATION CODE

7. AUTHOR(S)
C. R. MILLER and C. M. SONNENSCHEIN

8. PERFORMING ORGANIZATION REPORT NO.

9. PERFORMING ORGANIZATION NAME AND ADDRESS
RAYTHEON COMPANY
Equipment Division
Electro-optics Department
Sudbury, Massachusetts 01776

10. PROGRAM ELEMENT NO.
1AA010

11. CONTRACT/GRANT NO.
68-02-1752

12. SPONSORING AGENCY NAME AND ADDRESS
U. S. Environmental Protection Agency
Office of Research and Development
Washington, D. C. 20460

13. TYPE OF REPORT AND PERIOD COVERED
FINAL REPORT

14. SPONSORING AGENCY CODE

15. SUPPLEMENTARY NOTES
Prepared in cooperation with: National Environmental Research Center
Research Triangle Park, N. C. 27711

16. ABSTRACT
This report describes the successful demonstration of the ability of a CO_2 Laser Doppler Velocimeter (LDV) to measure remotely the velocity of the effluent from a power plant smoke stack. The basis of the technique is that laser radiation backscattered from particulates in the effluent is Doppler shifted in frequency in proportion to the velocity of the effluent. Measurements were made against a coal burning power plant equipped with electrostatic precipitators to remove particulates from the boiler flue gases. Based on the results of the measurements a study on the design of an LDV optimized for the measurement of power plant effluent velocities was performed.

17. KEY WORDS AND DOCUMENT ANALYSIS

a. DESCRIPTORS	b. IDENTIFIERS/OPEN ENDED TERMS	c. COSATI Field/Group

18. DISTRIBUTION STATEMENT
This document is available to the public for sale through the National Technical Information Service, Springfield, Virginia 22161

19. SECURITY CLASS *(This Report)*
UNCLASSIFIED

20. SECURITY CLASS *(This page)*
UNCLASSIFIED

21. NO. OF PAGES
123

22. PRICE

EPA Form 2220-1 (9-73)